

Properties of Rindler Horizon and Some Aspects of Black Hole Chemistry in Massive Gravity

Thesis

submitted in partial fulfillment of the requirements for the degree of

DOCTOR OF PHILOSOPHY

by

SAFIR T K



**DEPARTMENT OF PHYSICS
NATIONAL INSTITUTE OF TECHNOLOGY KARNATAKA (NITK),
SURATHKAL, MANGALORE - 575 025**

AUGUST, 2023

DECLARATION

By the Ph.D. Research Scholar

I hereby *declare* that the Research Thesis entitled “**Properties of Rindler Horizon and Some Aspects of Black Hole Chemistry in Massive Gravity**”, which is being submitted to the *National Institute of Technology Karnataka, Surathkal* in partial fulfillment of the requirements for the award of the Degree of *Doctor of Philosophy in Physics* is a *bonafide report of the research work carried out by me*. The material contained in this thesis has not been submitted to any University or Institution for the award of any degree.



Safir T K

Register No.: 148040 PH14P04

Department of Physics

National Institute of Technology Karnataka

Surathkal.

Place: NITK - Surathkal

Date: 17 August 2023

CERTIFICATE

This is to *certify* that the Research Thesis entitled “**Properties of Rindler Horizon and Some Aspects of Black Hole Chemistry in Massive Gravity**”, submitted by **Safir T K** (Register Number: 148040 PH14P04) as the record of the research work carried out by him, is *accepted* as the *Research Thesis submission* in partial fulfillment of the requirements for the award of degree of *Doctor of Philosophy*.



Dr. Deepak Vaid
Research Guide
Assistant Professor
Department of Physics
NITK Surathkal - 575025


18/8/2023

Chairman - DRPC
(Signature with Date and Seal)

Dr. N.K. UDAYASHANKAR
PROFESSOR & HEAD
DEPARTMENT OF PHYSICS
NITK SURATHKAL, SRINIVASNAGAR
MANGALORE - 575 025, INDIA

Dedicated to
my beloved mother, father, sister, brothers,
my dear wife Shadiya and my sweet kids Nafi and Naba

ACKNOWLEDGEMENT

First and foremost, I thank my Ph.D. supervisor, Dr. Deepak Vaid, for allowing me to work under his supervision. His assistance helped me to understand the exciting research areas in theoretical physics and enabled me to achieve one of the best careers in physics.

I am so grateful to Dr. Ajith K. M, Associate Professor, Department of Physics, NITK Suarthkal, for his valuable support and suggestions. Without his interventions made during this period, this work would not have been completed. I am thankful to all our department faculties for the discussions and support during the research. I want to express my profound appreciation to my research progress assessment committee members, including Dr. Ajith K.M and Dr. Santhosh George, Professor, Department of Mathematical and computational sciences, for their timely suggestions and support. I remember all my teachers and mentors taught me during school life to the present time. Especially teachers from Daruddawa Madrassa Valillapuzha, G.L.P. School Panikkara-puraya, Mina A.M.U.P. school Cheruvayoor, G.H.S.S. Vazhakad, Sullamussalam Science College Areacode, Govt. College Kottayam and N.S.S Training College, Pandalam. They all made me a better and more thoughtful person.

I am very thankful to my friends, Dr. C.L Ahmed Rizwan, Dr. A.Naveena Kumara, Dr C. Fairoos, and Kartheek Hegde, for their active discussions and their valuable support to complete this research work. I cannot move out of NITK, Surthkal without mentioning the names of research scholars and M.Sc Students of the department of physics Dr. Rajani K.V, Dr. Siby Thomas, Dr. Manoj Kumar, Dr. Sreejesh, Dr. Nimith K.M, Dr. Manju M S, Ahmed Khasim, Sibeesh P P, Amrutha S.V, Dr Shreyas Punacha and MSc students Yadhu Krishna, Mrudul, Sreedevi, Aswathi P, Lekshmi Sreekala, whose help were unforgettable.

I am fortunate to have the best colleagues at T.K.M College of Arts and Science, Kollam, in my teaching life whose support I cannot avoid completing this Ph.D. As a part-time research scholar, such support is crucial for the completion. I received this valuable support from the head of the department Aparna L.R, Dr. Mohammed Salim, Dr. P.K Manoj, Dr. Fairoos C, Dr. Shargina Beegum, Dr. Anshad, Dr. Saritha Devi, Dr.

Abdul Raheem, and Nisamudeen Ashique. Also, our principal Dr Chithra Gopinath has given valuable support to complete this research on time.

I am so grateful to my family for their unfailing support and encouragement. My grandmother Late Ayisha was one of the happiest people when I got Ph.D. admission at NITK. She has given me much encouragement and support all my life. My parents, T.K Alikutty and T.K Sainaba, Parents-in-law Abdul Hameed PN and Ayishakutty, My brothers Jabir, Jaseem, Jamshid, Sajad and my lovely sister Poovi. My brother-in-law Fadi, Hadi, my sister-in-laws Shakkira K, Nasreena E, Hiba M, Ajmala, and Rifa. I am very happy with my niblings Ziya, Dilu, Vasil, Ihsan, Ayisha, Dina, Sana, Abu, Aidu, and Eira. I am grateful for their support and prayers. I am also grateful to Ahmed Rizwan CL and his family for giving me nice hospitality many times during the research period.

Last but not least, I offer heartfelt gratitude to my soul mate Shadiya Nihla P.N. and my sweet kids, Nafi Aman and Naba Nourin, for their love and support. I am so lucky to have a supportive family like this. Their care and affection led me to reach the best career in my life. Above all, I would like to express my gratitude to Almighty God Allah for all his countless blessings bestowed on me that kept me happy in my life. Thank you all.

T.K. Safir

Statement of Contribution

THIS THESIS IS BASED ON THE FOLLOWING ARTICLES.

- **T. K. Safir**, C.L. Ahmed Rizwan, Deepak Vaid. “Ruppeiner geometry, P- V criticality and interacting microstructures of black holes in dRGT massive gravity”. **International Journal of Modern Physics A Vol. 37, No. 25 (2022)**.
- **T. K. Safir**, C.Fairoos, Deepak Vaid. “Physical Process First Law and the Entropy Change of Rindler Horizons”. **Annals of Physics Volume 450, March 2023, 169237**.
- **T. K. Safir**, A. Naveena Kumara, Shreyas Punacha, C.L. Ahmed Rizwan, C.Fairoos, Deepak Vaid. “Dynamic phase transition of black hole in massive gravity”. **Communicated with journal- Under Review**.

ABSTRACT

One of the biggest challenges in theoretical physics, beyond any doubt, is the lack of a successful theory that describes how gravity works quantum mechanically. Exploring black holes provides many promising pathways that might lead us to a positive solution for the problem at hand. One of the tools in this regard is the thermodynamic behavior of black holes. To this extent, this thesis deals with certain aspects of black hole thermodynamics. First, we probe the microstructure of the dRGT massive black hole in an anti-de Sitter background. The calculations are performed in an extended phase space with pressure and volume taken as fluctuation variables. We analyze the microstructure by exploiting the Ruppeiner geometry, where the thermodynamic curvature scalar is constructed via adiabatic compressibility. The nature of the curvature scalar along the coexistence line of small (SBH) and large (LBH) black holes is investigated. In the microscopic interaction, we observe that the SBH phase behaves as an anyonic gas and the LBH phase is analogous to a boson gas. Further, we study the effect of graviton mass on the underlying microstructure of the black hole.

The thermodynamic study in the massive gravity theory can be extended further by considering the dynamics of phase transition. The dynamical properties of the stable small-large black hole phase transitions in dRGT non-linear massive gravity theory are studied based on the underlying free energy landscape. The free energy landscape is constructed by specifying the Gibbs free energy to every state, and the free energy profile is used to study the different black hole phases. The small-large black hole states are characterized by a probability distribution function, and the kinetics of phase transition is described by the Fokker-Planck equation. Further, a detailed study of the first passage process is presented, which describes the dynamics of phase transition. We have investigated the effect of mass and topology on the dynamical properties of phase transitions of black holes in dRGT massive gravity theory.

Finally, we concentrate on the characteristics and features of the first law of black hole thermodynamics. The physical process version of the first law can be obtained for bifurcate-Killing horizons with certain assumptions. Especially, one has to restrict to the situations where the horizon evolution is quasi-stationary, under perturbations.

We revisit the analysis of this assumption considering the horizon perturbations of the Rindler horizon by a spherically symmetric object. We demonstrate that even if the quasi-stationary assumption holds, the change in entropy in four-dimensional space-time dimensions diverges when considered between asymptotic cross-sections. However, these divergences do not appear in higher dimensions. We also analyze these features in the presence of a positive cosmological constant. In the process, we prescribe a recipe to establish the physical process first law in such ill-behaved scenarios.

Keywords: Black hole thermodynamics; Thermodynamic geometry; Massive gravity theory; Free energy landscape; Physical process version of first law;

Contents

List of Figures	v
1 Introduction	1
1.1 The AdS Spacetime	4
1.2 Black holes and thermodynamics	6
1.3 Massive gravity	10
1.4 Objectives of the present research work	11
1.5 Organization of the thesis	12
2 An overview of black hole chemistry	13
2.1 Black hole chemistry	14
2.2 Four laws of black hole thermodynamics	15
2.3 Smarr relation and black holes	16
2.4 Smarr relation in AdS black holes	19
2.5 P-V criticality	21
2.5.1 Van der Waals fluid	21
2.5.2 Phase transitions in charged AdS black hole	22
2.6 Discussions	25
3 Ruppeiner geometry and interacting microstructures of black holes in dRGT massive gravity	27
3.1 Introduction	27
3.2 Thermodynamics of black holes in massive gravity	28
3.3 Microstructure of black holes	31

3.3.1	Thermodynamic geometry	32
3.3.2	Scalar curvature	37
3.3.3	Ruppeiner geometry and microstructure of massive black Hole	38
3.4	Discussions	40
4	Dynamic phase transition of black holes in massive gravity	43
4.1	Introduction	43
4.2	Thermodynamic characterisation and phase transition	45
4.3	Gibbs free energy landscape	48
4.4	Probabilistic evolution on the free energy landscape	52
4.4.1	Fokker-Planck equation and probabilistic evolution	52
4.4.2	First passage time	56
4.5	The effect of mass and topology	58
4.6	Discussions	60
5	Physical process version of first law	61
5.1	Introduction	61
5.2	Evolution of the horizon and the formation of caustic	63
5.3	Perturbation of Rindler horizon by a freely falling object	67
5.3.1	Caustic avoidance of Rindler horizon in four spacetime dimension	67
5.3.2	Caustic avoidance for higher dimensional Rindler horizon	70
5.4	General structure of physical process first law and the law for arbitrary horizon cross-sections	71
5.4.1	Divergences in four spacetime dimension	74
5.4.2	Dimensions greater than four	78
5.5	Horizon perturbation in arbitrary dimensional de-Sitter spacetime	82
5.5.1	PPFL for arbitrary horizon cross sections in de-Sitter spacetime	84
5.6	Discussions	87
6	Summary and future work	89
	Appendices	93

A Komar integrals in AdS space	95
B Rindler approximations of black hole space-times	99
Bibliography	103
Curriculum Vitae	111

List of Figures

1.1	The topological structure of anti-de sitter space	5
2.1	P-V isotherms and Gibbs free energy is plotted against temperature for VdW gas	22
2.2	P-v isotherms for charged AdS Black holes. Took $v = 2r_+$ for AdS black holes	24
2.3	Gibbs free energy is plotted against pressure and temperature for charged AdS Black holes	24
2.4	Coexistent curve for Charged Black holes. Critical points are labelled with a circle.	25
3.1	$P - V$ isotherms of the massive dRGT-AdS black hole	30
3.2	The behaviour of R_N as a function of P and V	39
3.3	The behaviour of the R_N against the reduced volume V_r at constant pressure.	40
3.4	The behaviour of R_N along the coexistence curve.	41
3.5	The effect of parameter k on the microstructure interactions.	41
3.6	The effect of parameter m on the microstructure interactions.	42
4.1	Black hole temperature as a function of event horizon radius	47
4.2	Behaviour of Gibbs free energy as a function of r_+ for $P < P_c$ at different temperatures	49
4.3	The phase diagram of dRGT black holes. Here, T_{max} , T_{min} , and T_{trans} are plotted as a function of P fro 0 to P_c	51

4.4	The time evolution of the probability distribution function $\rho(r,t)$	54
4.5	The time evolution of the probability distribution $\rho(r,t)$	55
4.6	The time evolution of the distribution of the probability $\Sigma(t)$ that the system remains at the initial state.	57
4.7	The probability distribution of the first passage time $F_p(t)$	58
4.8	The effect of the parameters on the time evolution of the probability distribution $\rho(r,t)$	59
4.9	The effect of the spacetime parameters on the probability distribution of the first passage time $F_p(t)$	60
5.1	Behaviour of the Weyl tensor against $\kappa\bar{t}$ for two different values of $\frac{\rho}{z_0}$	69

Chapter 1

Introduction

The term “gravity” was introduced to us as the weakest among the four fundamental forces in nature. Sir Isaac Newton developed the universal law of gravitation in 1687, which explains how two objects attract each other with a force that is directly proportional to the product of their masses and inversely proportional to the square of their distance. The quantitative description of gravity was a milestone in the history of physics and, was successful in explaining many phenomena such as the motion of planets around the sun. It is worth mentioning that Newton’s law of gravitation survived nearly 200 years! However, during the late 19th century, as the observational results become more precise, Newton’s theory of gravitation failed to explain certain situations such as the perihelion precision of planet Mercury. Later at the beginning of 20th century, the formulation of the special theory of relativity (STR) by Albert Einstein caused a paradigm shift in the understanding of space and time. In 1915 he extended the relativity theory by incorporating gravity and formulated the general theory of relativity(GTR). This theory explains how gravity works classically in an elegant way!

According to the general theory of relativity, it is the curvature in space-time that makes the planets revolve around the sun. In this description, a matter object can curve the space-time around it, and the space-time curvature is related to the matter object through Einstein’s field equations:

$$R_{\mu\nu} - \frac{1}{2}Rg_{\mu\nu} = 8\pi T_{\mu\nu} \quad (1.1)$$

Here, $R_{\mu\nu}$ is the Ricci tensor, and $g_{\mu\nu}$ is the metric tensor describing space-time. Note that the LHS of the above equation is purely geometrical. The energy-momentum tensor $T_{\mu\nu}$ in the RHS represents the matter content in space-time. The above set of equations can be summed up using the famous quote by John Wheeler “space-time tells matter how to move; matter tells space-time how to curve”. For a given $T_{\mu\nu}$, one can solve the above set of non-linear partial second-order differential equations to obtain the metric tensor $g_{\mu\nu}$ as the solution. The simplest solution is obtained by putting $T_{\mu\nu} = 0$, and the corresponding result is known as the Schwarzschild metric, which represents the space-time outside a spherically symmetric object of mass M .

$$ds^2 = - \left(1 - \frac{2M}{r} \right) dt^2 + \frac{dr^2}{\left(1 - \frac{2M}{r} \right)} + r^2 (d\theta^2 + \sin^2 \theta d\phi^2) \quad (1.2)$$

The above metric predicts some unusual features of space-time, such as space-time singularity at $r = 0$, in which the curvature scalar becomes infinite. Further, the region around the singularity is causally disconnected from the rest of space-time and is called a black hole. The surface $r = 2M$ is known as the event horizon, which defines the boundary of the black hole. One can come up with more solutions to Eq. [1.1](#) by using the appropriate energy-momentum tensor. A charged black hole solution was obtained by Hans Reissner and Gunnar Nordström independently in 1918 as,

$$ds^2 = -f(r)dt^2 + \frac{dr^2}{f(r)} + r^2 (d\theta^2 + \sin^2 \theta d\phi^2), \quad (1.3)$$

where,

$$f(r) = 1 - \frac{2M}{r} + \frac{Q^2}{r^2}. \quad (1.4)$$

Here, M and Q are the mass and charge of the black hole, respectively. The inner (r_-) and outer (r_+) horizons are obtained from $f(r) = 0$ as,

$$r_{\pm} = M \pm \sqrt{M^2 - Q^2} \quad (1.5)$$

In 1963, Roy Kerr found a rotating black hole solution to EFE. The metric of the

Kerr black hole is given by

$$\begin{aligned}
ds^2 = & -\frac{\Delta - a^2 \sin^2 \theta}{\rho^2} dt^2 - 2a \frac{2Mr \sin^2 \theta}{\rho^2} dt d\phi \\
& + \frac{(r^2 + a^2)^2 - a^2 \Delta \sin^2 \theta}{\rho^2} \sin^2 \theta d\phi^2 \\
& + \frac{\rho^2}{\Delta} dr^2 + \rho^2 d\theta^2
\end{aligned} \tag{1.6}$$

where $\Delta = r^2 - 2Mr + a^2$, $\rho^2 = r^2 + a^2 \cos^2 \theta$ and a, M are angular momentum and mass of black hole respectively. Using Eq. [1.6](#), the inner and outer horizon of Kerr metric can be found as

$$r_{\pm} = M \pm \sqrt{M^2 - a^2} \tag{1.7}$$

By adding an electric charge to the Kerr black hole, Newman found a new solution for EFE in 1965. it is known as Kerr- Newman black hole solution. This black hole refers to an electrically charged rotating black hole. The metric form of the Kerr- Newman black hole differs from Kerr black only in the definition of Δ , which is given by $\Delta = r^2 - 2Mr + a^2 + Q^2$. The event horizon of the Kerr- Newman black hole is found as

$$r_{\pm} = M \pm \sqrt{M^2 - a^2 - Q^2} \tag{1.8}$$

The background space-time for the above black hole solutions is asymptotically flat. This means that far from the matter object, space-time is described by a Minkowski metric. One can have black holes in space-time that is not asymptotically flat. The history of such models starts with Einstein. He introduced a parameter called the cosmological constant (Λ) to modify Eq. [1.1](#) so that the universe would be static, i.e., the infinite space-time neither expands nor contracts. However, the observational results in those times proved that the universe was indeed expanding, and subsequently, Einstein renounced his cosmological constant. Much later, advanced observational results confirmed the accelerated expansion of the universe which can be explained by Einstein's field equations with a positive Λ , and the space-time is called de Sitter (dS). Another important model of space-time that is not asymptotically flat is the Anti-de Sitter space-time (AdS). The AdS model of the universe is the one with constant negative curvature.

In light of AdS/CFT correspondence, AdS space-time is extensively studied, especially the thermodynamics of AdS black holes. It is essential to outline a few details of AdS space-time since we will be using this model often in this thesis.

1.1 The AdS Spacetime

Anti-de Sitter(AdS) is a maximally symmetric solution to the Einstein equation. This is also a Vacuum solution but has a negative cosmological constant. So it's a negatively curved space-time. It's the Lorentzian analogue of hyperbolic space. The space with constant negative curvature is known as hyperbolic space H^2 . Hyperbolic can be embedded into three-dimensional Minkowski space. The hyperbolic space is defined by

$$ds^2 = -dZ^2 + dX^2 + dY^2 \quad (1.9)$$

$$-Z^2 + X^2 + Y^2 = -L^2 \quad (1.10)$$

Hyperbolic space has $SO(1,2)$ invariance. Any point on the surface can be mapped to other points by an $SO(1,2)$ Lorentz transformation. In order to solve the constraint [1.10](#), take a coordinate system

$$X = L \sinh \rho \cos \phi, \quad Y = L \sinh \rho \sin \phi, \quad Z = L \cosh \rho.$$

Then metric becomes

$$ds^2 = L^2(d\rho^2 + \sinh^2 \rho d\phi^2) \quad (1.11)$$

It does not have a timelike direction even though it is embedded in Minkowskian space-time. So it's a space, not a space-time. Its curvature is constantly negative. Now we consider AdS_2 space-time can be embedded into flat space-time with two timelike directions.

$$ds^2 = -dZ^2 - dX^2 + dY^2. \quad (1.12)$$

$$-Z^2 - X^2 + Y^2 = -L^2 \quad (1.13)$$

The parameter L is the AdS radius. AdS_2 spacetime has $SO(2,1)$ invariance. Take a

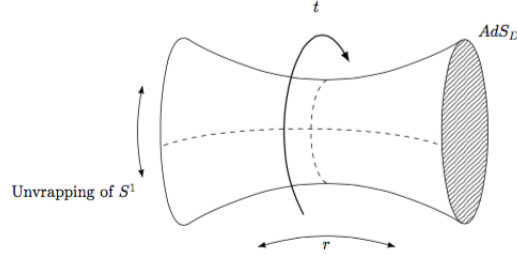


Figure 1: The topological structure of anti de- Sitter.

Figure 1.1: The topological structure of anti-de sitter space

coordinate system

$$Z = L \cosh \rho \cos \tilde{t}, \quad X = L \cosh \rho \sin \tilde{t}, \quad Y = L \sinh \rho \quad (1.14)$$

now the metric becomes

$$ds^2 = L^2 (-\cosh^2 \rho d\tilde{t} + d\rho^2) \quad (1.15)$$

This coordinate (\tilde{t}, ρ) , is called global coordinates. Here we have one time-like direction. The \tilde{t} coordinate has periodicity 2π , so the time like is periodic. But we can unwrap the time-like direction, then consider space of AdS_2 space-time where $-\infty < \tilde{t} < \infty$. The AdS space-time in AdS/CFT is this covering space. AdS space-time can be described through different types of coordinate systems.

For static coordinate (\tilde{t}, \tilde{r}) \tilde{r} is defined by $\tilde{r} = \sinh \rho$ now the metric become

$$\frac{ds^2}{L^2} = -(\tilde{r}^2 + 1)d\tilde{t}^2 + \frac{d\tilde{r}^2}{\tilde{r}^2 + 1}$$

In conformal coordinate (\tilde{t}, θ) θ coordinate is defined by $\tan \theta = \sinh \rho$. θ has values from $-\frac{\pi}{2}$ to $\frac{\pi}{2}$. Metric is in the form

$$\frac{ds^2}{L^2} = \frac{1}{\cos^2 \theta} (-d\tilde{t}^2 + d\theta^2)$$

. The value at $\theta = \pm\frac{\pi}{2}$ is called AdS boundary. This boundary is located at $\tilde{r} \rightarrow \infty$ in static coordinate and $r \rightarrow \infty$ in Poincare coordinate.

In Poincare coordinates(t,r) coordinate can defined as $Z = \frac{Lr}{2}(-t^2 + \frac{1}{r^2} + 1)$, $X = Lrt$, $Y = \frac{Lr}{2}(-t^2 + \frac{1}{r^2} - 1)$ where $r > 0$ and t varies from $-\infty \rightarrow \infty$ then metric becomes

$$\frac{ds^2}{L^2} = -r^2 dt^2 + \frac{dr^2}{r^2}$$

Any space-time which can be conformally compactified to match the conformal structure of AdS is called asymptotically AdS space-time. Consider Einstein's equation in a vacuum with a cosmological constant Λ

$$R_{\mu\nu} - \frac{1}{2}Rg_{\mu\nu} + \Lambda g_{\mu\nu} = 0 \quad (1.16)$$

Here the Ricci scalar R can be written in terms of Λ ,

$$R = \frac{2d}{d-2}\Lambda \quad (1.17)$$

1.2 Black holes and thermodynamics

A black hole is a region of space-time with a strong gravitational field from which even light cannot escape. A body becomes a black hole when its mass is smaller than the gravitational radius $r_g = \frac{2GM}{c^2}$. Any black hole is characterized by the parameters like mass, angular momentum, and electric charge. The surface boundary of the black hole in space-time is called the event horizon. It is a light-like surface. Wheeler introduced the term black hole in 1967. Oppenheimer and Snyder, in 1931, described that the gravitational collapse of a massive star results in black holes. Nowadays, we are sure that black holes with stellar masses exist in many binaries in our galaxies. Also, supermassive black holes exist in the center of the galaxies. If the black hole mass is small, it decays over a shorter than the universe's age. Such black holes are known as primordial black holes. They are formed at a very early stage of universe evolution. In 1974 Hawking's findings were very unexpected. His finding was the instability of a vacuum in a very strong gravitational field of a black hole, such an object act as a source of ra-

diation. Also, it should show a thermal spectrum. These findings stimulate the study of understanding features of quantum effects in black holes. Grand Unified theory(GUT) unifies all three fundamental interactions at a higher energy scale of the order $10^{15} GeV$ except gravity. Quantum gravity theory is an attempt to unify all interactions together. A black hole is a macroscopically quantum mechanical system. So the study of black holes helps to connect quantum gravity theory.

The quest for the quantum nature of gravity exploiting the properties of black holes has been active for a long time. In the early 1970s, Hawking proved that the area of the event horizon would never decrease under any physical processes (Bekenstein [1973], Hawking [1975]). Considering this property as a characteristic of thermodynamic entropy, Bekenstein argued that black holes could be attributed to entropy, which is related to the event horizon area. This was the first hint which indicated that black holes behave like thermodynamic objects. Soon, four laws were established for a general black hole in stationary, asymptotically flat space-time, where the first law of thermodynamics features a relation between the infinitesimal changes in mass, charge, the angular momentum of a black hole and the change of its horizon area. These infinitesimal changes are in the space of stationary black hole solutions, and this relation is referred to as the stationary state version of the first law.

Later the tools of thermodynamics, which are used extensively in an ordinary system, are also applied to black hole systems. Accordingly, further studies in black hole thermodynamics showed that thermally stable black holes exist only in anti-de Sitter (AdS) space-time. The thermal properties of black holes in AdS space differ significantly from their asymptotically flat counterpart. The AdS space acts as a thermal cavity and a black hole can exist in a stable equilibrium with radiation. A milestone in this direction was provided by Hawking and Page in the 1980s. They found a phase transition in Schwarzschild AdS black hole known as Hawking Page transition, which is between radiation and large black hole phases. Later, the inconsistency between the first law and the Smarr relation led to the identification of the cosmological constant as the pressure term in the thermodynamics studies of a black hole. Subsequently, it was observed that the P- V criticality of charged AdS black holes shows a resemblance

with that of the Van der Waals (vdW) fluid. The thermodynamics of AdS black holes in the extended phase space with a PdV term exhibits a first-order phase transition similar to the liquid/gas transition in vdW fluid. In AdS black holes, the transition is between a small black hole (SBH) and a large black hole (LBH) phases (Hawking and Page 1983a). These thermal properties find new meaning in light of AdS/CFT correspondence which relates classical gravitational theories to strongly coupled conformal field theory on its boundary.

From the statistical point of view, the thermodynamics of a system always demands a microscopic description. Even though the thermodynamics of black holes is widely studied, understanding the microscopic structure of the black hole was a challenging problem. In this regard, the Ruppeiner geometry approach (Ruppeiner 1995a) is a handy tool that extracts certain aspects of microscopic information from macroscopic properties. In this approach, a metric is defined on the thermodynamic state-space, which measures the distance between nearby fluctuating states. The Ruppeiner curvature scalar (R), which can be calculated from the metric, provides crucial details about phase transitions and the nature of interactions in the microstructure of the system under consideration. The important information obtained from this construction is the nature of the microstructure interaction, the strength of the interaction, and critical behaviour. The sign of curvature scalar specifies the type of interactions. For a noninteracting system like an ideal gas, the curvature scalar vanishes. In an interacting system, the positive and negative values of the scalar curvature represent repulsive and attractive interactions, respectively. Also, the magnitude of the Ruppeiner curvature scalar measures the strength of interaction. An added feature of the construction is that, for the system with critical behavior, the curvature scalar shows divergence at the critical point. The singularity of the curvature scalar is related to the singular nature of response functions near the critical point. The Ruppeiner geometric method was found effective in describing the microstructure details of a variety of known systems in conventional thermodynamics. This success eventually led to the application of the Ruppeiner geometry method to a black hole system.

A variety of approaches have been presented within the framework of Ruppeiner

geometry to understand the microstructure of black holes. Recently, it was proposed that the thermodynamic curvature scalar can be constructed by taking the pressure and volume as fluctuating variables, and the curvature scalar is normalized by adiabatic compressibility(Dehyadegari et al. 2020). This construction makes an observation that strong repulsive interactions dominate among the microstructures of small black holes where the thermodynamic curvature diverges to positive infinity. In our work, we focus on the microscopic interactions of massive dRGT black holes using the curvature scalar normalized via adiabatic compressibility.

An innovative move to ponder the black hole phase transition is by investigating Gibbs free energy landscape together with stochastic Fokker-Planck equation(Wei and Liu 2015a)(Wei et al. 2019a). That helps one to analyze the kinetics and dynamics of the transition process. The extremum in the off-shell Gibbs free energy curves are identified as the stable and unstable states of the black hole. The transition point is identified from symmetric double wells in the free energy. Nevertheless, in the ensemble perspective, two stable phases separated by a finite-height barrier of the intermediate phase can transit into another stable state due to thermal fluctuations. The dynamics of this probabilistic evolution are governed by the Fokker-Planck equation. Deploying the free energy landscape, in our work we have studied the dRGT massive black hole in an anti-de Sitter background.

Apart from the stationary state version of the first law of black hole thermodynamics, there exists a “physical process” version(PPFL). Black holes, as found in nature, are far from being appropriately described by global stationary black hole solutions. They evolve due to falling matter, and the area of the horizon changes with time. Unlike the infinitesimal change in the stationary state version of the first law, which is a change in the space of solutions, in the physical process” version, there is an evolution in time due to the process of matter falling into the black hole. Consequently, a different version of the first law holds and appropriately describes this situation. In this version, one relates the time evolution of the entropy to the matter influx across the horizon(Hawking and Hartle 1972, Carter 1979, Wald 1995b). The physical process version of the first law can be obtained for bifurcating Killing horizons with certain assumptions. Especially,

one has to restrict to the situations where the horizon evolution is quasi-stationary, under perturbations. We revisit the analysis of this assumption considering the horizon perturbations of the Rindler horizon by a spherically symmetric object.

1.3 Massive gravity

Even though recent observations from LIGO/VIRGO collaborations confirm the predictions of the general theory of relativity, there are enough reasons to look beyond Einstein's theory of gravity. There is no doubt that Einstein's general relativity gives an accurate model for gravitational interactions at a low energy scale, where the quantum effect does not come to play. But when energy increases, quantum effects start to dominate. We know the general theory of relativity is a purely classical theory of gravity. It does not account for the impact of quantum mechanics. So it is impossible to explain what was going on at energy thig as the Planck energy or at distances as small as the Planck length. On the observational side, the mass content expected from general theory relativity exceeds the mass estimated from astronomical observations. It is believed that such discrepancies can be accounted for by considering the presence of an unknown form of mass known as dark matter. Also, the presence of dark matter is proven through many observations of the motions of galaxies and gravitational lensing. So the general relativity prediction fails and hence the gravity laws should be modified. Another discrepancy is about the expansion of the universe, which accelerated expansion. It is confirmed by the measurements done on cosmic microwave background radiation (CMBR). This accelerated expansion of the universe demands a positive cosmological constant to exist. The measured value of the cosmological constant is many orders of magnitude smaller than the estimated value in quantum field theoretic calculations. This difference can not be incorporated into Einstein's general relativity. These issues related to general relativity point out the incompleteness in our understanding of either matter or gravity or both. So, problems like the cosmological constant problem, the hierarchy problem, and the accelerated expansion demand a modification to the General theory of relativity. In the history of modified theories of gravity, many models were proposed, which include Lovelock gravity, Einstein-Yang-Mills theory, $f(R)$ theories, Massive gravity, Hořava gravity(Capozziello and Laurentis 2011, Clifton et al. 2012).

The general theory of relativity is a unique massless spin two-field theory. Among the several modified versions, massive gravity theories explain the universe's accelerated expansion without introducing a cosmological constant or dark energy. Massive gravity theories have a long and remarkable history. The initial studies were carried out by Fierz and Pauli in 1939 (Fierz and Pauli 1939). The proposed theory was linear and ghost-free but did not reduce to general relativity in the massless limit. Non-linear modifications of Fierz and Pauli's theory lead to "Boulware-Deser" ghost instability (Boulware and Deser 1972). Later, de Rham, Gabadadze, and Tolley (dRGT) came up with a special class of non-linear massive gravity theory, which is "Boulware-Deser" ghost free (de Rham et al. 2011). Further, the thermodynamics of the black holes in massive gravity were widely investigated (Cai et al. 2015, Xu et al. 2015, Hendi et al. 2017a, 2016, Mirza and Sherkatghanad 2014, Fernando 2016, Ning and Liu 2016).

1.4 Objectives of the present research work

The main objective of this thesis is the study of "Properties of Rindler Horizon and Some Aspects of Black Hole Chemistry in Massive Gravity". The work specifically focuses on:

- Study the phase transitions in the dRGT massive black hole in an anti-de Sitter space-time by analysing Hawking temperature, mass, entropy, heat capacity and Gibbs free energy in the extended phase space.
- Probe the microstructure of the dRGT massive black hole in an anti-de Sitter background in an extended phase space with pressure and volume taken as fluctuation variables.
- Analyse the dynamics and kinetics of phase transition via Gibbs free energy landscape aided with stochastic Fokker-Planck equation.
- Investigate physical process version of first law (PPFL) and the entropy change of Rindler horizons.
- Explore the first law in PPFL version of thermodynamics and its modification in the presence of positive cosmological constant.

1.5 Organization of the thesis

The thesis is organised as follows:

Chapter 1 gives a brief introduction to black holes, AdS space-times and massive gravity. The scope and objectives of the present research work, together with the organisation of the thesis, are also included at the end of this chapter.

Chapter 2 presents a brief introduction to black hole chemistry and VdW like phase transition of RN AdS black holes.

In **Chapter 3**, Thermodynamic geometry and microstructure of black holes are discussed. Microstructure of the dRGT massive black hole in an anti-de Sitter background in an extended phase space with pressure and volume taken as fluctuation variables are discussed.

In **Chapter 4**, a thermodynamic study in the massive gravity theory can be extended further by considering the dynamics of phase transition. The dynamical properties of the stable small-large black hole phase transitions in dRGT non-linear massive gravity theory are studied and discussed on the underlying free energy landscape.

In **Chapter 5**, we concentrate on the characteristics and features of the first law of black hole thermodynamics. The physical process version of the first law can be obtained for bifurcate-Killing horizons with certain assumptions. We discussed the analysis of this assumption considering the horizon perturbations of the Rindler horizon by a spherically symmetric object.

Chapter 6 summarises the important findings of the present research work by highlighting the remarkable results of the thesis along with conclusions.

Chapter 2

An overview of black hole chemistry

Thermodynamics is one of the classical theory in physics. It developed through the work of Carnot, Clausius, Joule, Kelvin and many others. Thermodynamics is an empirical science which describes the macroscopic behaviour of systems. The fundamental principles of thermodynamics are stated in three laws. The zeroth law establishes temperature as a fundamental property of matter. It states that if two bodies are in separately thermal equilibrium with the third body, then they are also in thermal equilibrium with each other. The first law assures the principle of conservation of energy, and the second law introduces the concept of entropy. The key highlight of thermodynamics is that the microscopic details are not necessary to explore the macroscopic behaviour of systems.

Black holes are important objects in physics. It is the region of spacetime where a large amount of mass is concentrated with strong gravity, and nothing can escape from it. It is one of the best candidates to study the theory of quantum gravity because where gravity and quantum mechanics hold simultaneously. The understanding of the thermodynamic behaviour of black holes using the concepts of chemistry will be discussed here. To establish the complete correspondence between the thermodynamics of an ordinary system and that of black holes, the recent literature suggests that identification of the mass of a black hole, cosmological constant, surface gravity, and horizon area of a black hole with the chemical enthalpy, pressure, temperature, and entropy of an ordinary thermodynamic system respectively. Consequently, the thermodynamics of black

holes behave analogously to a variety of everyday phenomena.

2.1 Black hole chemistry

The subject of black hole physics serves as a bridge between gravity and quantum mechanics. Taking into account the quantum mechanics at the black hole horizon, Stephen Hawking found that the black hole emits radiation proportional to its surface gravity (Hawking 1975). Prior to the Hawking's work, Jacob Bekenstein had suggested that in order to have consistent second law, the entropy of the black hole should depend on the area of a black hole (Bekenstein 1973). This enables one to consider a black hole as a thermodynamic object. Hence, in parallel with ordinary thermodynamics, four laws of black hole mechanics were proposed (Bardeen et al. 1973b). Later studies in black hole thermodynamics showed that the thermally stable black hole exists only in anti-de Sitter (AdS) space. A milestone in this direction was provided by Hawking and Page in the 1980s. They found that a phase transition, the so-called Hawking-Page phase transition, is exhibited by Schwarzschild- AdS black hole, which is a transition between radiation and large black hole phase (Hawking and Page 1983a).

Since then, the thermodynamic phase transitions in AdS black holes have been extensively studied. Later, the inconsistency between the first law and the Smarr relation leads to identifying the cosmological constant as the pressure term in thermodynamics (Kastor et al. 2009a). Subsequently, with the pressure and volume term, it was observed that the $P - V$ criticality of charged AdS black holes shows a resemblance with that of the van der Waals (vdW) fluid (Kubiznak and Mann 2012). The thermodynamics of AdS black holes in this extended phase space with a PdV term exhibits a first-order phase transition between a small black hole (SBH) phase and a large black hole (LBH) phase. Also, various other thermodynamic features of AdS black holes analogous to the van der Waals fluid, like the Joule-Thomson effect and heat engine, were observed (Ökcü and Aydiner 2017, Johnson 2014). This was the beginning of a new domain in black hole research called 'black hole chemistry'.

An arbitrary black hole can be treated as a thermodynamic system. A stationary black hole in an equilibrium state is completely described by three parameters mass(M), angular momentum (J) and charge(Q). Also, the area of a black hole is written as the

function of these parameters,

$$A = 4\pi \left(2M^2 - Q^2 + 2M\sqrt{M^2 - Q^2 - \frac{J^2}{M^2}} \right) \quad (2.1)$$

from this internal energy of a black hole in terms of three parameters can be obtained

$$M = M(A, J, Q) = \sqrt{\frac{\pi(Q^2 + \frac{A}{4\pi})^2 + 4J^2}{A}} \quad (2.2)$$

The differential of internal energy is written as the slight change of area(dA), angular momentum (dJ) and electric charge (dQ),

$$dM = \frac{\kappa}{8\pi}dA + \Omega dJ + \Phi dQ \quad (2.3)$$

where $\kappa = \frac{4\pi\sqrt{M^2 - Q^2 - \frac{J^2}{M^2}}}{A}$ is surface gravity. $\Omega = \frac{4\pi J}{MA}$ is angular velocity. $\Phi = \frac{4\pi Qr_+}{A}$ is electric potential of black hole. This equation is very similar to the first law of classical thermodynamics. Hawking's remarkable finding of radiation of stationary black hole gives the relation between temperature and surface gravity.

$$T = \frac{\hbar\kappa}{2\pi ck} \quad (2.4)$$

Where c is the speed of light and k is the Boltzmann constant. Bekenstein- Hawking entropy relation relates the area of a black hole with entropy

$$S = \frac{A}{4l_p^2} \quad (2.5)$$

where $l_p^2 = \frac{\hbar G}{c^3}$ is plank length. These arguments strongly support taking an analogy between black hole physics and thermodynamics.

2.2 Four laws of black hole thermodynamics

Bardeen, Carter and Hawking 1973 formulated four laws of black hole physics, which are similar to four laws in thermodynamics [Bardeen et al. \(1973a\)](#).

1. **Zeroth law:** The surface gravity κ is constant over the event horizon of a stationary black hole. As similar to the zeroth law in thermodynamics, where temperature is constant for a thermodynamic equilibrium state.
2. **First law:** First law of thermodynamics features a relation between the infinitesimal changes in mass, charge, angular momentum of a black hole and the change of its horizon area. These infinitesimal changes are in the space of stationary black hole solutions

$$dM = \frac{\kappa}{8\pi G} dA + \Omega dJ + \Phi dQ \quad (2.6)$$

Where κ is surface gravity, M is mass, Q is the charge, A is event horizon area, J is angular momentum, Φ is electric potential.

3. **Second law** (Hawking's Area theorem): The area of the event horizon of a black hole never decreases i.e. $dA \geq 0$
4. **Third law:** it is never possible to reduce the surface gravity κ to zero by a finite number of processes. In other words, it is difficult to form an extremal black hole.

2.3 Smarr relation and black holes

Smarr relation is the relation which connects the black hole parameters. Eulers theorem provides a bridge between the first law of black hole mechanics and the Smarr formula for a stationary black hole. It states that if a function $f(x, y)$ takes the scaling relation, $f(\alpha^p x, \alpha^q y) = \alpha^r f(x, y)$, then it should satisfy the relation

$$r(f(x, y)) = p \left(\frac{\partial f}{\partial x} \right) x + q \left(\frac{\partial f}{\partial y} \right) y. \quad (2.7)$$

Even though the correspondence between the thermodynamics of a physical system and a black hole exists, they were not comparable for the first law. We know the first law of thermodynamics as,

$$dE = TdS - PdV + \text{work term} \quad (2.8)$$

and black hole first law can be written as,

$$dM = \frac{\kappa}{8\pi}dA + \Omega dJ + \Phi dQ, \quad (2.9)$$

where ΩdJ , ΦdQ are refers to work term and here we chosen $c = \hbar = k = 1$. By comparing these two Eq. [2.8](#) and [2.9](#), we can easily conclude that there is no counterpart term for pressure and volume in black hole thermodynamics. For d-dimensional Schwarzschild AdS black hole solution([Kastor 2008](#)),

$$ds^2 = -f(r)dt^2 + \frac{dr^2}{f(r)} + r^2 d\Omega_{d-2}^2 \quad (2.10)$$

where

$$f(r) = 1 - \frac{1}{d-2} \frac{16\pi}{\lambda_{d-2}} \frac{M}{r^{d-3}} - \frac{2\Lambda}{(d-1)(d-2)} \quad (2.11)$$

$d\Omega_{d-2}^2$ is the line element of unit sphere S^d with volume $\lambda_{d-2} = \frac{2\pi^{\frac{d-1}{2}}}{\Gamma(\frac{d-1}{2})}$. The Smarr relation for such a black hole can be derived using dimensional analysis and Euler's theorem. For a d-dimensional black hole, mass $M(A, J)$ is the function of the area of event horizon (A) and angular momentum (J). From dimensional analysis,

$$M \propto L^{d-3}, \quad A \propto L^{d-2}, \quad J \propto L^{d-2}. \quad (2.12)$$

Under the scaling $L \rightarrow \alpha L$

$$M \rightarrow \alpha^{d-3}M, \quad A \rightarrow \alpha^{d-2}A, \quad J \rightarrow \alpha^{d-2}J. \quad (2.13)$$

Now the relation using the scaling relation $M(A, J)$ can be written as

$$\alpha^{d-3}M = M(\alpha^{d-2}A, \alpha^{d-2}J). \quad (2.14)$$

Differentiating with respect to α gives

$$(d-3)\alpha^{d-4}M = (d-2)\frac{\partial M}{\partial(\alpha^{d-2}A)}\alpha^{d-3}A + (d-2)\frac{\partial M}{\partial(\alpha^{d-2}J)}\alpha^{d-3}J, \quad (2.15)$$

by setting $\alpha = 1$, we will have Smarr formula,

$$(d-3)M = (d-2)TA + (d-2)\Omega J. \quad (2.16)$$

Where $T = \frac{\partial M}{\partial S} = 4G \frac{\partial M}{\partial A}$ and $\Omega = \frac{\partial M}{\partial J}$. Thus Smarr relation for a 4-d case can be written as,

$$M = \frac{\kappa}{4\pi G}A + 2\Omega J. \quad (2.17)$$

In charged Kerr solution, we see that M is a homogeneous function horizon area A, angular momentum J and charge Q.

$$M = M(A, J, Q^2) \quad (2.18)$$

$$M = \left(\frac{A}{16\pi} + \frac{4\pi J^2}{A} + \frac{Q^2}{2} + \frac{\pi Q^4}{A} \right)^{1/2} \quad (2.19)$$

Now using scaling relation, we write,

$$\alpha M = M(\alpha^2 A, \alpha^2 J, \alpha^2 Q^2) \quad (2.20)$$

Then, Euler's theorem tells,

$$M = 2 \frac{\partial M}{\partial A} A + 2 \frac{\partial M}{\partial J} J + \frac{\partial M}{\partial Q} Q. \quad (2.21)$$

From equation [2.17](#) L.H.S can be replaced,

$$\frac{\kappa}{4\pi G}A + 2\Omega J + \phi Q = 2 \frac{\partial M}{\partial A} A + 2 \frac{\partial M}{\partial J} J + \frac{\partial M}{\partial Q} Q. \quad (2.22)$$

Comparing the coefficients, one gets ie,

$$2A \left\{ \frac{\kappa}{8\pi G} - \frac{\partial M}{\partial A} \right\} + 2J \left\{ \Omega - \frac{\partial M}{\partial J} \right\} + Q \left\{ \phi - \frac{\partial M}{\partial Q} \right\} = 0. \quad (2.23)$$

$$\frac{\partial M}{\partial A} = \frac{\kappa}{8\pi G}; \quad \frac{\partial M}{\partial J} = \Omega; \quad \frac{\partial M}{\partial Q} = \phi \quad (2.24)$$

Differential of $M(A, J, Q)$ can be obtain,

$$dM(A, J, Q) = \frac{\partial M}{\partial A} dA + \frac{\partial M}{\partial J} dJ + \frac{\partial M}{\partial Q} dQ \quad (2.25)$$

Using Eq. (2.24), we obtain differential mass relation,

$$dM = \frac{\kappa}{8\pi G} dA + \Omega dJ + \phi dQ \quad (2.26)$$

This is the differential mass formula, which is commonly known as the first law of black hole thermodynamics, similar to the first law in classical thermodynamics given by,

$$dE = T dS + \text{work terms.} \quad (2.27)$$

Analysing various terms in the first law, one can easily identify the mass (M) of the black hole with energy (E) in classical thermodynamics. Similarly, horizon area (A) and surface gravity (κ) are identified with entropy (S) and temperature (T) in ordinary thermodynamics, respectively. The remaining terms in the first law (ΩJ and ϕQ) are identified as work terms in thermodynamics.

$$\begin{aligned} E &\longleftrightarrow M \\ S &\longleftrightarrow \frac{A}{4G} \\ T &\longleftrightarrow \frac{\kappa}{2\pi} \end{aligned}$$

2.4 Smarr relation in AdS black holes

Smarr formula does not remain the same in spacetime with the cosmological constant. As we know from gravitational action for AdS black holes,

$$S = \frac{1}{8\pi G} \int d^d x \sqrt{-g} (R - 2\Lambda), \quad (2.28)$$

cosmological constant Λ has the dimension of $(length)^{-2}$. The quantity M is a function of horizon area(A) and cosmological constant Λ . The quantities scale as

$$M \propto L^{d-3}, \quad A \propto L^{d-2}, \quad \Lambda \propto L^{-2}. \quad (2.29)$$

Using the Eulers theorem and dimensional analysis, we can write the mass of a black hole, which satisfies the Smarr relation by,

$$(d-3)M = (d-2) \left(\frac{\partial M}{\partial A} \right) A - 2 \left(\frac{\partial M}{\partial \Lambda} \right) \Lambda \quad (2.30)$$

Here, by setting $\Lambda = 0$ and $\frac{\partial M}{\partial A} = \frac{\kappa}{8\pi G}$ gives well-known Smarr formula for an asymptotically flat black hole. From the Komar integral formalism, we get the Smarr formula for AdS/dS (Appendix [A](#)) as,

$$(d-3)M = (d-2) \frac{\kappa A}{8\pi G} - 2 \frac{\Theta}{8\pi G} \Lambda \quad (2.31)$$

Calculation of Θ for 4-d Schwarzschild AdS black holes found to be,

$$\Theta = -\frac{4\pi r_h^3}{3} = -V \quad (2.32)$$

which is the volume of a 3-dimensional sphere. Comparing two different version of Smarr relation (Eq. [2.30](#) and [2.31](#)) we get,

$$(d-2) \left(\frac{\partial M}{\partial A} \right) A - 2 \left(\frac{\partial M}{\partial \Lambda} \right) \Lambda = (d-2) \frac{\kappa A}{8\pi G} - 2 \frac{\Theta}{8\pi G} \Lambda \quad (2.33)$$

This helps us to identify $\frac{\partial M}{\partial A} = \frac{\kappa}{8\pi G}$ and $\frac{\partial M}{\partial \Lambda} = \frac{\Theta}{8\pi G}$. Differentiation of Smarr relation gives the first law of black hole thermodynamics in this new extended phase space,

$$dM = \frac{\kappa}{8\pi G} dA + \left(\frac{\partial M}{\partial \Lambda} \right) d\Lambda \quad (2.34)$$

The result of Θ equal to geometrical volume led to the idea of considering the conjugate quantity Λ as the thermodynamic pressure (Teitelboim 1985).

$$P = -\frac{\Lambda}{8\pi} \quad (2.35)$$

The second term in the Smarr relation and the first law fills the obvious omission of PV term in black hole thermodynamics. The addition of $P - V$ term in the phase space modifies the Smarr relation and first law.

$$M = 2(TS + \Omega J - VP) + \phi Q \quad (2.36)$$

$$dM = TdS + VdP + \phi dQ + \Omega dJ \quad (2.37)$$

where J and Ω are angular momenta and angular velocity, respectively. Similarly, Q and ϕ are electromagnetic charges and potential, respectively. This version of black hole thermodynamics is popularly known as ‘extended phase space’. The immediate implication of $P - V$ addition is that the mass is replaced with enthalpy rather than internal energy.

2.5 P-V criticality

Since thermodynamically stable black holes exist only in AdS space-time, thermodynamical studies of the black hole were mainly focused on asymptotically AdS black holes. The thermodynamics in the extended phase space with a PdV term exhibits a first-order phase transition similar to the liquid/gas transition in vdW fluid (Kubizňák and Mann 2012). In AdS black holes, the transition is between a small black hole (SBH) and a large black hole (LBH) phase. Also, a variety of other thermodynamic properties of vdW fluids, like the Joule-Thomson effect and heat engine, were found in AdS black holes (Ökcü and Aydiner 2017, Johnson 2014).

2.5.1 Van der Waals fluid

The ideal gas equation $PV = RT$ was modified by Van der Waals in 1879 with the consideration of intermolecular attraction and the finite size of a molecule. He added

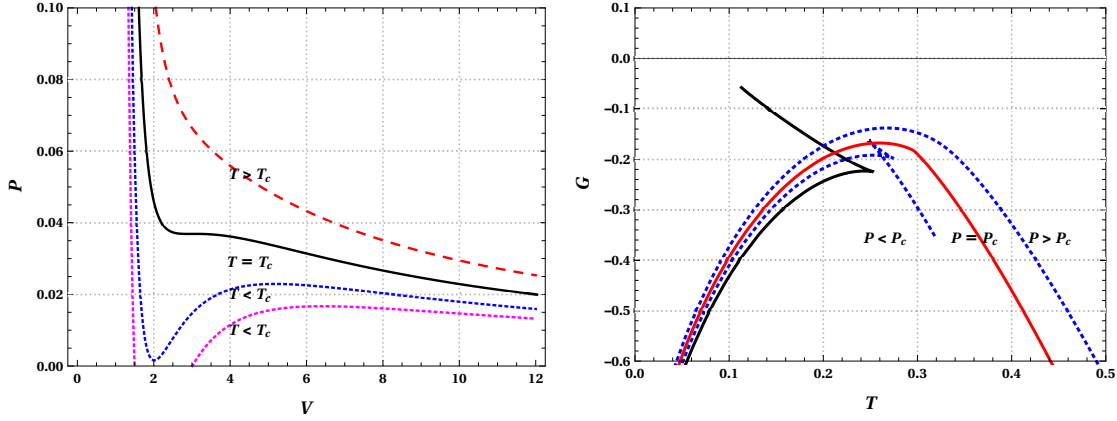


Figure 2.1: P-V isotherms and Gibbs free energy is plotted against temperature for VdW gas

some correction terms for pressure and volume and wrote a new equation state for a real gas.

$$\left(P + \frac{a}{V^2}\right)(V - b) = RT \quad (2.38)$$

$$P = \frac{RT}{(V - b)} - \frac{a}{V^2} \quad (2.39)$$

where a and b are Van der Waals constants. The pressure-volume (P-V) isotherms are plotted for various temperatures using the vdW equation of state. The plot is shown in figure 2.1. From the plot, we can determine the critical point using the condition, $\frac{dP}{dV} = 0$ and $\frac{d^2P}{dV^2} = 0$. Using this condition, the critical parameters for VdW gas are determined. The critical volume $V_c = 3b$, temperature $T_c = \frac{8a}{27bR}$ and the pressure $P_c = \frac{a}{27b^2}$. The universal value $\frac{P_c V_c}{kT_c} = \frac{3}{8}$ predicted for all fluids. Below the critical point, a phase change occurs between a liquid and gaseous phase. More signatures about first-order liquid/gas phase transition can be obtained from Gibbs free energy plots in the G-T plane. A swallowtail behaviour appears in the plots below the critical point, as shown in figure 2.1.

2.5.2 Phase transitions in charged AdS black hole

The metric of the charged RN-AdS black hole is given by,

$$ds^2 = -f(r)dt^2 + \frac{dr^2}{f(r)} + r^2 d\Omega^2 \quad (2.40)$$

where $d\Omega^2$ is the standard line element on a two dimensional unit sphere and,

$$f(r) = 1 - \frac{2M}{r} + \frac{Q^2}{r^2} + \frac{r^2}{l^2}. \quad (2.41)$$

The mass function $M(r)$ gives the distribution of black hole mass as,

$$M(r) = \frac{r^3}{2l^2} + \frac{r}{2} + \frac{1}{2r}. \quad (2.42)$$

In the extended phase space, the cosmological constant Λ is treated as the thermodynamic pressure as $P = -\Lambda/8\pi$, and the volume as the conjugate quantity. With this identification, one can interpret the mass of an AdS black hole as the enthalpy of the spacetime (Kastor et al. 2009b). The Hawking temperature of the black hole is associated with the surface gravity $T = \frac{\kappa}{2\pi}$, with $\kappa = \frac{f'(r_+)}{2}$,

$$T = \frac{f'(r_+)}{4\pi} = \frac{r}{2\pi l^2} + \frac{M}{2\pi r^2} - \frac{1}{2\pi r^3} \quad (2.43)$$

The entropy of the RN-AdS black hole is simply the area of the event horizon, $S = \pi r^2$.

The equation of state is thus obtained from Eqn. 2.43 as,

$$P = \frac{1}{8\pi r^4} - \frac{1}{8\pi r^2} + \frac{T}{2r}. \quad (2.44)$$

With the specific volume $v = 2r_+$, the equation has the proper dimensions, and then we have the physical equation of state,

$$P = \frac{T}{v} + \frac{2}{\pi v^4} - \frac{1}{2\pi v^2}. \quad (2.45)$$

Using the above expressions for pressure Eqn. 2.45 and temperature Eqn. 2.43, we obtain the isotherms in the $P - v$ plane. It is clear from the figures 2.2 and 2.3 that the black hole under consideration exhibits a van der Waals (vdW) like critical behaviour. The $P - v$ isotherms in figure 2.2 have an oscillatory behaviour below a certain critical temperature T_c . The positive slope regions in the curve below T_c , correspond to an unstable state of the system. And the negative slope region indicates stable phase of

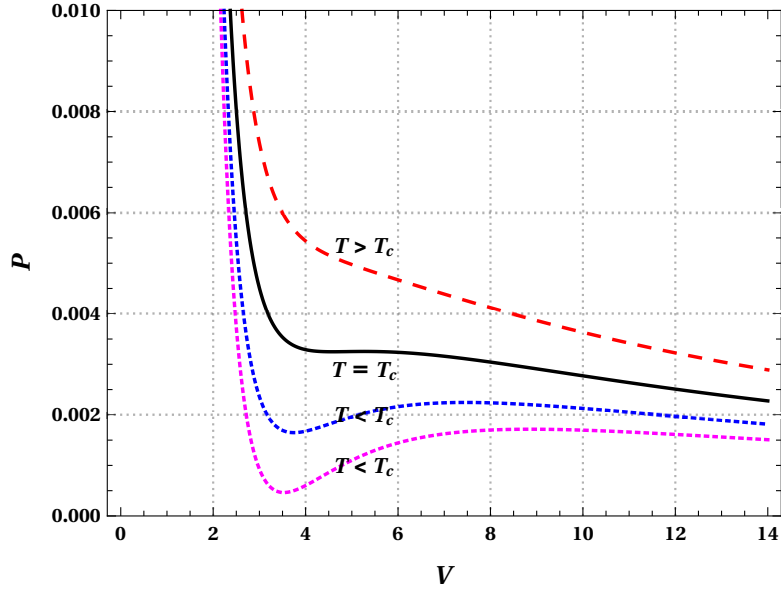


Figure 2.2: P - v isotherms for charged AdS Black holes. Took $v = 2r_+$ for AdS black holes

the system. This slope disappears at critical point $T = T_c$, which is an inflection point. Above the critical temperature, the isotherms moves towards the ideal gas behaviour. It

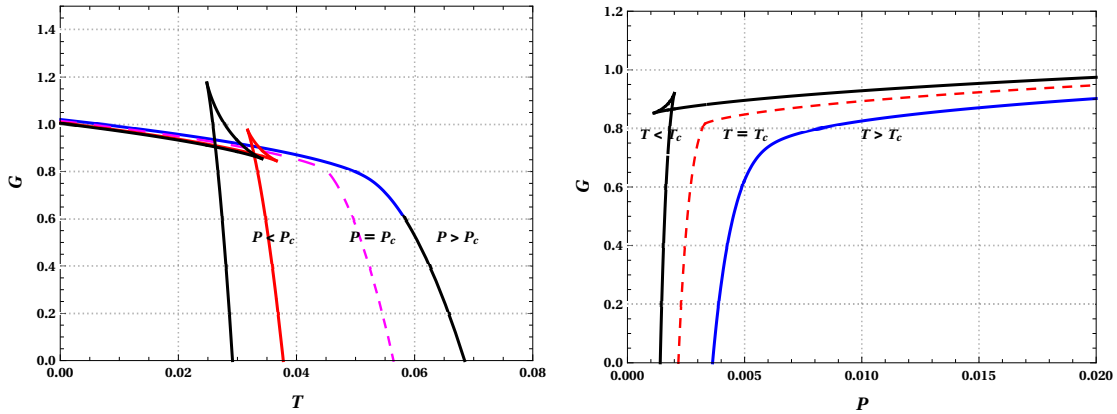


Figure 2.3: Gibbs free energy is plotted against pressure and temperature for charged AdS Black holes

is interesting that van der Waals gas and AdS black holes have similar phase structures. The Gibbs free energy $G = U - TS$ together with $P - v$ isotherms are important to study the critical phenomenon during a phase transition. Phases in a black hole are named as *Small black hole phase (SBH)* and *Large black hole phase (LBH)* (Kubizňák and Mann 2012). Further, a coexistence curve is obtained in figure 2.4, along which temperature

and Gibbs free energy coincide for both phases SBH and LBH. On the coexistence line, both SBH and LBH phases coexist, and the line terminates at a critical point. The

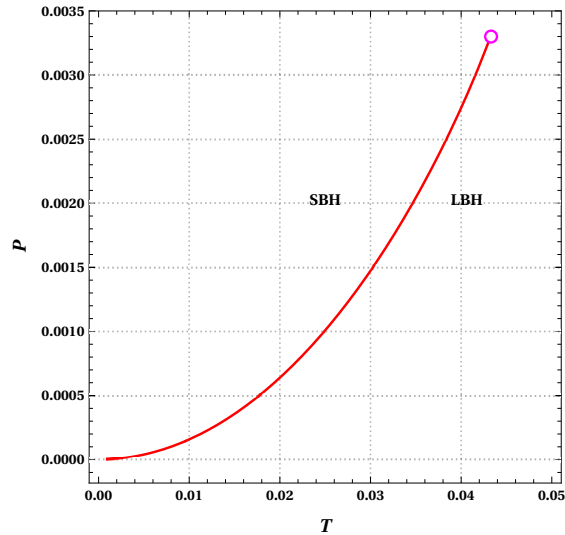


Figure 2.4: Coexistent curve for Charged Black holes. Critical points are labelled with a circle.

singular behaviour around the critical point is characterised by four numbers known as critical exponents $\alpha, \beta, \gamma, \delta$. All the critical exponents of SBH-LBH phase transition exactly match with that of van der Waals fluid and belong to the same universality class. Critical values are

2.6 Discussions

Black holes are, hopefully, an excellent tool that could be used to unravel the nature of gravity at the quantum mechanical level. The well-established connection between black holes and thermodynamics has laid a strong foundation for this prospect. Understanding gravity from the viewpoint of thermodynamics and statistical physics has made a great deal of advancements in recent years. One of the profound results of this prospect is the analogy between the van der Waal liquid-gas system and a charged black hole in AdS space. This formulation was achieved by treating the cosmological constant as thermodynamic pressure in the extended phase space. Subsequently, a gear deal of thermodynamics was studied in asymptotically AdS black holes resembling a first-order vdW phase structure.

Chapter 3

Ruppeiner geometry and interacting microstructures of black holes in dRGT massive gravity

3.1 Introduction

A variety of approaches have been presented within the framework of Ruppeiner geometry to understand the microstructure of black holes (Wei and Liu 2015b, Wei et al. 2019b, Xu et al. 2020b, Miao and Xu 2018, Xu 2020, Xu et al. 2020a, Ghosh and Bhamidipati 2020b,a, Yerra and Bhamidipati 2020b, Wu et al. 2021). Recently, it was proposed that the thermodynamic curvature scalar can be constructed by taking the pressure and volume as fluctuating variables, and the curvature scalar is normalized by adiabatic compressibility (Dehyadegari et al. 2020). This construction makes an observation that strong repulsive interactions dominate among the microstructures of small black holes where the thermodynamic curvature diverges to positive infinity. Further, this method has been successfully applied to the Gauss-Bonnet AdS black hole spacetime (Naveena Kumara et al. 2020). In this chapter, we focus on the microscopic interactions of massive dRGT black holes using the curvature scalar normalized via adiabatic compressibility.

The van der Waals like feature of dRGT massive gravity black holes and other ap-

plications such as triple point, Reentrant phase transitions, heat engines, and throttling process were also studied (Zou et al. 2017, Liu et al. 2020, Hendi et al. 2018, Yerra and Bhamidipati 2020a, Lan 2019). In addition, several works to probe the microstructure were also studied using various thermodynamic-geometry approaches (Chabab et al. 2019, Wu et al. 2021, Yerra and Bhamidipati 2020b).

3.2 Thermodynamics of black holes in massive gravity

In this section, we discuss the spacetime and thermodynamic structure of black holes in massive gravity theory. Here we consider dRGT non-linear massive gravity theory. In four-dimensional AdS space, the action for the Einstein-dRGT gravity coupled to a non-linear electromagnetic field reads as

$$S = \int d^4x \sqrt{-g} \left[\frac{1}{16\pi} \left[R + \frac{6}{l^2} + m^2 \sum_{i=1}^4 c_i \mathcal{U}_i(g, f) \right] - \frac{1}{4\pi} F_{\mu\nu} F^{\mu\nu} \right], \quad (3.1)$$

where $F_{\mu\nu} = \partial_\mu A_\nu - \partial_\nu A_\mu$ is the electromagnetic field tensor with vector potential A_μ , l is AdS radius, m is related to the graviton mass, and c_i are coupling parameters. Further, $f_{\mu\nu}$ is a symmetric tensor as reference metric coupled to the space-time metric $g_{\mu\nu}$. Graviton interaction terms are represented by symmetric polynomials \mathcal{U}_i , and are obtained from a 4×4 matrix $\mathcal{K}_\nu^\mu = \sqrt{g^{\mu\alpha} f_{\nu\alpha}}$, which have the following forms,

$$\begin{aligned} \mathcal{U}_1 &= [\mathcal{K}] \\ \mathcal{U}_2 &= [\mathcal{K}]^2 - [\mathcal{K}^2] \\ \mathcal{U}_3 &= [\mathcal{K}]^3 - 3[\mathcal{K}^2][\mathcal{K}] + 2[\mathcal{K}^3] \\ \mathcal{U}_4 &= [\mathcal{K}]^4 - 6[\mathcal{K}^2][\mathcal{K}]^2 + 8[\mathcal{K}^3][\mathcal{K}] + 3[\mathcal{K}^2]^2 - 6[\mathcal{K}^4] \end{aligned}$$

The solution to the above action for various horizon topologies are given by (Hendi et al. 2017b, Cai et al. 2015),

$$ds^2 = -f(r)dt^2 + \frac{1}{f(r)}dr^2 + r^2 h_{ij} dx_i dx_j, \quad (3.2)$$

where h_{ij} is the metric for two dimensional hypersurface. The topological parameter (k) can take values 0, -1 or 1, representing planar, hyperbolic, and spherical topology, respectively. With the choice of reference metric $f_{\mu\nu} = \text{diag}(0, 0, c_0^2 h_{ij})$, the values of \mathcal{U}_i becomes $\mathcal{U}_1 = \frac{2c_0}{r}$, $\mathcal{U}_2 = \frac{2c_0^2}{r^2}$, $\mathcal{U}_3 = \mathcal{U}_4 = 0$. Now, the metric function reduces to,

$$f(r) = k - \frac{m_0}{r} - \frac{\Lambda r^2}{3} + \frac{q^2}{r^2} + m^2 \left(\frac{c_0 c_1}{2} r + c_0^2 c_2 \right), \quad (3.3)$$

where integration constants m_0 and q are related to black hole mass and charge, respectively. m is the parameter for graviton mass, and in the limiting case of $m = 0$ the spacetime reduces to Reissner- Nordstrom black hole solution.

With this quick review of spacetime, we now turn to its thermodynamics in the extended phase space. Here the cosmological constant Λ is dynamic and is related to the pressure as $P = -\Lambda/8\pi$, and its conjugate quantity gives the black hole volume (normalized) (Kastor et al. 2009a). In extended thermodynamics, the mass of the black hole is interpreted as enthalpy of the spacetime rather than energy. The Hawking temperature of the black hole is associated with the surface gravity $T = \frac{\kappa}{2\pi}$, with $\kappa = \frac{f'(r_h)}{2}$, where r_h is the horizon radius. Another important thermodynamic parameter, the entropy of the black hole can be obtained from the Bekenstein area law. These thermodynamics quantities can easily be obtained as,

$$\begin{aligned} M &= \left(\frac{r_h}{2} (k + c_0^2 c_2 m^2) + \frac{c_0 c_1 m^2 r_h}{2} + \frac{8}{3} \pi P r_h^2 + \frac{q^2}{4r_h^2} \right), \\ T &= \left(2P r_h + \frac{k + c_0^2 c_2 m^2}{4\pi r_h} - \frac{q^2}{16\pi r_h^3} + \frac{c_0 c_1 m^2}{4\pi} \right), \\ S &= \pi r_h^2. \end{aligned}$$

The first law of black hole mechanics can be readily written using the above quantities, using which we can calculate the remaining thermodynamic quantities. Thermodynamic volume is,

$$V = \left(\frac{\partial M}{\partial P} \right)_{S, Q} = \frac{4}{3} \pi r_h^3 = \frac{\pi}{6} v^3, \quad (3.4)$$

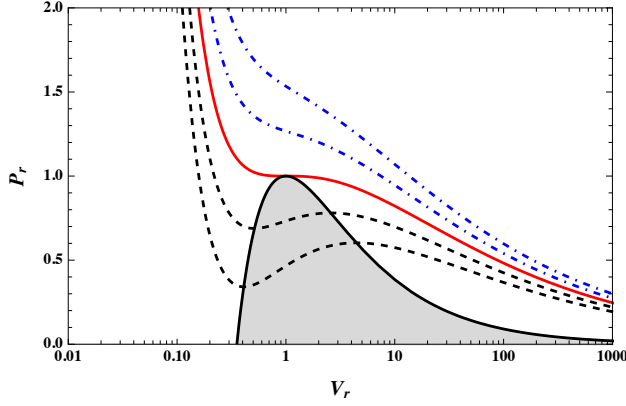


Figure 3.1: $P - V$ isotherms of the massive dRGT-AdS black hole. The shaded region below the solid black line corresponds to the unstable states. (Parameters are in reduced terms and the x axis is in the log scale).

where $v = 2r$ is the specific volume. The equation of state of the system is,

$$P = \frac{q^2}{2\pi v^4} - \frac{k + c_0^2 c_2 m^2}{2\pi v^2} + \frac{T}{v} - \frac{c_0 c_1 m^2}{4\pi v}. \quad (3.5)$$

The black hole exhibits a vdW like behaviour. The critical values can be derived from the conditions,

$$\left(\frac{\partial P}{\partial v}\right)_T = 0, \quad \text{and} \quad \left(\frac{\partial^2 P}{\partial v^2}\right)_T = 0, \quad (3.6)$$

we obtain,

$$P_c = \frac{(k + m^2 c_2 c_0^2)^2}{24\pi q^2}, \quad v_c = \frac{\sqrt{6}\pi q}{(k + m^2 c_2 c_0^2)^{1/2}}, \quad T_c = \frac{2(k + m^2 c_2 c_0^2)^{(3/2)}}{3\sqrt{6}\pi q} + \frac{m^2 c_1 c_0}{4\pi}. \quad (3.7)$$

Using the above critical values, we define the reduced thermodynamic quantities as,

$$P_r = \frac{P}{P_c}, \quad T_r = \frac{T}{T_c}, \quad v_r = \frac{v}{v_c}, \quad V_r = \frac{V}{V_c}. \quad (3.8)$$

In the reduced parameter space, the equation of state reduces to,

$$P_r = \frac{8}{3v} \left\{ T_r \left[1 + \frac{c_0 c_1 m^2 q}{16} \left(\frac{6}{k + c_0^2 c_2 m^2} \right)^{3/2} \right] - \frac{c_0 c_1 m^2 q}{16} \left(\frac{6}{k + c_0^2 c_2 m^2} \right)^{3/2} \right\} + \frac{1}{3v^4} - \frac{2}{v^2}. \quad (3.9)$$

In fact, we can write the equation of state in terms of thermodynamic volume V as,

$$P = \frac{-4c_0^2 c_2 m^2 - 4k}{8 \cdot 6^{2/3} (\pi)^{1/3} V^{2/3}} + \frac{16\pi T - 4c_0 c_1 m^2}{16 (6)^{1/3} \pi^{2/3} (V)^{1/3}} + \frac{(\frac{\pi}{6})^{1/3} q^2}{12V^{4/3}}. \quad (3.10)$$

The above equation $P(V, T)$ (since $r = (\frac{3V}{4\pi})^{1/3}$) is often called the geometric form. Now, one can construct the Maxwell equal area law. The observed coexistence line determines the small-large black hole transition region. In the next sections, we examine the microstructure of the dRGT black hole using Ruppeiner geometry and present our observations in detail.

3.3 Microstructure of black holes

From statistical physics point of view, the thermodynamics of a system always demands a microscopic description. The scenario is not much different in black hole thermodynamics. Even though the thermodynamics of black holes is widely studied, the understanding the microscopic structure of the black hole was a challenging problem always. An alternate way of approaching phase transitions in classical thermodynamics is by constructing thermodynamic geometry through the construction of a thermodynamic metric on the thermodynamic space (P, V, T) . This idea was introduced by Weinhold and Ruppeiner, who constructed thermodynamic metric to study phase transitions and microscopic interactions in thermodynamic systems (Ruppeiner 1995a) (Weinhold 1975).

A Riemannian geometry can be built in the thermodynamic equilibrium space, whose metric tells us about the fluctuations between the states. These studies show that the thermodynamic geometry encodes the information about the microscopic interaction. In this regard Ruppeiner geometry approach is a very useful tool, which extracts

certain aspects of microscopic information from macroscopic properties. In this approach, a metric is constructed on the thermodynamic equilibrium state space which measures the distance between two nearby fluctuating states (Ruppeiner 1995a, 2008a). The Ruppeiner scalar curvature hence calculated from the metric provides the crucial details about phase transitions and the nature of interactions in the microstructure of the system under consideration. The important information obtained from this construction are: (1) nature of microstructure interaction, (2) strength of interaction and (3) critical behaviour. The sign of Ruppeiner scalar curvature indicates the type of interactions. For a non interacting system like ideal gas, it will vanish. In an interacting system, the positive and negative values of scalar curvature represent repulsive and attractive interactions respectively. The magnitude of the Ruppeiner curvature scalar is the measure of strength of interaction. An added feature of the construction is that, for the system with critical behaviour, the curvature scalar shows divergence near the critical point. The singularity of the curvature scalar is related to the singular nature of response functions near the critical point. The Ruppeiner geometric method found effective in describing the micro structure details of a variety of known systems in conventional thermodynamics (Ruppeiner (1995b), Janyszek and Mrugaa (1990), Oshima et al. (1999), Mirza and Mohammadzadeh (2008), May et al. (2013)). This success eventually lead to the application of the Ruppeiner geometry method to a black hole system (Ruppeiner (2008b)).

3.3.1 Thermodynamic geometry

Thermodynamic geometry can explained using fluctuation theory. Which tells that any physical quantities describing a macroscopic body in equilibrium is always equal to their mean value, even though they fluctuate, this fluctuation requires some probability distribution for the physical quantity. Consider thermodynamic system has two independent variable x^0 and x^1 . The probability of finding the system in $x^0 + dx^0$ and $x^1 + dx^1$ is proportional to the number of micro states.

$$P(x^0, x^1) dx^0 dx^1 = C \Omega(x^0, x^1) dx^0 dx^1 \quad (3.11)$$

where C is normalization constant. From Boltzmann entropy formula, $S = k_B \ln \Omega$,

$$\Omega = \exp\left(\frac{S}{k_B}\right) \quad (3.12)$$

Eq. 3.11 become

$$P(x^0, x^1) = C \exp\left(\frac{S}{k_B}\right) \quad (3.13)$$

Now consider total thermodynamic system is divided in to system and surrounding. System plus surrounding is called environment. Now total entropy can be written as

$$S(x^0, x^1) = S_s(x^0, x^1) + S_E(x^0, x^1) \quad (3.14)$$

where $S_s \ll S_E \approx S$. Now using the Taylor expansion entropy can expand at $x^\mu = x_0^\mu$.

Total entropy become

$$S = S_0 + \left. \frac{\partial S_s}{\partial x^\mu} \right|_{x^\mu = x_0^\mu} \Delta x_s^\mu + \left. \frac{\partial S_E}{\partial x^\mu} \right|_{x^\mu = x_0^\mu} \Delta x_E^\mu + \frac{1}{2} \left. \frac{\partial^2 S_s}{\partial x^\mu \partial x^\nu} \right|_{x^\mu = x_0^\mu} \Delta x_s^\mu \Delta x_s^\nu + \frac{1}{2} \left. \frac{\partial^2 S_E}{\partial x^\mu \partial x^\nu} \right|_{x^\mu = x_0^\mu} \Delta x_E^\mu \Delta x_E^\nu \quad (3.15)$$

where μ, ν can take values (0,1,2,..). For closed system $x_s^\mu + x_E^\mu = x_{Total}^\mu = \text{Constant}$

$$\left. \frac{\partial S_s}{\partial x^\mu} \right|_{x^\mu = x_0^\mu} \Delta x_s^\mu = \left. \frac{\partial S_E}{\partial x^\mu} \right|_{x^\mu = x_0^\mu} \Delta x_E^\mu \quad (3.16)$$

Therefore, Eq. 3.15 become,

$$\Delta S = \frac{1}{2} \left. \frac{\partial^2 S_s}{\partial x^\mu \partial x^\nu} \right|_{x^\mu = x_0^\mu} \Delta x_s^\mu \Delta x_s^\nu + \frac{1}{2} \left. \frac{\partial^2 S_E}{\partial x^\mu \partial x^\nu} \right|_{x^\mu = x_0^\mu} \Delta x_E^\mu \Delta x_E^\nu \quad (3.17)$$

since $S_E \approx S_{total}$, the second term is much smaller than first term, so we can ignore it.

Now, Eq. 3.13 become,

$$P(x^0, x^1) = C \exp\left(\frac{1}{2k_B} \left. \frac{\partial^2 S_s}{\partial x^\mu \partial x^\nu} \right|_{x^\mu = x_0^\mu} \Delta x_s^\mu \Delta x_s^\nu\right) \quad (3.18)$$

$$P(x^0, x^1) = C \exp\left(-\frac{1}{2}\Delta l^2\right) \quad (3.19)$$

Δl^2 gives the distance between two neighbouring fluctuating states.

$$\Delta l^2 = \frac{-1}{k} g_{\mu\nu} \Delta x_s^\mu \Delta x_s^\nu \quad (3.20)$$

$$g_{\mu\nu} = \frac{\partial^2 S_s}{\partial x^\mu \partial x^\nu} \quad (3.21)$$

For simplicity we can take $k = 1$ and take $S_s = S$. Here Δl^2 can be treated as distance between two neighbouring states in state space. As we know Riemannian geometry, once we know the metric of spacetime we can develop the scalar curvature. By employing same procedure we can compute scalar curvature in terms of parameter space. By using the same conventions like,

$$\Gamma_{\mu\nu}^\sigma = \frac{1}{2} g^{\sigma\rho} (\partial_\nu g_{\rho\mu} + \partial_\mu g_{\rho\nu} - \partial_\rho g_{\mu\nu}) \quad (3.22)$$

$$R_{\rho\mu\nu}^\sigma = \partial_\nu \Gamma_{\rho\mu}^\sigma - \partial_\mu \Gamma_{\rho\nu}^\sigma + \Gamma_{\rho\mu}^\delta \Gamma_{\delta\nu}^\sigma - \Gamma_{\rho\nu}^\delta \Gamma_{\delta\mu}^\sigma \quad (3.23)$$

$$R_{\mu\nu} = R_{\mu\sigma\nu}^\sigma \quad (3.24)$$

$$R = g^{\mu\nu} R_{\mu\nu} \quad (3.25)$$

where $g^{\mu\nu}$ is inverse of metric $g_{\mu\nu}$. For thermodynamic system first law can be written as,

$$dU = TdS - PdV + \sum_i y_i dx^i \quad (3.26)$$

where x_i corresponds to thermodynamic variables and y_i indicate chemical potential. For simplicity by absorbing PdV term in to the last term

$$dU = TdS + \sum_i y_i dx^i \quad (3.27)$$

since entropy is taken as thermodynamic potential in Ruppeiner geometry

$$dS = \frac{dU}{T} - \sum_i \frac{y_i}{T} dx^i \quad (3.28)$$

$$dS = z_\mu dx^\mu \quad (3.29)$$

where μ takes values (0,1,2,3..), i running as (1,2,3..), $z^\mu = (U, V..)$, $y_i = (-P, ..)$ and $z_\mu = \frac{\partial S}{\partial x^\mu} = (\frac{1}{T}, \frac{-y_i}{T})$. The line element can be written as

$$\Delta l^2 = -\Delta z_\mu \Delta x^\mu \quad (3.30)$$

$$\Delta l^2 = \frac{1}{T} \Delta T \Delta S + \frac{\Delta y_i}{T} \Delta x^i \quad (3.31)$$

Here we can choose two choices of parameter space coordinate. (T, x^i) coordinate or (T, y_i) coordinate.

For the first choice T and x^i are independent variables. Helmholtz free energy can choose as potential here. (T, V) parameter space is good choice for in this category. $F = U - TS$ and its differential form is,

$$dF = -SdT + y_i dx^i \quad (3.32)$$

From this expression we have the relation

$$\frac{\partial S}{\partial x^i} = -\frac{\partial y_i}{\partial T}. \quad (3.33)$$

Now expand ΔS and Δy_i in terms of independent variables T and x^i

$$\Delta S = \frac{\partial S}{\partial T} \Delta T + \frac{\partial S}{\partial x^i} \Delta x^i \quad (3.34)$$

$$\Delta y_i = \frac{\partial y_i}{\partial T} \Delta T + \frac{\partial y_i}{\partial x^j} \Delta x^j \quad (3.35)$$

Now the Eq. [3.31](#) can be written as

$$\Delta l^2 = \frac{-1}{T} \left(\frac{\partial^2 F}{\partial T^2} \right) \Delta T^2 + \frac{1}{T} \left(\frac{\partial^2 F}{\partial x^i \partial x^j} \right) \Delta x^i \Delta x^j \quad (3.36)$$

For T, V as state space coordinate Eq. [3.36](#) can be written as

$$\Delta l^2 = \frac{-1}{T} C_V \Delta T^2 - \frac{1}{T} \left(\frac{\partial P}{\partial V} \right) \Delta V^2. \quad (3.37)$$

Curvature scalar can be easily obtained from this line element for (T,V) fluctuation coordinates.

For the second choice T and y_i are fluctuation coordinates. Corresponding thermodynamic potential is $W = U - TS - y_i x^i$. (P,V) parameter space is good choice for in this category. Differential form of W can be written as,

$$dW = -SdT - x^i dy_i \quad (3.38)$$

Here we have

$$S = -\frac{\partial W}{\partial T}, \quad x^i = -\frac{\partial W}{\partial y_i} \quad (3.39)$$

Now expand ΔS and Δx^i in Eq. 3.31 in terms of independent variables T and y_i .

$$\Delta S = \frac{\partial S}{\partial T} \Delta T + \frac{\partial S}{\partial y_i} \Delta y_i \quad (3.40)$$

$$\Delta x^i = \frac{\partial x^i}{\partial T} \Delta T + \frac{\partial x^i}{\partial y_j} \Delta y_j \quad (3.41)$$

Eq. 3.31 now can simplified to

$$\Delta l^2 = \frac{-1}{T} \left(\frac{\partial^2 W}{\partial P_\mu \partial P_\nu} \right) \Delta P_\mu \Delta P_\nu \quad (3.42)$$

where $P_\mu = (T, y_i)$. For representing metric in (S,P) parameter space,

$$\Delta T = \frac{\partial T}{\partial S} \Big|_P \Delta S + \frac{\partial T}{\partial P} \Big|_S \Delta P \quad (3.43)$$

$$\Delta V = \frac{\partial V}{\partial S} \Big|_P \Delta S + \frac{\partial V}{\partial P} \Big|_S \Delta P \quad (3.44)$$

Now, metric can be written as

$$\Delta l^2 = \frac{\Delta S^2}{C_P} + \frac{V}{T} \kappa_S \Delta P^2 \quad (3.45)$$

where $\kappa_S = \frac{-1}{V} \left(\frac{\partial V}{\partial P} \right)_S$ is the adiabatic compressibility. Since entropy of black hole depends only on volume (S, P) plane is equivalent to (P, V) plane.

3.3.2 Scalar curvature

From thermodynamic geometric perspective, we can investigate the information about spacetime from scalar curvature. It will diverge at critical point of phase transition, so this property is used to find the phase transition. The sign of scalar curvature indicate the type of interaction. Positive scalar curvature gives repulsive interaction, whereas negative indicate attractive interaction. $R = 0$ indicate there is no interaction. As we discussed in the first case of parameter space, that is Fluctuation coordinate as (T, x), where x can take any variable like V, Q, J, \dots . For two dimension case metric can be written as

$$g_{\mu\nu} = \frac{1}{T} \begin{pmatrix} \left(\frac{-\partial^2 F}{\partial T^2} \right)_x & 0 \\ 0 & \left(\frac{\partial^2 F}{\partial x^2} \right)_T \end{pmatrix} \quad (3.46)$$

$$g_{\mu\nu} = \frac{1}{T} \begin{pmatrix} \left(\frac{\partial S}{\partial T} \right)_x & 0 \\ 0 & \left(\frac{\partial y}{\partial x} \right)_T \end{pmatrix} \quad (3.47)$$

Heat capacity at constant x is $C_x = T \left(\frac{\partial S}{\partial T} \right)_x$ line element can be written as

$$dl^2 = \frac{C_x}{T^2} dT^2 - \frac{(\partial_{xy})_T}{T} dx^2 \quad (3.48)$$

from this metric scalar curvature can be calculated as

$$R = \frac{1}{2C_x^2 (\partial_{xy})^2} \{ T(\partial_{xy}) [(\partial_x C_x)^2 + (\partial_T C_x)((\partial_{xy}) - T\partial_{T,xy})] + C_x [(\partial_{xy})^2 + T((\partial_x C_x)(\partial_{x,xy}) - T(\partial_{T,xy})^2) + 2T(\partial_{xy})(-\partial_{x,x} C_x + T(\partial_{T,T,xy}))] \} \quad (3.49)$$

Here R can be diverge at $C_x = 0$ or $(\partial_{xy})_T = 0$. $(\partial_{x,xy})_T = (\partial_{xy})_T = 0$ are the condition for critical point. So it means R has diverging behaviour at critical point. For constant heat capacity C_x , the scalar curvature reduces to,

$$R = \frac{(\partial_{xy})^2 - T^2(\partial_{T,xy})^2 + 2T^2(\partial_{xy})(\partial_{T,T,xy})}{2C_x(\partial_{xy})^2} \quad (3.50)$$

in (T, V) parameter space, thermodynamic curvature is normalized with respect heat capacity at constant volume, whereas in (P, V) plane thermodynamic curvature is constructed via adiabatic compressibility(κ).

3.3.3 Ruppeiner geometry and microstructure of massive black Hole

In this section, we study the interacting microstructure of the massive black hole using Ruppeiner geometry method. Without compromising generality we will put $c_0 = 1$ and $m = 1$ in Eq. (4.3). In the thermodynamic parameter space of pressure and entropy, the line element can be simplified to the following form, (Dehyadegari et al. 2020)

$$dl^2 = \frac{dS^2}{C_P} + \frac{V}{T} \kappa_S dP^2, \quad (3.51)$$

here the heat capacity $C_P = T(\frac{\partial S}{\partial T})_P$ and $\kappa_S = -\frac{1}{V}(\frac{\partial V}{\partial P})_S$. Considering the interdependence of entropy and volume in the case of a spherically symmetric black hole, the above line element can be written as

$$dl^2 = \frac{1}{C_P} \left(\frac{\pi}{6V} \right)^{2/3} dV^2 + \frac{V}{T} \kappa_S dP^2 \quad (3.52)$$

Now, we have pressure and volume as the thermodynamic variables. Since the adiabatic compressibility κ_S is a vanishing quantity similar to the heat capacity at a constant volume, we define a normalized thermodynamic curvature as $R_N = R\kappa_S$. By performing a direct calculation of the curvature scalar, we obtain the normalized curvature scalar (R_N) of the dRGT black hole.

$$R_N = \frac{16V_r^{2/3}}{y^{5/2} \left(P_r V_r^{4/3} - 2V_r^{2/3} + 1 \right)^2 \left(36c_1 q V_r + \sqrt{6} y^{3/2} \left(3P_r V_r^{4/3} + 6V_r^{2/3} - 1 \right) \right)}{\times \left\{ 54\sqrt{6} c_1^2 q^2 V_r^2 + 9c_1 q V_r y^{3/2} \left(9P_r V_r^{4/3} + 6V_r^{2/3} + 1 \right) + \sqrt{6} \left(3V_r^{2/3} - 1 \right) y^3 \left(9P_r V_r^{4/3} - 6V_r^{2/3} + 5 \right) \right\}}. \quad (3.53)$$

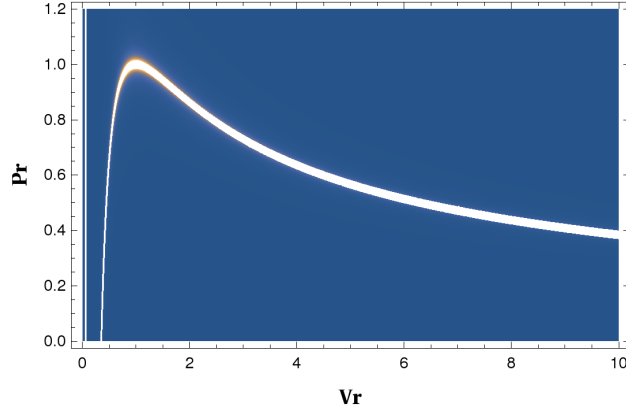


Figure 3.2: The behaviour of R_N as a function of P and V

Here, the variable y is defined as $y = k + c_2$. The behaviour of R_N with reduced volume V_r for a fixed parameter is studied in the figures 3.3(a) to 3.3(d). For $P_r < 1$, R_N has two negative divergences. These divergences merge at $V_r = 1$ for $P_r = 1$. For $P_r > 1$, these divergences of R_N disappears. The divergence of R_N is along the curve is defined by,

$$P_{div} = \frac{2V_r^{2/3} - 1}{V_r^{4/3}} \quad P_{div} = \frac{1 - 2V_r^{2/3}}{3V_r^{4/3}} - \frac{0.003061}{V_r^{1/3}} \quad (3.54)$$

Here, the dominant interaction is attractive in nature because the R_N is always negative. In the figure 3.4(b), the red dashed curve represents the coexistence curve and the blue solid represents the divergent curve. The shaded region in the graph indicates the positive values of the normalized scalar curvature and the other remaining regions R_N take negative values. SBH and LBH phases simultaneously coexist under the coexistence curve. From this figure, it is apparent that a certain range of volume in SBH has positive R_N , which implies the domination of repulsive interaction. The region where R_N is negative signifies attractive microstructure interactions.

One can study the plot for R_N along the coexistence curve for both SBH and LBH phases from critical temperature to zero. Here we observe that R_N for both SBH and LBH diverges to $-\infty$ at the critical temperature. The figure 3.4(a) shows that LBH possesses only negative values of R_N , and it gradually increases while approaching the critical temperature. However, for the SBH phase R_N changes sign and become a positive value below a particular temperature. Also, R_N goes to positive infinity as T tends to zero, where strong repulsive interaction dominates.

We also investigate the effect of graviton mass ($m = 0, 1, 2$) and horizon topology on the micro-states of dRGT black holes for SBH and LBH phases. It is clear from the figure 3.6 that the repulsive interaction of SBH becomes strongly repulsive as graviton mass increases. However, the attractive nature of the LBH phase becomes weaker as graviton mass increases. Figures 3.5(a) and 3.5(b) show the repulsive interaction SBH is stronger for spherical topology, followed by flat and hyperbolic topology. Hyperbolic topology has the most attractive LBH interactions, followed by flat and spherical topology.

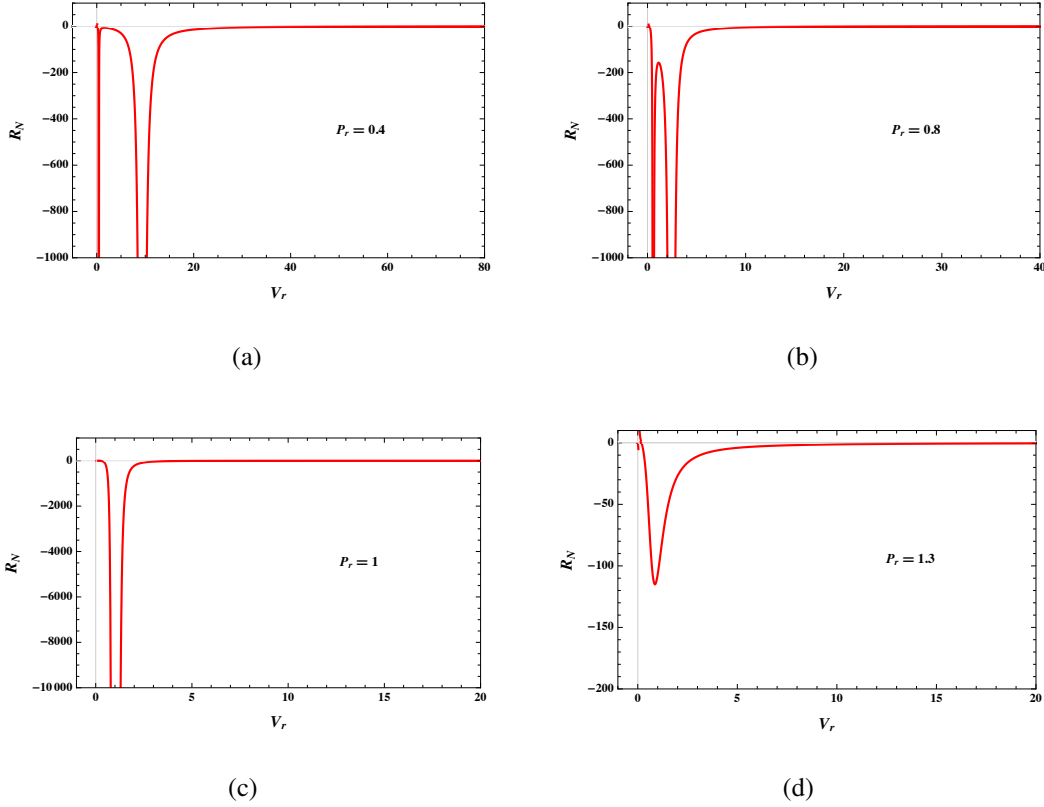


Figure 3.3: The behaviour of the R_N against the reduced volume V_r at constant pressure.

3.4 Discussions

we have constructed the Ruppeiner geometry for an AdS black hole in dRGT massive gravity to the phenomenological understanding of the nature and the strength of the microstructure interactions. The underlying motivation for this study lies in the fact that the black hole phase transition is related to its microstructure details. The construction

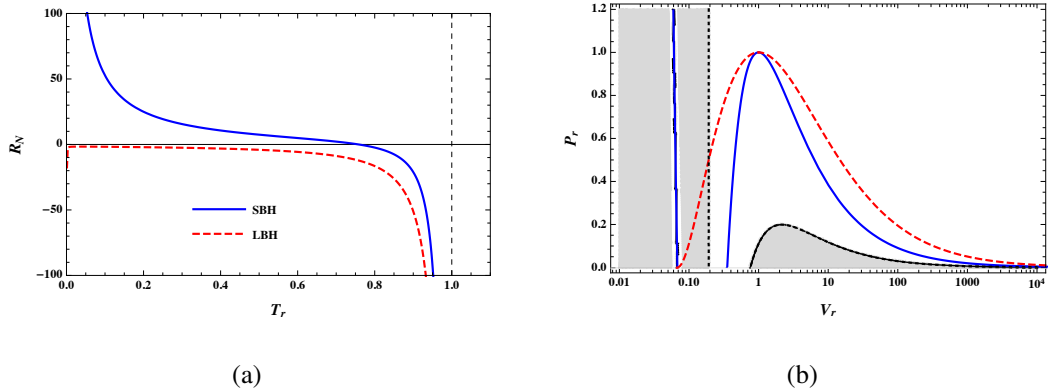


Figure 3.4: Left: The behaviour of R_N along the coexistence curve. The red (dashed) and blue (solid) lines correspond to LBH and SBH, respectively. Right: The vanishing curve (black dot-dashed line) and diverging curve (blue solid line) of R_N along with the coexistence curve (red dashed line). The shaded regions indicate positive R_N ; otherwise, R_N is negative (Parameters are in reduced terms, and the x axis is in the log scale).

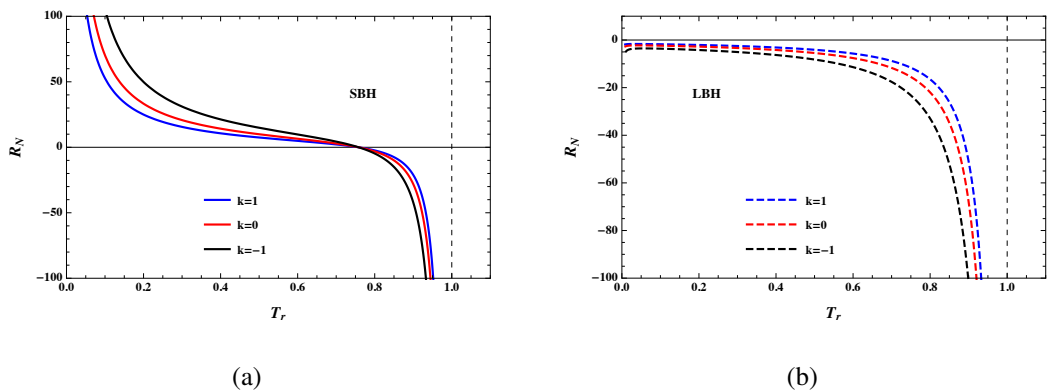


Figure 3.5: The effect of parameter k on the microstructure interactions. In the left SBH and in the right LBH are shown.

is carried out by defining a normalized curvature scalar R_N in the parameter space of pressure P and the volume V , which are the fluctuation coordinates, via the adiabatic compressibility κ . The phenomenological understanding of the nature and the strength of the microstructure follows from the observation of the behavior of R_N along the coexistence line for the small-large black hole phase transition, which is a first-order transition with universal behavior. The validity of the construction of normalized curvature scalar is confirmed by looking at the divergence of the curvature scalar at the critical point of the phase transition. The study shows that the microstructure details

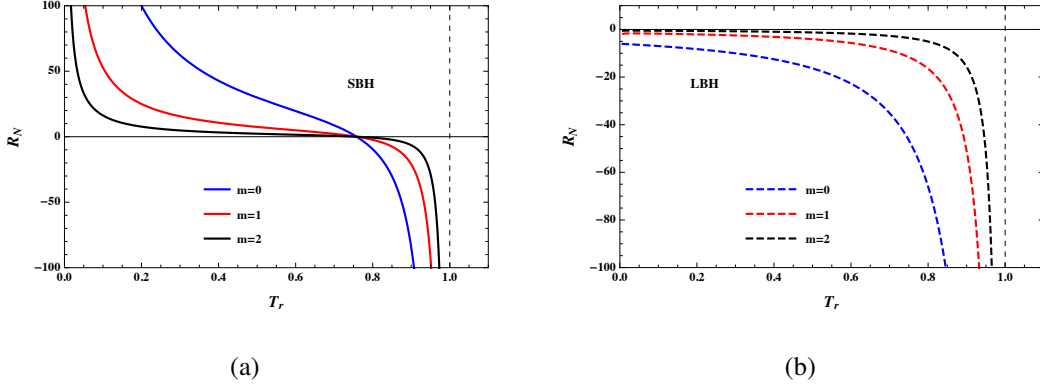


Figure 3.6: The effect of parameter m on the microstructure interactions. In the left SBH and in the right LBH are shown.

of the dRGT massive black holes are similar to the charged AdS black holes; however, it is influenced by the parameters of the spacetime that govern the massive gravity background.

The small black hole phase has microstructures analogous to anyon gas with attractive and repulsive interactions. The result is interesting due to the presence of a repulsive interaction at some parameter space, which differs from the microstructure properties of a vdW fluid (where we have only dominant attractive interactions), though the phase transition properties are akin to both black hole and VdW systems. In other words, the universality in the critical behavior does not imply the similarity in the microstructure interactions. We note that the repulsive interaction is suppressed by the graviton mass m . The effect of the topology on the repulsive interaction was also investigated, which shows a trend of stronger to weaker in the order $k = -1, 0, 1$. The LBH exhibits only attractive interactions all over the parameter space, which is similar to a boson gas. In both the small and large black hole phases, the attractive interactions of the black hole microstructure have the same dependence on the spacetime parameters m and k . The effect of charge on the microstructure is also explored, which we find negligible.

Chapter 4

Dynamic phase transition of black holes in massive gravity

4.1 Introduction

Phase transitions are useful tools in thermodynamics and statistical physics. Hawking and Page (Hawking and Page 1983b) studied the first-order phase transition from a thermal AdS phase to a large black hole phase by considering the black holes as thermodynamic states. The analogy between black holes and van der Waal systems has been explored in modified gravity theories as well as higher curvature gravity theories (Cai et al. 2013, Wei and Liu 2013, Zou et al. 2014, Rajagopal et al. 2014, Mo and Liu 2014, Xu et al. 2015, Yazdikarimi et al. 2019, Dayyani et al. 2018). In thermodynamics studies, the macroscopic properties of a system can be determined by the microscopic degrees of freedom. In this regard, a phase of a thermodynamics system is a macroscopic emergent state. The probability in which a state emerges from many possible micro states is related to the thermodynamic free energy of the system. The free energy distributed among the state space constitutes a free energy landscape. Further, the free energy landscape can be characterised by specifying an order parameter. In a van der Waal liquid-gas system, the density can be used as order parameter. The transition between different states, caused by thermal fluctuations, can be addressed in terms of free energy minima.

Black holes, being a thermal entity, can be considered as macroscopic emergent states of some underlying microscopic degrees of freedom. Therefore, we can construct a free energy landscape by taking the radius of the black hole as order parameter (Wei and Liu 2015a, Wei et al. 2019a). Also, one can study the kinetics of black hole phase transitions using probabilistic Fokker-Planck equation on the free energy landscape. This formalism has been applied to study the phase transitions in Einstein as well as massive gravity theories (Li and Wang 2020). The calculation can be extended by solving the Fokker-Planck equation subjected to suitable boundary conditions to obtain the stationary distributions of black hole states at different temperatures as well as the first passage time of the probabilistic evolution between black hole states. Considering this, the dynamics and kinetics of the Hawking-Page phase transition for Reissner-Nordstrom anti-de Sitter (RNAdS) black holes are investigated in (Li et al. 2020).

The general theory of relativity is a massless spin two field theory. One can ask about the possibilities of a self-consistent gravity theory with massive graviton. The answer is yes! And among the several modified versions of massive gravity theories can explain the accelerated expansion of our universe without introducing a cosmological constant or dark energy. Massive gravity theories have a long and remarkable history. The initial studies were carried out by Fierz and Pauli in 1939 (Fierz and Pauli 1939). The proposed theory was linear and ghost-free but did not reduce to general relativity in the massless limit. Non-linear modifications of Fierz and Pauli's theory lead to "Boulware-Deser" ghost instability (Boulware and Deser 1972). Later, de Rham, Gabadadze, and Tolley (dRGT) came up with a special class of non-linear massive gravity theory, which is "Boulware-Deser" ghost free (de Rham et al. 2011). As mentioned before, the thermodynamics of the black holes in massive gravity were widely investigated (Cai et al. 2015, Xu et al. 2015, Hendi et al. 2017a, 2016, Mirza and Sherkatghanad 2014, Fernando 2016, Ning and Liu 2016). The van der Waals like feature of dRGT massive gravity black holes and other applications such as triple point, Reentrant phase transitions, heat engines, and throttling process were also studied (Zou et al. 2017, Liu et al. 2020, Hendi et al. 2018, Yerra and Bhamidipati 2020a, Lan 2019). In addition, several works to probe the microstructure were also studied using various

thermodynamic-geometry approaches (Chabab et al. 2019, Wu et al. 2021, Yerra and Bhamidipati 2020b, Safir et al. 2022).

In this chapter, we extend the calculation of black hole phase transitions within free energy landscape by considering a dRGT non-linear massive gravity theory. The free energy landscape is constructed by specifying the Gibbs free energy to every states, and the free energy profile is used to study the different black hole phases. A detailed study on the first passage process is presented which describes the dynamics of phase transitions. Finally, we will investigate the effect of mass and topology on the dynamical properties of phase transitions of black holes in dRGT non-linear massive gravity theory.

4.2 Thermodynamic characterisation and phase transition

We start with a brief discussion on the spacetime and thermodynamic structure of black holes in massive gravity theory. As mentioned above, we consider the dRGT non-linear massive gravity theory in four-dimensional AdS space. The action for the Einstein-dRGT gravity coupled to a non-linear electromagnetic field is given by (Vegh 2013),

$$S = \int d^4x \sqrt{-g} \left[\frac{1}{16\pi} \left[R + \frac{6}{l^2} + m^2 \sum_{i=1}^4 c_i \mathcal{U}_i(g, f) \right] - \frac{1}{4\pi} F_{\mu\nu} F^{\mu\nu} \right], \quad (4.1)$$

where $F_{\mu\nu} = \partial_\mu A_\nu - \partial_\nu A_\mu$ is the electromagnetic field tensor with vector potential A_μ , l is AdS radius, m is related to the graviton mass, and c_i are coupling parameters. Further, $f_{\mu\nu}$ is a symmetric tensor as reference metric coupled to the space-time metric $g_{\mu\nu}$. Graviton interaction terms are represented by symmetric polynomials \mathcal{U}_i , and are obtained from a 4×4 matrix $\mathcal{K}_\nu^\mu = \sqrt{g^{\mu\alpha} f_{\nu\alpha}}$, which have the following forms,

$$\begin{aligned} \mathcal{U}_1 &= [\mathcal{K}] \\ \mathcal{U}_2 &= [\mathcal{K}]^2 - [\mathcal{K}^2] \\ \mathcal{U}_3 &= [\mathcal{K}]^3 - 3[\mathcal{K}^2][\mathcal{K}] + 2[\mathcal{K}^3] \\ \mathcal{U}_4 &= [\mathcal{K}]^4 - 6[\mathcal{K}^2][\mathcal{K}]^2 + 8[\mathcal{K}^3][\mathcal{K}] + 3[\mathcal{K}^2]^2 - 6[\mathcal{K}^4] \end{aligned}$$

The solution to the above action for various horizon topologies are given by (Cai et al. 2015, Hendi et al. 2017b),

$$ds^2 = -f(r)dt^2 + \frac{1}{f(r)}dr^2 + r^2 h_{ij} dx_i dx_j, \quad (4.2)$$

where h_{ij} is the metric for two dimensional hypersurface. The topological parameter (k) can take values 0, -1 or 1 , representing planar, hyperbolic, and spherical topology, respectively. With the choice of reference metric $f_{\mu\nu} = \text{diag}(0, 0, c_0^2 h_{ij})$, the values of \mathcal{U}_i becomes $\mathcal{U}_1 = \frac{2c_0}{r}$, $\mathcal{U}_2 = \frac{2c_0^2}{r^2}$, $\mathcal{U}_3 = \mathcal{U}_4 = 0$. Now, the metric function reduces to,

$$f(r) = k - \frac{m_0}{r} - \frac{\Lambda r^2}{3} + \frac{q^2}{r^2} + m^2 \left(\frac{c_0 c_1}{2} r + c_0^2 c_2 \right), \quad (4.3)$$

where integration constants m_0 and q are related to black hole mass and charge, respectively. m is the parameter for graviton mass, and in the limiting case of $m = 0$ the spacetime reduces to Reissner- Nordstrom black hole solution.

Now, the event horizon (r_+) is determined by the largest root of the equation $f(r) = 0$. The Hawking temperature of the black hole is related to its surface gravity by the relation $T_H = \frac{\kappa}{2\pi}$, where the surface gravity $\kappa = \frac{1}{2} f'(r_+)$. As in the case of an asymptotically AdS black hole in four dimension, one can relate the thermodynamic pressure with cosmological constant (Kastor et al. 2009a, Dolan 2011b,a) as,

$$P = -\frac{\Lambda}{8\pi}$$

At this point, the mass, temperature, and the entropy of the black hole in Einstein-dRGT gravity coupled to a non-linear electromagnetic field can be expressed in terms of the horizon radius and pressure as following:

$$\begin{aligned} M &= \left(\frac{r_+}{2} (k + c_0^2 c_2 m^2) + \frac{c_0 c_1 m^2 r_+}{2} + \frac{8}{3} \pi P r_+^2 + \frac{q^2}{4r_+^2} \right), \\ T_H &= \left(2P r_+ + \frac{k + c_0^2 c_2 m^2}{4\pi r_+} - \frac{q^2}{16\pi r_+^3} + \frac{c_0 c_1 m^2}{4\pi} \right), \\ S &= \pi r_+^2. \end{aligned}$$

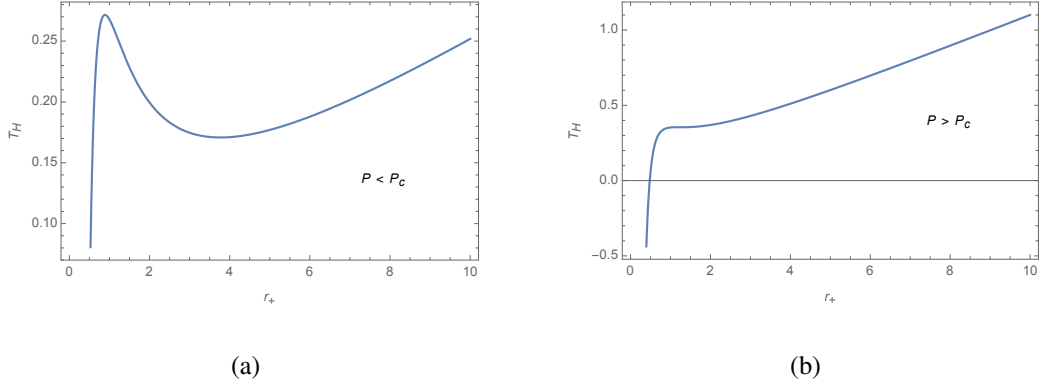


Figure 4.1: Black hole temperature as a function of event horizon radius (a) when $P < P_c$ and (b) $P > P_c$.

The first law of black hole mechanics can be readily written using the above quantities. Further, thermodynamic volume is obtained as,

$$V = \frac{4}{3}\pi r_+^3 = \frac{\pi}{6}v^3, \quad (4.4)$$

where $v = 2r_+$ is the specific volume. The equation of state of the system $P = P(T_H, v)$ is,

$$P = \frac{q^2}{2\pi v^4} - \frac{k + c_0^2 c_2 m^2}{2\pi v^2} + \frac{T_H}{v} - \frac{c_0 c_1 m^2}{4\pi v}. \quad (4.5)$$

This expression indicates that the black hole exhibits a vdW fluid like behaviour. The critical points for the first order phase-transition between a large black hole phase (LBH) and small black hole phase (SBH) in the extended phase space can be derived from the conditions,

$$\left(\frac{\partial P}{\partial v}\right)_{T_H=0}, \quad \text{and} \quad \left(\frac{\partial^2 P}{\partial v^2}\right)_{T_H} = 0, \quad (4.6)$$

we obtain,

$$P_c = \frac{(k + m^2 c_2 c_0^2)^2}{24\pi q^2}, \quad (4.7)$$

Above the critical pressure P_c , the black hole temperature T_H is a monotonic function of black hole radius. Whereas below the critical pressure black hole temperature have the local minimum and local maximum values (this characteristics is independent of the topology of the system). In Fig. [\[4.1\]](#) we have depicted a typical behaviour of T_H

as a function of r_+ for both $P < P_c$ and $P > P_c$.

The local minima and local maxima of black hole temperature for $P < P_c$ are determined by,

$$\frac{\partial T_H}{\partial r_+} = 0,$$

giving the solutions,

$$r_{min/max} = \frac{1}{4\sqrt{\pi}} \left[\frac{k + c_0^2 m^2 c_2 \mp (k + c_0^2 m^2 c_2 - 24\pi P q^2)^{\frac{1}{2}}}{P} \right]^{\frac{1}{2}}.$$

And the corresponding values of black hole temperatures are given by,

$$T_{min/max} = \frac{1}{4\sqrt{\pi}} \left[c_0 c_1 m^2 \pi^{\frac{3}{2}} - \frac{16\pi q^2}{\left(\frac{k + c_0^2 m^2 c_2 \mp (k + c_0^2 m^2 c_2 - 24\pi P q^2)^{\frac{1}{2}}}{P} \right)^{\frac{3}{2}}} \right. \\ \left. + \frac{4(k + c_0^2 m^2 c_2)}{\left(\frac{k + c_0^2 m^2 c_2 \mp (k + c_0^2 m^2 c_2 - 24\pi P q^2)^{\frac{1}{2}}}{P} \right)^{\frac{1}{2}}} + 2P \left(\frac{k + c_0^2 m^2 c_2 \mp (k + c_0^2 m^2 c_2 - 24\pi P q^2)^{\frac{1}{2}}}{P} \right)^{\frac{1}{2}} \right]$$

Further analysis shows, when the black hole temperature lies $T_{min} < T_H < T_{max}$, there exists three branches of black hole solution (i.e. small, intermediate, and large black hole), in which the intermediate solution is unstable. Also, there is a first order phase transition from the small black hole to the large black hole similar to the van der Waals liquid-gas system.

The characteristics of the first-order phase transition of black hole is further studied in the following section using Gibbs free energy landscape.

4.3 Gibbs free energy landscape

As discussed before, the free energy is an effective tool to study the dynamic phase transition of black holes. We consider the canonical ensemble composed of a series of black holes at a given temperature T . The free energy landscape is constructed by specifying a Gibbs free energy to every spacetime states. Now, the Gibbs free energy

(on-shell) can be obtained either from the Euclidean action (Dolan 2011a) or from the thermodynamic relationship $G = M - T_H S$. Note that the expression for off-shell Gibbs free energy is obtained by replacing the Hawking temperature (T_H) with the ensemble temperature (T), and is given by,

$$G = M - T S = \frac{r_+}{2} \left(k + \frac{q^2}{r_+^2} + \frac{8}{3} P \pi r_+^2 + m^2 \left(c_0^2 c_2 + \frac{c_0 c_1 r_+}{2} \right) \right) - \pi T r_+^2 \quad (4.8)$$

In this construction, the black hole radius is taken as the order parameter describing the microscopic degrees of freedom of the system. Now, the Gibbs free energy landscape as a function of the black hole radius for $P < P_c$ at different values of the temperature can be studied Fig. [4.2]. When $T < T_{min}$, there is only one global minimum for the Gibbs free energy, and corresponds to pure radiation phase. At $T = T_{min}$, there is an inflection point. Above this temperature two black hole phases emerge (small and large black hole phases). The smaller black hole corresponds to a local maximum of Gibbs free energy and the larger black hole has a local minimum. For $T_{min} < T < T_{max}$, the

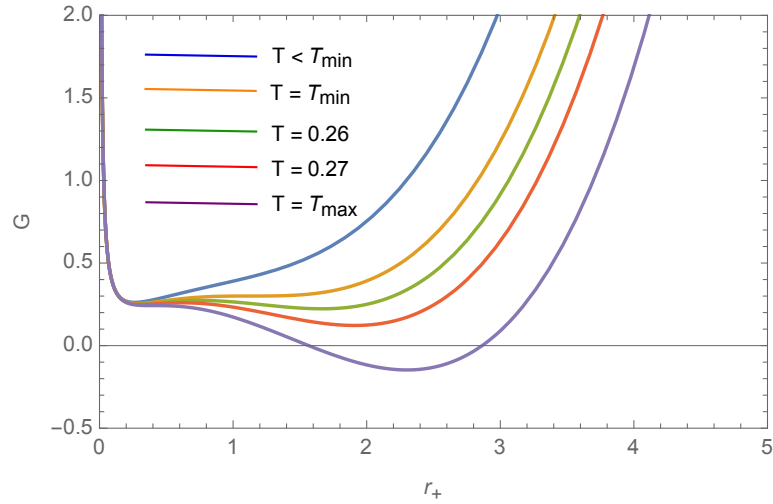


Figure 4.2: Behaviour of Gibbs free energy as a function of r_+ for $P < P_c$ at different temperatures

Gibbs free energy has three local extremals, in which two are stable and one is unstable.

The extremum values are determined by,

$$\begin{aligned} \frac{\partial G}{\partial r_+} &= 0 \\ \Rightarrow \frac{k}{2} + \frac{m^2}{2} (c_0^2 c_2 + c_0 c_1 r_+) - \frac{q^2}{2r_+^2} - 2\pi r_+ (T - 2Pr_+) &= 0 \end{aligned} \quad (4.9)$$

Solving this equation for radius, we obtain the radii for small, intermediate, and large black holes. The intermediate black hole which has the maximum value of Gibbs free energy is unstable. The small and large black holes are locally stable as they corresponds to minimal Gibbs free energy. Further, the Gibbs free energy can be obtained as,

$$G_{s/m/l} = \frac{r_{s/m/l}}{2} \eta + \frac{3q^2}{4r_{s/m/l}} - \frac{2}{3} P \pi r_{s/m/l}^3, \quad (4.10)$$

where $\eta = k + c_2 m^2$. As the temperature increases, the local minimum of Gibbs free energy lowers until it becomes zero at $T = T_{trans}$. T_{trans} is known as the transition temperature. At this point, the Gibbs free energy of large and small black holes are equal. Therefore, the transition temperature can be obtained from the following equations:

$$\begin{aligned} \frac{1}{2} (\eta + c_1 r_s) - \frac{q^2}{2r_s^2} - 2\pi r_s (T - 2Pr_s) &= 0, \\ \frac{1}{2} (\eta + c_1 r_l) - \frac{q^2}{2r_l^2} - 2\pi r_l (T - 2Pr_l) &= 0, \\ \text{and } \frac{r_s}{2} \eta + \frac{3q^2}{4r_s} - \frac{2}{3} P \pi r_s^3 &= \frac{r_l}{2} \eta + \frac{3q^2}{4r_l} - \frac{2}{3} P \pi r_l^3; \end{aligned}$$

The expressions for the small and large black hole radii is readily obtained as,

$$\begin{aligned} r_s &= \frac{1}{8(\pi P)^{\frac{3}{2}}} \left[(\eta + \omega) (\eta (\eta + \omega) - 12P\pi q^2) \right]^{\frac{1}{2}}, \\ r_l &= \frac{1}{4\pi P(\eta + \omega)} \left[\eta (\eta + \omega) - 12P\pi q^2 + 4\sqrt{\pi} (P(\eta + \omega) (\eta (\eta + \omega) - 12P\pi q^2)) \right]^{\frac{1}{2}}. \end{aligned} \quad (4.11)$$

Here, $\omega = \sqrt{\eta^2 - 24P\pi q^2}$. These expressions can be substituted back to obtain the transition temperature.

$$T_{trans} = \frac{6\sqrt{P\pi}t^2(\eta + \omega) - 2q^2(P\pi)^{\frac{3}{2}}(49\eta + 13\omega) + c_1m^2(\eta + \omega)^{\frac{3}{2}}\sqrt{\eta(\eta + \omega) - 12Pq^2}}{2\pi(\eta + \omega)^{\frac{3}{2}}\sqrt{\eta(\eta + \omega) - 12Pq^2}}$$

A thermodynamic phase diagram is given by plotting T_{max} , T_{min} , and T_{trans} as a function of P . For a chosen parameters of the system ($k = 1, m = 1, q = c_1 = c_2 = 0.05$), the curves divide the $P - T$ plane into four thermodynamic phase regions. In Fig. [4.3], the blue, black, and red lines represent T_{max} , T_{trans} , and T_{min} respectively.

Note that the structure of phase diagram is similar to the case of AdS black hole .

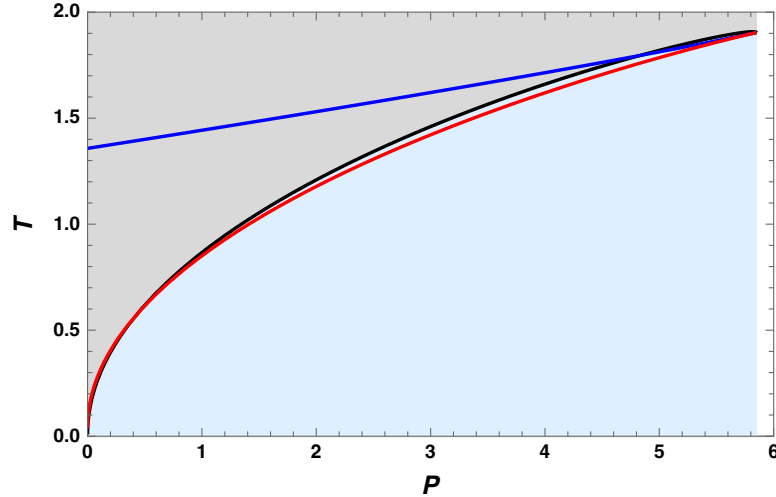


Figure 4.3: The phase diagram of dRGT black holes. Here, T_{max} , T_{min} , and T_{trans} are plotted as a function of P from 0 to P_c . The small black hole is stable in the blue region whereas the large black hole is stable in the grey region. In this plot, the black line represents the coexisting curve.

The region above the blue line as well as below the red line has only one black hole solution which is always thermodynamically stable. The rest of the phase-diagram represents three black hole solutions. Along the black curve the free energies of small and large black holes are equal, and both these solutions coexist along this curve with equal probability. Therefore, the black line is called the coexisting curve. The free energy of the small black hole phase is less than the free energy of the large black hole in the phase region between the black and red curves, and the free energy of small black hole phase is greater than the free energy of the larger black hole in the region

between the black and blue curves. As the system having less Gibbs free energy is thermodynamically stable, we conclude that the small black hole is stable in the region between the red and black curves whereas the large black hole is thermodynamically stable in the region enclosed by the black and blue lines. However, from the ensemble point of view, one stable black hole state may turn into another stable state due to thermal fluctuations. The dynamics of such evolution of the system is described by the probabilistic Fokker-Planck equation. We will investigate the dynamics of the phase transition in the following section.

4.4 Probabilistic evolution on the free energy landscape

In this section, we study the kinetics of black hole phase transition by considering black holes as thermodynamic states in the extended phase space. We have observed that the large and small black hole phases can switch into each other due to the presence of thermal fluctuations. Note that the black hole radius r_+ is taken as the order parameter which characterises the black hole phases. Therefore, the probability distribution of the thermodynamic state can be consider as a function of r_+ and time t .

4.4.1 Fokker-Planck equation and probabilistic evolution

We denote the distribution function $\rho(r_+, t)$. Now, the evolution of the distribution is governed by the probabilistic Fokker-Planck equation given by

$$\frac{\partial \rho(r_+, t)}{\partial t} = D \frac{\partial}{\partial r} \left\{ e^{-\beta G(r_+)} \frac{\partial}{\partial r} \left[e^{\beta G(r_+)} \rho(r_+, t) \right] \right\} \quad (4.12)$$

Here, D is the diffusion coefficient and is given by $D = kT/\xi$, with k , ξ denoting the Boltzmann constant and dissipation coefficient respectively. Also, the quantity $\beta = 1/(kT)$ is the inverse temperature of the system. For convenience, we take $k = \xi = 1$ without the loss of generality.

To solve the Fokker-Planck equation, we need to impose two boundary conditions. The first one is the reflecting boundary condition which preserves the normalisation of the

probability distribution. At $r_+ = r_0$, we set,

$$e^{-\beta G(r_+)} \frac{\partial}{\partial r} [e^{\beta G(r_+)} \rho(r_+, t)] \Big|_{r_+=r_0} = 0,$$

which can be rewritten as,

$$\beta G'(r_+) \rho(r_+, t) + \rho'(r_+, t) \Big|_{r_+=r_0} = 0, \quad (4.13)$$

where the prime denotes the derivative with respect to the order parameter r_+ . The second boundary condition sets the value of the distribution function to zero,

$$\rho(r_0, t) = 0 \quad (4.14)$$

In the following analysis, we chose the reflecting boundary condition at $r_0 = 0$ and $r_0 = \infty$. The initial distribution is taken to be a Gaussian wave packet located at r_i , which is a good approximation of δ - distribution.

$$\rho(r_+, 0) = \frac{1}{\sqrt{\pi a}} e^{-\frac{(r-r_i)^2}{a^2}}, \quad (4.15)$$

where the parameter a is a constant which determines the initial width of the wave packet. Note that the initial distribution is well normalised, and as a consequence of the reflection boundary condition $\rho(r_+, t)$ will remain normalised during the evolution. The parameter r_i denotes the radius of the initial black hole state. We may choose either $r_i = r_s$ representing SBH as the initial state or $r_i = r_l$ for LBH. Suppose we chose $r_i = r_l$ at $t = 0$. As the distribution evolve, we observe a non-zero probability distribution for both SBH and LBH states. This indicates the phase transition between LBH and SBH phases due to the thermal fluctuations. The time evolution of $\rho(r_+, t)$ is plotted in Fig. (4.4).

In Fig. (4.4)(a) and (4.4)(b), we set $r_i = r_s$, and studied the evolution of the distribution for two values of the transition temperatures ($T_{trans} = 0.4, 0.5$). Initially, the probabilistic distribution is peaked at $r_+ = r_s$. The probabilistic distribution becomes

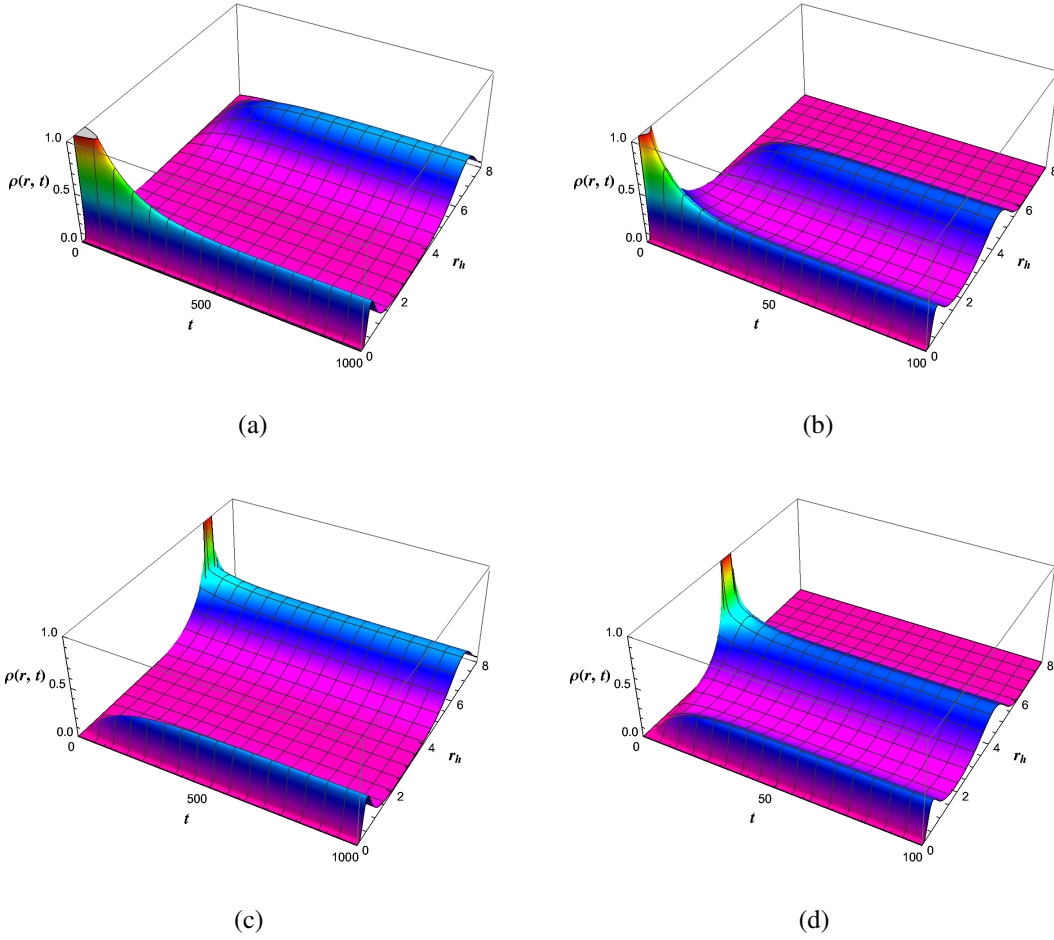


Figure 4.4: The time evolution of the probability distribution function $\rho(r, t)$. In (a) and (b) the initial condition is chosen at SBH state and in (c) and (d) it is at LBH state. The reflecting boundary conditions are imposed at $r = 0$ and $r = \infty$. The coexistent temperatures are $T_E = 0.4$ in left panel) and $T_E = 0.5$ in right panel) with $c_1 = 2, q = 1, m = 1, c_0 = 1, c_2 = 5$ and $k = 1$.

quasi-stationary in a short time with peaks at small and large black hole states. After some time, the height of $\rho(r_+, t)$ at $r_+ = r_s$ decreases while another peak starts to develop at $r_+ = r_l$. This implies the leakage of small black hole state to large black hole state. Further, as $t \rightarrow \infty$, $\rho(r_+, t)$ becomes a stationary state. A similar behaviour is observed if we take the initial state to be a large black hole. The corresponding evolution for two different temperatures are depicted in Fig. 4.4(c), and 4.4(d).

The above analysis can be made more apparent by comparing the behaviour of $\rho(r_s, t)$ and $\rho(r_l, t)$ as time progresses, where $\rho(r_s, t)$, $\rho(r_l, t)$ represent the probability

distribution of SBH and LBH states respectively. In Fig. 4.5, the evolution of probability distribution for both black hole states are depicted for two different transition temperatures. In both cases, we have taken the initial black hole state to be SHM. In other words, at $t = 0$, $\rho(r_s)$ takes a finite value but $\rho(r_l)$ vanishes. Fig. 4.5(a) describes the evolution of both probability distributions for a transition temperature $T_{trans} = 0.4$. Now, as time increases, the height of $\rho(r_s, t)$ decreases while that of $\rho(r_l, t)$ increases, indicating the leakage of black hole states from SBH to LBH. For large values of time, both $\rho(r_s, t)$ and $\rho(r_l, t)$ approaches a final stationary state where $\rho(r_s) = \rho(r_l)$. In Fig. ??(b), the same evolution is drawn but for a higher transition temperature, $T_{trans} = 0.5$. From the figure, we observe that for larger transition temperatures, both distribution reaches the stationary state more rapidly. A similar analysis can be carried out by taking other black hole state as the initial configuration giving the same results.

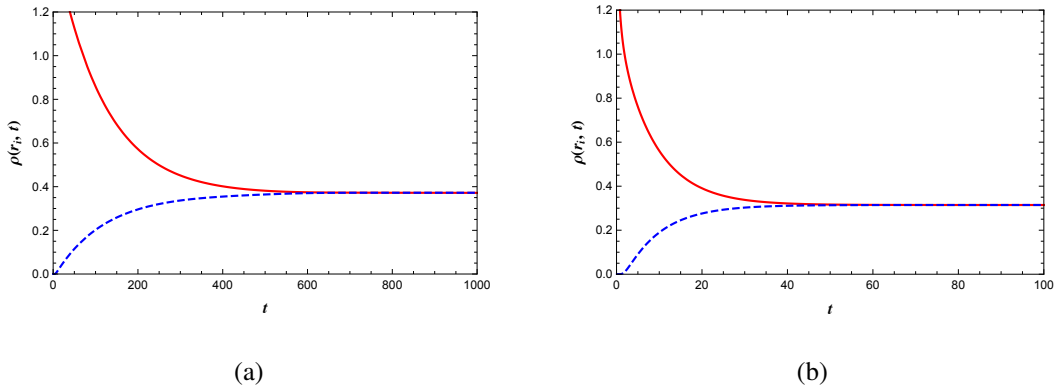


Figure 4.5: The time evolution of the probability distribution $\rho(r, t)$. The solid red and dashed blue curves correspond to the functions $\rho(r_{hs}, t)$ and $\rho(r_{hl}, t)$, respectively. The initial Gaussian wave packet is located at SBH state. The coexistent temperatures are (a) $T_E = 0.4$. (b) $T_E = 0.5$, with $c_1 = 2, q = 1, m = 1, c_0 = 1, c_2 = 5$ and $k = 1$.

In the coming session, we will study the kinetics by first passage process from one black hole state to another black hole state on the underlying free energy landscape. First passage time is a very important quantity in transition state theory, and is used to find out the time that it takes for a state starting from one stable phase to reach another stable phase.

4.4.2 First passage time

A key factor to describe LBH-SBH phase transition is the first passage time. The first passage time is defined as the time required for the state of black hole from a stable phase (described by the minimum of Gibbs free energy) to reach the intermediate transition state (described by the maximum of Gibbs free energy) for the first time. Note that the black hole phase transition between two states under consideration is due to the thermal fluctuations in the system. Therefore, the first passage time will be a random variable. The probability that the present state of SBH that has not made a first passage by time t is defined as,

$$\Sigma(t) = \int_0^{r_m} \rho(r_+, t) dr_+, \quad (4.16)$$

where r_m is the radius of the intermediate black hole state obtained from Eq. (4.9). As the time progress, the probability that the system remains at SBH decreases and approaches to zero as $t \rightarrow \infty$, i.e., $\Sigma(t)_{t \rightarrow \infty} = 0$. This is due to the fact that the normalization of the probability distribution is preserved in this case. Similarly, one can start with an LBH state and define the probability distribution that the initial LBH state has not made a first passage by time t as,

$$\Sigma(t) = \int_{r_m}^{\infty} \rho(r_+, t) dr_+, \quad (4.17)$$

The time evolution of $\Sigma(t)$ for both SBH and LBH for two values of transition temperatures are plotted in Fig. 4.6. The probability distribution is clearly seen to vanish for long time evolutions. Further, the probability distribution decrease faster for transitions at higher temperature. Now, the first passage time is the probability that a small black hole state passes through the intermediate state for the first time in the interval $(t, t + dt)$. The distribution of first passage time is given by,

$$F_p(t) = -\frac{d\Sigma(t)}{dt} \quad (4.18)$$

Substituting for $\Sigma(t)$ and using the Fokker-Planck's equation along with the reflecting boundary condition at $r_+ = 0$ and absorbing boundary condition at $r_+ = r_m$, we get the

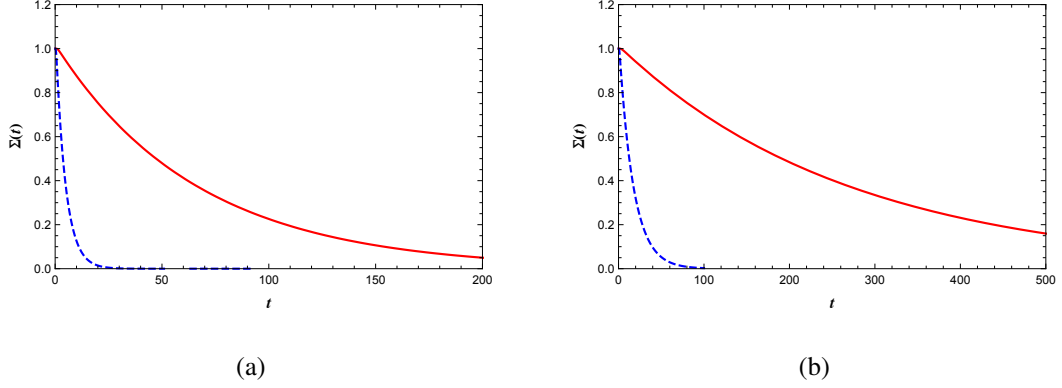


Figure 4.6: The time evolution of the distribution of the probability $\Sigma(t)$ that the system remains at the initial state. (a) Initially at SBH and (b) initially at LBH state. Red solid and blue dashed curves are for the coexistent temperatures $T_E = 0.4$ and $T_E = 0.5$, respectively, with $c_1 = 2, q = 1, m = 1, c_0 = 1, c_2 = 5$ and $k = 1$.

following expression for the first passage time.

$$F_p(t) = -D \frac{\partial}{\partial t} \rho(r_+, t) \Big|_{r=r_m} \quad (4.19)$$

The distribution of first passage time for both SBH to LBH and LBH to SBH phase transitions are plotted for different transition temperatures (Fig. 4.7). In Fig. 4.7(a), the initial distributions are Gaussian wave packets located at the small black hole state. The single peak in the first passage time within a short period of time indicates that a considerable fraction of the first passage events have occurred before the distribution attains its exponential decay form. As time increases the peak becomes more sharper. The curves corresponding to different transition temperatures show similar behaviour of the first time. Further, when the initial state is SBH, the location of the peak moves to left (lower value of time) when the transition occur at larger transition temperatures. This characteristics can be justified by looking at the behaviour of the barrier height between the small and intermediate black hole states as a function of temperature. As mentioned in section 4.3, $G(r_m) - G(r_s)$ decreases as temperature increases. Therefore, the small black hole state can cross the barrier to reach the intermediate state easily at higher transition temperatures. However, if the initial distribution is peaked at large black hole state, the location of the peak moves to right (higher values of time) when

the transition occur at larger transition temperatures Fig. 4.7(b). Similar to the previous case, this behaviour is explained as follows: As the barrier height $G(r_m) - G(r_l)$ increases with the temperature, the large black hole state takes more time to cross the barrier under thermal fluctuations. These results are qualitatively similar to the case of dynamics of phase transitions charged AdS black holes presented in Li et al. (2020).

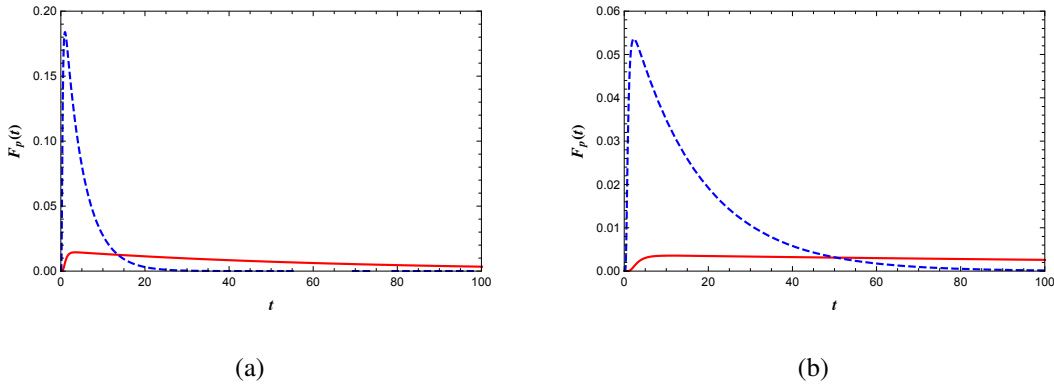


Figure 4.7: The probability distribution of the first passage time $F_p(t)$. Red solid and blue dashed curves are for the coexistent temperatures $T_E = 0.4$ and $T_E = 0.5$, respectively. (a) From SBH state to LBH state. (b) From LBH state to SBH state. Here, $c_1 = 2, q = 1, m = 1, c_0 = 1, c_2 = 5$ and $k = 1$.

In the following, we investigate the role of mass and the topological parameter on the results discussed above on the dynamic phase transition of black holes in massive gravity theory.

4.5 The effect of mass and topology

Note that the numerical results presented so far in the investigation of the dynamics of black hole phase transition in dRGT non-linear massive gravity theory consider only certain values of the parameters in the system. It still remains to study the behaviour of time evolution of the probability distribution and the first passage time by varying those parameters. However, as the theory possess too many variables, we will be considering the effect of mass and the topology only.

In Fig. 4.8, the evolution of probability distribution function is plotted for different topologies and masses. Here, we have considered planar ($\kappa = 0$), hyperbolic ($\kappa = -1$),

and spherical ($\kappa = 1$) topologies. For the sake of demonstration the initial black hole is taken as small black hole (SBH) state and the transition temperature to be $T_E = 0.4$ (Fig. 4.8(a)). One can see from the figure that the height of $\rho(r_s, t)$ decreases rapidly for $\kappa = -1$, indicating a quick leakage of black hole state from SBH to LBH. For the case of planar topology, the transition is less rapid and for the spherical case, the evolution is slow. This means that out of three, the spherical black holes attain the stationary state only after a long evolution. Further, the value of the probability distribution at the stationary state ($\rho(r_s) = \rho(r_l)$) is highest for the spherical case compared to the planar and hyperbolic cases. The effect of mass parameter shows a similar behaviour. As m increases, the system attains its final stationary state slowly. We conclude, as the mass increases the small black hole state leaks towards the large black hole state slowly (Fig 4.8(b)).

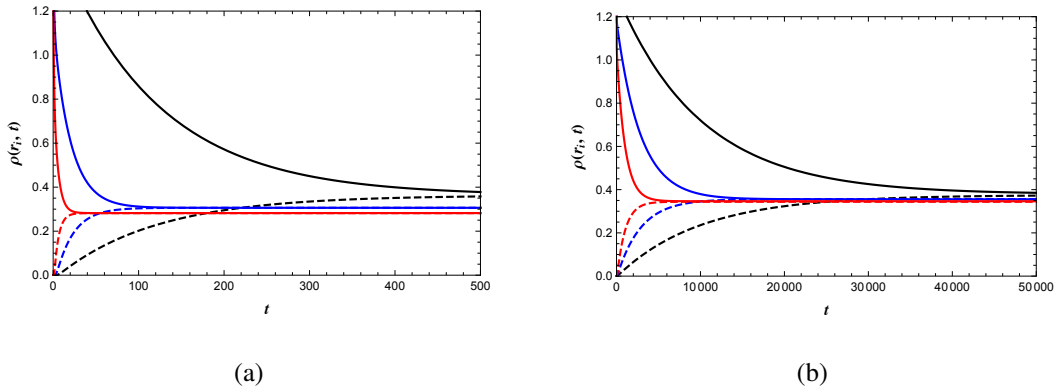


Figure 4.8: The effect of the parameters on the time evolution of the probability distribution $\rho(r, t)$. The solid and dashed curves correspond to the functions $\rho(r_{hs}, t)$ and $\rho(r_{hl}, t)$, respectively. The initial Gaussian wave packet is located at SBH state. (a) The effect of topology. Black, blue and red correspond to $k = 1, 0, -1$, respectively. The coexistent temperature is $T_E = 0.4$. (b) The effect of mass parameter m . Red, blue and black correspond to $m = 0, 0.07, 0.1$, respectively. The coexistent temperature is $T_E = 0.03$. The other parameters in these two plots are, $c_1 = 2, q = 1, m = 1, c_0 = 1, c_2 = 5$ and $k = 1$.

The effect of topology and mass on the probability distribution of first passage time is in accordance with the above findings Fig. 4.9. We have considered an initial small black hole state within the topologies $\kappa = 0, -1$ and 1. For a given transition tempera-

ture, the small black hole state reaches the intermediate state in a small duration of time for hyperbolic topology. In the case of spherical topology the corresponding time is maximum Fig. 4.9(a). Further, we observe that the time taken to reach the intermediate state, starting from SBH increases as mass increases (Fig. 4.9(b)).

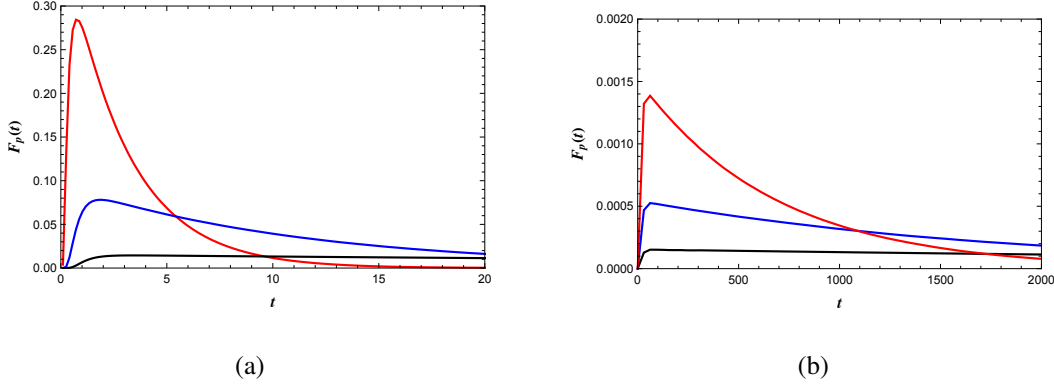


Figure 4.9: The effect of the spacetime parameters on the probability distribution of the first passage time $F_p(t)$. We consider the case for SBH (initial) state to LBH state. (a) The effect of topology. Black, blue and red solid lines are for $k = 1, 0, -1$, respectively. The coexistent temperature is $T_E = 0.4$. (b) The effect of mass parameter m . Red, blue and black correspond to $m = 0, 0.07, 0.1$, respectively. The coexistent temperature is $T_E = 0.03$. The other parameters in these two plots are, $c_1 = 2, q = 1, m = 1, c_0 = 1, c_2 = 5$ and $k = 1$.

4.6 Discussions

We have studied the dynamics of black hole phase transitions in dRGT non-linear massive gravity theory using the free energy landscape. Thermodynamic characterization and different black hole phases are discussed by considering the black hole radius as an order parameter. Emergent phases of small and large black holes as well as the coexisting curve between these states are shown. The switching of one black hole phase to another due to thermal fluctuations is addressed in terms of first passage time. Further, we have solved the Fokker-Planck equation numerically and the results are explained. The results we have presented are qualitatively similar to the findings of (Li et al. 2020). Finally, we have discussed the effect of mass parameters and the topology on the evolution of black hole phase transition between small and large black hole states.

Chapter 5

Physical process version of first law

5.1 Introduction

Black holes are perhaps the simplest non-trivial solutions of Einstein's field equations. However, the implications of its geometry are both interesting and intriguing. The presence of a horizon prevents classical information, inside the horizon, from reaching an asymptotic observer. Due to this fact, the black hole horizon can be treated as an inner boundary of spacetime. It is this feature that gives rise to a relation between the infinitesimal changes in mass, charge, angular momentum of a black hole and the change of its horizon area, akin to the first law of thermodynamics (Bardeen et al. 1973b). These infinitesimal changes are on the space of stationary black hole solutions, and this relation is referred to as the *stationary state* version of the first law. Further, it was argued that black holes, in general relativity, can be endowed with an entropy which is proportional to the area of the horizon (Bekenstein 1972, 1973). The result of (Hawking 1972, 1975) that black holes radiate, quantum mechanically, like a black body, at a temperature equal to that of its surface gravity, further lends support to the fact that black holes indeed behave like thermodynamic objects. These further raise important questions regarding the quantum origin of this entropy and motivates the quest for a quantum theory of gravity. However, the first law, which is purely of classical origin, remains an important aspect to explore.

Black holes, as found in nature, are far from being appropriately described by global stationary black hole solutions. They evolve due to infalling matter, and the area of the

horizon changes with time. Unlike the infinitesimal change in the stationary state version of the first law, which is a change in the space of solutions, this is an evolution in time due to the process of matter falling into the black hole. Consequently, a different version of the first law holds and appropriately describes this situation. In this version one relates the time evolution of the entropy to the matter influx across the horizon (Hawking and Hartle 1972, Carter 1979, Wald 1995a) and is therefore called as the "physical process" version of the first law (PPFL). As will be explicit, PPFL can be locally characterized, and therefore, it also holds for a wider class of horizons, which does not require the specification of the asymptotic structure. As a result, PPFL holds in the context of Rindler (Jacobson and Parentani 2003), or for that matter, any bifurcate Killing horizon (Amsel et al. 2008).

If a stationary horizon is perturbed by some matter stress-energy tensor $T_{\mu\nu}$ and, once the black hole settles down to another stationary state, then PPFL provides a mathematical expression for the change in horizon area A_H as,

$$\frac{\kappa}{8\pi} \Delta A_H = \int_{\mathcal{H}} T_{\alpha\beta} \chi^\alpha \chi^\beta dA dt, \quad (5.1)$$

where dA is the area element of the horizon cross-section, t is the Killing parameter associated with the horizon-generating Killing vector χ^μ and κ denotes the surface gravity of the unperturbed horizon. Much like the equilibrium version of the usual first law of thermodynamics, the above relation will fail to hold, if considered between two nonequilibrium states, due to dissipative effects. This would mean that the process of evolution of an initial equilibrium state has taken place in a non-quasi-static manner. Then one can ask, what are the processes that are quasi-static such that PPFL continues to hold. It is important to note that while deriving the above relation, by a straightforward integration of the Raychaudhuri equation, there are two assumptions made. First, the process of horizon evolution must be quasi-static so that the terms which are of higher order in expansion and shear of the horizon can be neglected. Second, upon perturbation and in the course of evolution, no additional generators are added to the horizon. When an object falls into the black hole causing the evolution of the horizon, the interesting question is, what are the restrictions on the parameters of the object such

that the above assumptions remain valid. This query was first examined by (Thorne et al. 1986, Suen et al. 1988) and further extended for general perturbations by (Amsel et al. 2008) and (Bhattacharjee and Sarkar 2015).

A necessary condition such that the above assumptions remain valid during the evolution, is the avoidance of caustic formation along the horizon, a situation where the expansion becomes negative infinity. Not only does the formation of caustic violates the first assumption, but it also indicates the addition of new generators to the horizon. In $D = 4$, if a black hole of mass M is perturbed by a spherically symmetric object of mass m and radius r then in order to avoid caustic formation, along the horizon, the radius of the object (r) must satisfy $r > 2\sqrt{2Mm}$ (Thorne et al. 1986). Such a constraint on the size of the perturbing matter has also been obtained for Rindler horizon in arbitrary dimensions (Amsel et al. 2008) as well as for perturbing matter which is charged or rotating (Bhattacharjee and Sarkar 2015).

In this work, we demonstrate that even if such a constraint holds, the change in horizon entropy diverges, when considered between asymptotic cross-sections as pointed out in (Jacobson and Parentani 2003). However, we present an interesting observation that such divergences are absent for dimensions greater than 4. The question now is whether one can modify the PPFL to account for such situations or in more general situations where caustics ‘do’ form to the future of the bifurcation surface. The hint comes from a modification of PPFL suggested in (Mishra et al. 2018), where it was shown that one could choose arbitrary cross-sections as the initial and final slices, at the cost of introduction of an extra term in the first law expression. Hence we show that even if a caustic forms to the future of the bifurcation surface, one can take our initial slice beyond that point and write a modified PPFL. Finally, we discuss the same problem in the presence of a positive cosmological constant.

5.2 Evolution of the horizon and the formation of caustic

In this section, we briefly review the derivation of PPFL as well as the conditions on the perturbation strength, along the lines of (Amsel et al. 2008) and (Bhattacharjee

and Sarkar (2015), such that caustic is avoided to the future of the bifurcation surface. Consider a space-time with a bifurcate Killing horizon. Suppose some energy flux falls across an initially stationary bifurcate Killing horizon. Due to the teleological nature of the event horizon, it starts expanding even when there is no flux across it and finally settles down to another stationary state once the passage of all matter has ceased. The corresponding change in the expansion θ , of the horizon, is governed by the Raychaudhuri equation for null-congruences, associated with the horizon generating Killing vector χ^μ ,

$$\frac{d\theta}{dt} = \kappa\theta - \frac{1}{2}\theta^2 - \sigma_{\mu\nu}\sigma^{\mu\nu} - R_{\alpha\beta}\chi^\alpha\chi^\beta. \quad (5.2)$$

We have parametrized the geodesics by the Killing time t and $t = -\infty$ corresponds to the bifurcation surface. Further, κ is defined as $\chi^\mu\nabla_\mu\chi^\nu = \kappa\chi^\nu$ and $\sigma_{\mu\nu}$ represents the shear of this congruence. The basic assumption one takes while deriving the physical process version of the first law is that the process of horizon evolution is quasi-stationary (quasi-static in the thermodynamic sense), such that one can neglect terms which are higher-order in θ and $\sigma_{\mu\nu}$, in Raychaudhuri equation. Under this assumption, Eq. (5.2) becomes,

$$-\frac{d\theta}{dt} + \kappa\theta = \mathcal{S}(t), \quad (5.3)$$

where $\mathcal{S}(t) = 8\pi T_{\alpha\beta}\chi^\alpha\chi^\beta$ is the perturbing energy flux. One exploits the Green's function technique to solve this differential equation. Further, using the expression $\theta = \frac{1}{\Delta A} \left(\frac{d(\Delta A)}{dt} \right)$, one gets the final result as,

$$\frac{d(\Delta A)}{dA} = \frac{8\pi}{\kappa} \int_{-\infty}^{\infty} dt T_{\alpha\beta}\chi^\alpha\chi^\beta, \quad (5.4)$$

where A denotes the area of horizon cross-section. The right-hand side of the above equation can be identified as the Killing energy (E_χ) associated with χ^μ , which is the amount of energy crossing the horizon. Thus we have the first law,

$$\frac{\kappa\Delta A}{8\pi} = \Delta E_\chi, \quad (5.5)$$

where ΔA represents the difference between the area of the perturbed horizon in the asymptotic future and the initial area of the horizon before perturbation. The lower limit of the integration was taken to be the bifurcation surface ($t = -\infty$). As we have discussed before, the crucial assumption one has to make while deriving the first law is the quasi-stationarity of the horizon evolution. This statement about quasi-stationarity can be quantified by calculating a threshold value of θ , beyond which caustics set in. To arrive at an expression for the threshold value, consider the homogeneous version ($\mathcal{S} = \sigma^2 = 0$) of the Raychaudhuri equation,

$$\left(-\frac{d}{dt} + \kappa\right) \frac{\theta}{2\kappa} - \kappa \left(\frac{\theta}{2\kappa}\right)^2 = 0. \quad (5.6)$$

Solving for $(\theta/(2\kappa))$ we obtain,

$$\frac{\theta}{2\kappa} = \frac{1}{\left(1 + \left(\frac{2\kappa}{\theta_0} - 1\right) e^{\kappa(t_0 - t)}\right)}, \quad (5.7)$$

where θ_0 is the expansion of the horizon at some time t_0 before the driving force acts. We can clearly see that, if $\theta_0/(2\kappa) > 1$, then θ increases to the past and becomes infinite at some finite time $t < t_0$ (Thorne et al. 1986). This means, if the expansion becomes greater than 2κ at any instance during the evolution, then the Raychaudhuri equation implies that the horizon would develop a caustic at a finite earlier time. Evidently, our earlier approximation in deriving the first law breaks down in this case. Our goal is to see what this condition means in terms of the parameters of the perturbing object. Before proceeding, we outline a few equations related to the horizon evolution.

The complete description of the horizon evolution is governed by two equations. The Raychaudhuri equation (Eq. (5.2)), which says how the expansion changes along the horizon Killing parameter and, the tidal force equation which gives the evolution of the shear $\sigma_{\mu\nu}$, i.e.,

$$\frac{d\sigma_{\mu\nu}}{dt} = (\kappa - \theta)\sigma_{\mu\nu} - \sigma_{\mu\sigma}\sigma^\sigma{}_\nu + \frac{1}{2}\sigma^2 h_{\mu\nu} + (2\sigma_{\mu\sigma} + \theta h_{\mu\sigma})\sigma^\sigma{}_\nu - \varepsilon_{\mu\nu}, \quad (5.8)$$

where $\varepsilon_{\mu\nu} = h_\mu^\alpha h_\nu^\beta C_{\alpha\lambda\beta\sigma} \chi^\lambda \chi^\sigma$ is the electric part of the Weyl tensor $C_{\alpha\lambda\beta\sigma}$, and, $h_{\mu\nu}$

is the projection operator onto the space-like cross-sections of the horizon and is defined as,

$$h_{\mu\nu} = g_{\mu\nu} + \chi_\mu l_\nu + \chi_\nu l_\mu. \quad (5.9)$$

Here l_μ is an auxiliary null vector, defined as $l_\mu \chi^\mu = -1$. If the horizon perturbation is weak, then both Eq. (5.2) and Eq. (5.8) will get simplified significantly. We take the tidal field, which sources the evolution of shear, to be of first-order in a small dimensionless parameter $m\kappa$. Here, m denotes the mass of the perturbing object, and κ is the surface gravity of the unperturbed horizon. Truncating both equations to lowest order in the perturbation parameter, we get,

$$-\frac{d\sigma_{\mu\nu}}{dt} + \kappa\sigma_{\mu\nu} = \varepsilon_{\mu\nu}, \quad (5.10)$$

and,

$$-\frac{d\theta}{dt} + \kappa\theta = \mathcal{S}(t) + \sigma^2. \quad (5.11)$$

The tidal field sources the evolution of the shear $\sigma_{\mu\nu}$ according to Eq. (5.10) and this $\sigma_{\mu\nu}$ along with the non-gravitational energy flux determines the horizon expansion through Eq. (5.11). The above equations can be solved to get,

$$\sigma_{\mu\nu}(t) = \int_{-\infty}^{\infty} \varepsilon_{\mu\nu}(t') e^{\kappa(t-t')} \Theta(t'-t) dt', \quad (5.12)$$

$$\theta(t) = \int_{-\infty}^{\infty} (\mathcal{S}(t') + \sigma^2(t')) e^{\kappa(t-t')} \Theta(t'-t) dt'. \quad (5.13)$$

Having laid out the necessary tools, we now proceed to calculate the conditions on the parameters of the perturbing object so that the PPFL remains valid. The investigation was first carried out in (Thorne et al. 1986, Suen et al. 1988), where authors considered the perturbation of a Kerr black hole by a freely falling object. The calculations were done by a justifiable approximation of a Kerr horizon by a Rindler horizon (RH), the horizon perceived by an accelerating observer in flat spacetime. They arrived at the following condition on the radius (r) of the perturbing object so that the PPFL remains

valid.

$$r > 2\sqrt{\frac{m}{2\kappa}}, \quad (5.14)$$

where κ is the surface gravity of the black hole and m is the mass of the perturbing object. If the radius of the perturbing object, falling into the horizon, is less than that of the threshold value give by Eq. (5.14), then caustic will form along the horizon invalidating the approximations made while deriving PPFL. This result, however, cannot be adopted for the case of Rindler horizon by taking $\kappa \rightarrow 0$ limit. This was pointed out later in (Amsel et al. 2008) and a result that holds for general bifurcate Killing horizons, in spacetime dimension $D \geq 3$, was obtained. Further, in (Bhattacharjee and Sarkar 2015), the authors considered situations where a freely falling charged or rotating object perturbs a Rindler horizon in $D = 4$.

5.3 Perturbation of Rindler horizon by a freely falling object

In this section, we briefly recap the problem regarding the validity of PPFL by considering a horizon perturbation by a freely falling object. We obtain a constraint on the size of the perturbing object so that caustic formation is avoided along the horizon. Further, we explicitly show how to establish the first law even if caustic forms along the horizon at some point in time. To calculate horizon expansion of a black hole, we approximate the black hole horizon by a horizon perceived by an accelerating observer in flat spacetime (Rindler horizon). This is very reasonable since we restrict the region of study very close to the event horizon, which can be approximated to be Rindler. Then, we can obtain the corresponding results for the perturbation of the black hole horizon, as explained in Appendix (B). From now on, we will be considering the evolution of the Rindler horizon only.

5.3.1 Caustic avoidance of Rindler horizon in four spacetime dimension

Consider a spherically symmetric object falling across a Rindler horizon. We assume that the mass of the perturbing matter is very small so that one can neglect the back-

reaction effects. Also, we neglect terms which are higher-order in m throughout the calculations, where m is the mass of the perturbing object. In Minkowski coordinates (T, Z, x, y) , the trajectory of the freely falling object is given as, $x = y = 0$, and $Z = z_0$. The perturbing object is characterized by the solution of the linearized Einstein's field equations. In isotropic coordinates, the perturbing metric is given as,

$$ds^2 = - \left(1 - \frac{2m}{\sqrt{\rho^2 + (Z - z_0)^2}} \right) dT^2 + \left(1 + \frac{2m}{\sqrt{\rho^2 + (Z - z_0)^2}} \right) (dZ^2 + d\rho^2 + \rho^2 d\theta^2), \quad (5.15)$$

where $\rho^2 = x^2 + y^2$. We calculate the non-zero components of the electric part of the Weyl tensor. On the horizon ($T = Z$) we have,

$$\varepsilon_{\rho\rho} = -\frac{1}{\rho^2} \varepsilon_{\theta\theta} = \left(\frac{-3m\rho^2 \kappa^2 Z^2}{(\rho^2 + (Z - z_0)^2)^{\frac{5}{2}}} \right) + O(m^2). \quad (5.16)$$

Further, we express the above relation in terms of advanced Killing time which is related to the Minkowski time co-ordinate as,

$$t = \frac{1}{\kappa} \ln \left(\frac{\kappa}{2} (T + Z) \right). \quad (5.17)$$

Along the horizon we have,

$$T = Z = z_0 e^{\kappa \bar{t}}, \quad (5.18)$$

where $\bar{t} = t - t_0$ is the shifted Killing time and t_0 denotes the time at which matter crosses the horizon. For $\kappa \bar{t} \ll 1$ one can expand the above exponential. Thus the electric part of the Weyl tensor becomes,

$$\varepsilon_{\rho\rho} = -\frac{3\rho^2 \kappa^2 z_0^2 m}{(\rho^2 + z_0^2 \kappa^2 \bar{t}^2)^{\frac{5}{2}}}. \quad (5.19)$$

One can see that the maximum contribution to the electric part of the Weyl tensor comes from $\bar{t} = 0$. We assume $\rho/z_0 \ll 1$. Now, the time dependence of the above function can be effectively described by a delta function peaked at $\bar{t} = 0$ (Thorne et al. 1986). This

can be understood by plotting the behavior of the Weyl tensor as a function of $\kappa\bar{t}$. One can easily see from the figure (5.1) that the Weyl tensor behaves like a delta function in the region $\rho/z_0 \ll 1$. Therefore, we express the electric part of the Weyl tensor as,

$$\epsilon_{\rho\rho}(\bar{t}) = -\frac{4m\kappa z_0}{\rho^2} \delta(\bar{t}). \quad (5.20)$$

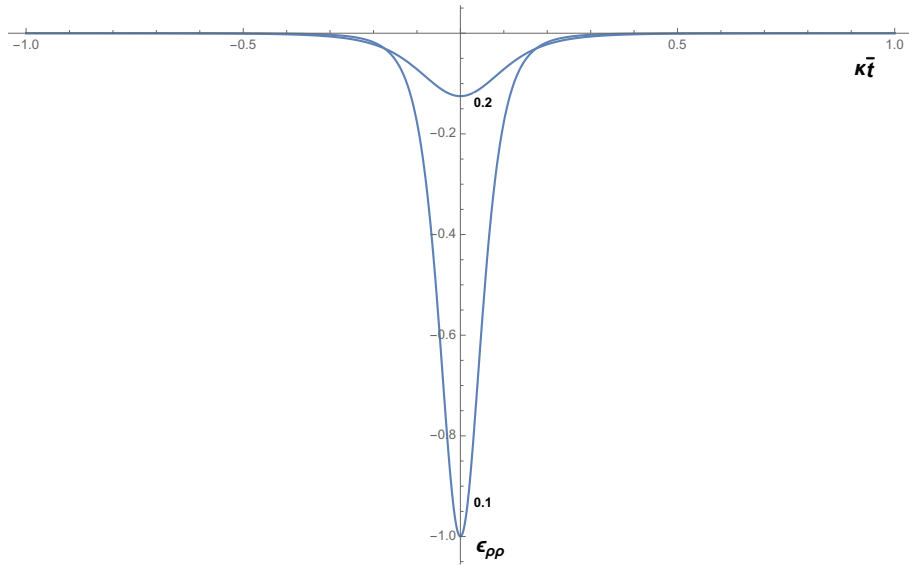


Figure 5.1: Behaviour of the Weyl tensor against $\kappa\bar{t}$ for two different values of $\frac{\rho}{z_0}$. One can see that the profile tends to look like a delta function as $\frac{\rho}{z_0} \rightarrow 0$.

The approximation of Eq. (5.19) by Eq. (5.20) is justified as follows. It is clear that the maximum expansion obtained using Eq. (5.20) will always be greater than the one obtained from Eq. (5.19). Hence, if the maximum value of expansion obtained using Eq. (5.20) satisfies the condition of caustic avoidance, it will hold true for the expansion resulting from Eq. (5.19). Now, we calculate the horizon shear using Eq. (5.12). We get,

$$\sigma_{\rho\rho} = -\frac{1}{\rho^2} \sigma_{\theta\theta} = -\frac{4m\kappa z_0}{\rho^2} e^{\kappa\bar{t}} \Theta(-\bar{t}). \quad (5.21)$$

This expression says that the horizon shear vanishes once the perturbing object crosses the horizon ($\bar{t} = 0$). We now calculate the expansion of the horizon using Eq. (5.13).

The integration can be done easily, resulting in the following expression.

$$\theta(\bar{t}) = \frac{2}{\kappa} \left(\frac{4m\kappa z_0}{\rho^2} \right)^2 (1 - e^{\kappa\bar{t}}) e^{\kappa\bar{t}} \Theta(-\bar{t}). \quad (5.22)$$

Similar to the shear, the expansion of the horizon also vanishes after the object has crossed the horizon. It is to be noted that, the expression above determines the expansion of those geodesics which pass outside the perturbing object. Our goal here is to find the allowed sizes of the perturbing object so that no caustic forms along the horizon, ensuring the validity of the physical process first law. Note that the expression, i.e., Eq. (5.22), describes the expansion of a Rindler horizon when a spherically symmetric charged matter falls freely onto it. One can also find the corresponding expression for a black hole horizon by replacing z_0 with $1/\kappa$, where κ is the surface gravity of the black hole (Appendix B). If we approximate ρ by the radius r of the perturbing object¹, the condition for caustic avoidance along the horizon ($\theta_{\max} < 2\kappa$) reads,

$$r > 2\sqrt{\frac{m}{2\kappa}}. \quad (5.23)$$

This result has been reported in Thorne et al. (1986), Amsel et al. (2008), Suen et al. (1988).

5.3.2 Caustic avoidance for higher dimensional Rindler horizon

In dimensions higher than 4, one can calculate the bound on the radius of the perturbing object by following the same steps and approximations as in section (5.3.1). The metric for the perturbing object in $(n+2)$ dimensional space-time is given by,

$$ds^2 = - \left(1 - \frac{Cm}{\left(\sqrt{\rho^2 + (Z - z_0)^2} \right)^{(n-1)}} \right) dT^2 + \left(1 + \frac{Cm}{(n-1) \left(\sqrt{\rho^2 + (Z - z_0)^2} \right)^{(n-1)}} \right) (dZ^2 + d\rho^2 + \rho^2 d\Omega_{n-1}^2), \quad (5.24)$$

¹This approximation is reasonable since we have shown that the electric part of the Weyl tensor behaves as a delta function peaked at $\bar{t} = 0$, which is the time at which perturbing matter crosses the horizon. At this point the radial co-ordinate ρ of the matter is essentially its radius r .

where $\rho^2 = \sum_{i=1}^n x_i^2$ and x_i 's are the Minkowski co-ordinates. The constant $C = \frac{16\pi}{n\Omega_n}$, with Ω_n being the volume of S^n . The non-zero components of the electric part of the Weyl tensor are calculated along the horizon ($Z - T = 0$) as,

$$\varepsilon_{\rho\rho} = -\frac{(n-1)}{g_{\theta_i\theta_i}} \varepsilon_{\theta_i\theta_i} = -\frac{(n-1)(n+1)Cm\kappa^2 Z^2 \rho^2}{2\left(\sqrt{\rho^2 + (Z-z_0)^2}\right)^{(n+3)}. \quad (5.25)$$

Proceeding with the same analysis as before, the formation of caustic is avoided if the radius of the object satisfies the following relation.

$$r > \left(\frac{4\pi\sqrt{n-1}mz_0}{\Omega_{n-1}}\right)^{\frac{1}{n}}. \quad (5.26)$$

This result was obtained in (Amsel et al. 2008). We would like to extend the analysis further. Suppose the radius of the perturbing object does not satisfy Eq. (5.23), then caustic may develop along the horizon at some finite earlier time. In such situations, the PPFL becomes invalid. However, we explicitly show that one can always recover the first law for a certain interval of horizon evolution according to (Mishra et al. 2018), in which the authors have obtained a first law expression for arbitrary horizon slices. During the analysis of such a first law, we, however, come across certain features related to the total entropy change of the horizon, which will be discussed thoroughly.

5.4 General structure of physical process first law and the law for arbitrary horizon cross-sections

Recall that in our earlier analysis, we had imposed a condition while deriving PPFL, that no caustic is formed to the future of the bifurcation surface. This assumption is necessary because one has to integrate the Raychaudhuri equation from the bifurcation surface to some stationary surface in the asymptotic future. However, one can always obtain a first law between two arbitrary horizon slices at the cost of an additional term in the first law. We begin with a brief outline of the modified PPFL as obtained in (Mishra et al. 2018). Consider the horizon perturbation due to some matter influx across the horizon. The entropy associated with the horizon is given by,

$$S = \frac{1}{4} \int_{\mathcal{H}} \sqrt{h} d^n x, \quad (5.27)$$

where the integration is over the horizon cross-section, and h denotes the determinant of the induced metric on its cross-section. The change in entropy along the horizon is given by,

$$\Delta S = \frac{1}{4} \int d^n x \int_{\lambda_1}^{\lambda_2} d\lambda \sqrt{h} \theta^{\text{aff}}, \quad (5.28)$$

where the expansion (θ^{aff}) along the affine parameter λ is $\theta^{\text{aff}} = \frac{d}{d\lambda} \ln \sqrt{h}$. One can integrate Eq. (5.28) by parts to obtain,

$$\Delta S = \Delta \left[\frac{1}{4} \int d^n x \lambda \theta^{\text{aff}} \sqrt{h} \right] - \frac{1}{4} \int d^n x \int_{\lambda_1}^{\lambda_2} d\lambda \lambda \sqrt{h} \left(\frac{d\theta^{\text{aff}}}{d\lambda} \right). \quad (5.29)$$

This relation can be recast in non-affine parametrization of the geodesics as,

$$\Delta S = \Delta \left[\frac{1}{4} \int d^n x \frac{1}{\kappa} \theta \sqrt{h} \right] - \frac{1}{4} \int d^n x \int_{t_1}^{t_2} dt \frac{1}{\kappa} \sqrt{h} \left(-\kappa \theta + \frac{d\theta}{dt} \right), \quad (5.30)$$

where κ is the same quantity as defined in section (5.2). The affine and the non-affine parameters are related by $d\lambda/dt = e^{\kappa t}$, and the relation between the expansions in different parametrizations is given by $\theta^{\text{aff}} = \theta/\kappa\lambda$. The evolution of θ along t is governed by the Raychaudhuri equation given by Eq. (5.2). We assume that the horizon perturbation is weak so that the higher-order terms can be neglected. Let the tidal field, which sources the evolution of shear is of the order of, $\varepsilon = m\kappa$. Truncating Eq. (5.2) to lowest order in ε , we get

$$-\frac{d\theta}{dt} + \kappa\theta = \mathcal{S}(t) + \sigma^2 + O(\varepsilon^2). \quad (5.31)$$

Consequently, the entropy change (Eq. (5.30)) becomes,

$$\Delta S = \Delta \left[\frac{1}{4} \int d^n x \frac{1}{\kappa} \theta \sqrt{h} \right] + \frac{1}{4} \int d^n x \int_{t_1}^{t_2} dt \frac{1}{\kappa} (\sigma^2 + \mathcal{S}(t)) \sqrt{h}. \quad (5.32)$$

We are interested in the dynamics of those geodesics which do not intersect the in-

falling body. Hence, the σ^2 is the leading order term in this case. The above expression is called the *modified version of the physical process first law*. The important point here is that the above relation determines the entropy change of the horizon between two arbitrary horizon Killing times. However, this relation holds only for some duration of the horizon evolution at which one can neglect the effect of θ^2 terms in the Raychaudhuri equation. The above expression, when evaluated for $t_2 \rightarrow \infty$ and $t_1 \rightarrow -\infty$, the first term vanishes, and one gets back the original form of the PPFL. The following assumptions are made in the process:

1. The horizon eventually settles down to a new stationary state. Therefore, the first term evaluated at $t_2 \rightarrow \infty$ is zero, by assumption.
2. The first term is of higher-order at the bifurcation surface, provided the radius of the perturbing body satisfies the bound Eq. (5.23). This bound also ensures that no caustic forms to the future of the bifurcation surface.

We will show that the first assumption does not hold for Rindler horizons in four space-time dimensions. In fact, there is a non zero contribution coming from the upper limit. We will show that though θ goes to zero at the asymptotic slice, its integral over the cross-section does not. Further, the second term in Eq. (5.32) diverge when the spatial integration is taken over the entire cross-section. Hence one is bound to define a PPFL for arbitrary cross-sections.

We will also relax the second assumption in the following sense. The horizon evolution should be quasi-stationary (i.e., no caustic forms) between the concerned horizon slices only. Exploiting our results, one can choose the interval of horizon evolution where such a modified PPFL will hold for a given perturbing object. This way of looking at the problem is different since earlier we were concerned about the size of the perturbing object to keep the horizon evolution quasi-stationary. But now, we look for a suitable interval of horizon Killing time where the first law remains valid. As a consequence, t_1 cannot be taken at $-\infty$ but must be some finite value. Hence, we ask, given a model of perturbation can one find the temporal span of the horizon evolution where

the entropy change satisfies the relation given by Eq. (5.32)?

We answer the question posed above as follows: Suppose an object falls freely across the horizon at $t = 0$, which generates a non-zero expansion of the geodesics for $t < 0$. This means that the horizon expands from $t = -\infty$ and ceases to expand when the object hits the horizon ($t = 0$). A careful analysis of the Raychaudhuri equation reveals that if $\theta \approx 2\kappa$, then one cannot neglect the effect of θ^2 term while calculating the entropy change. Now, our problem reduces to finding the horizon Killing time ($t = \tau$) at which $\theta \approx 2\kappa$. One can explicitly show that Eq. (5.32) holds for t satisfying the condition: $\tau < t < \infty$. Consider the perturbation of a Rindler horizon by a spherically symmetric object. Suppose the object crosses the horizon at $t = 0$. Using the expressions for shear and expansion, we estimate the time at which the expansion becomes 2κ as,

$$\tau = \frac{1}{\kappa} \ln \left[\frac{1}{2} \left(1 - \sqrt{1 - N^{-1}} \right) \right], \quad (5.33)$$

where,

$$N = 8n(n-1) \left(\frac{\pi m}{\Omega_{n-1} \kappa \rho^n} \right)^2. \quad (5.34)$$

Once we find the lower bound for the Killing time, we use Eq. (5.32) to calculate the entropy change for $\tau < t < \infty$. However, one must ensure that the integrations are finite. This will answer whether the first assumption is correct and how one has to use the general expression (Eq. (5.32)) to get a finite answer for the entropy change. In the next section, we will show that if the integration over the cross-sections is taken over $[a, \infty)$ (where a should be taken as the radius of the object), then the future slice should be taken at some finite Killing time.

5.4.1 Divergences in four spacetime dimension

In this section, we evaluate the terms in Eq. (5.32) separately. Note that the approximations made in the previous section essentially hides all the far region behavior of the perturbing Weyl tensor. However, we find that the shear and the expansion can be calculated from the exact profile, i.e., Eq. (5.16) of the Weyl tensor, without the assumptions

made in the above section. Therefore, we can find the large distance behavior of both the shear and expansion, which are ignored while trying to find a lower bound on the size of the object. We discuss all these features one by one and explain its impact on the validity of the physical process first law. Now, with the full profile, the horizon shear is given by,

$$\sigma_{\rho\rho}(t) = -\frac{1}{\rho^2}\sigma_{\theta\theta} = \frac{2\kappa m z_0 e^{\kappa t}}{\rho^2} \left[\frac{\left(z_0 (e^{\kappa t} - 1) \left(3\rho^2 + 2z_0^2 (e^{\kappa t} - 1)^2 \right) \right)}{2 \left(\rho^2 + z_0^2 (e^{\kappa t} - 1)^2 \right)^{3/2}} - 1 \right]. \quad (5.35)$$

The corresponding expression for expansion of the horizon is,

$$\theta(t) = \frac{\kappa m^2 z_0 e^{\kappa t}}{8\rho^4} \left[-15\pi\rho + \frac{64 \left(\rho^2 + 2z_0^2 (e^{\kappa t} - 1)^2 \right)}{\sqrt{\rho^2 + z_0^2 (e^{\kappa t} - 1)^2}} + 30\rho \tan^{-1} \left(\frac{z_0 (e^{\kappa t} - 1)}{\rho} \right) \right. \\ \left. - \frac{2z_0 (e^{\kappa t} - 1) \left(47\rho^4 + 64z_0^4 (e^{\kappa t} - 1)^4 + 113\rho^2 z_0^2 (e^{\kappa t} - 1)^2 \right)}{\left(\rho^2 + z_0^2 (e^{\kappa t} - 1)^2 \right)^2} \right]. \quad (5.36)$$

Note that these quantities don't vanish immediately after the perturbing object crosses the horizon ². However, both the shear and the expansion vanishes at $t = \infty$. This ensures that the final black hole configuration is stationary. However, at $\rho = 0$, these quantities diverge. If the particle were replaced by an extended object, then these divergences would not have appeared because one should consider the metric in the interior of the body as well. Since we are interested in the horizon generators which do not intersect the body, our range of integration would be from some non-zero value of ρ . Hence this divergence is not a problem. Alternatively, one can say that the lower bound on the particle size takes care of this divergence.

To write Eq. (5.32), we need to evaluate the integrations over the cross-sections. Our goal is to verify whether the expression for the entropy change is finite or not. We

²The horizon expansion and shear become zero just after the perturbing object crosses the horizon if we approximate the electric part of the Weyl tensor by a delta function as used in [Amsel et al. \(2008\)](#). As mentioned above, we do not make such approximation in this section.

go ahead and calculate the time and ρ integral of these quantities which appear in Eq. (5.32). One can show that the contribution to the entropy change due to the first term in Eq. (5.32) is finite. Hence, we will be interested in the quantity,

$$\int (\Sigma(t_2) - \Sigma(t_1)) \rho \, d\rho \, d\theta, \quad (5.37)$$

where $\Sigma(t)$ is defined as,

$$\Sigma(t) = \int dt \, \sigma^2 \sqrt{h}. \quad (5.38)$$

To demonstrate the divergences we will first find this integral over a finite range $\rho \in [a, b]$. This is given by the following expression.

$$\begin{aligned} & \frac{\pi \kappa m^2}{2} \left[16 \log \frac{\left(\sqrt{a^2 + z_0^2 z_2^2} + z_0 z_2 \right) \left(\sqrt{b^2 + z_0^2 z_1^2} + z_0 z_1 \right)}{\left(\sqrt{a^2 + z_0^2 z_1^2} + z_0 z_1 \right) \left(\sqrt{b^2 + z_0^2 z_2^2} + z_0 z_2 \right)} \right. \\ & + z_0^2 z_2 (z_2 + 1) \left(\frac{1}{b^2 + z_0^2 z_2^2} - \frac{1}{a^2 + z_0^2 z_2^2} \right) - z_0^2 z_1 (z_1 + 1) \left(\frac{1}{b^2 + z_0^2 z_1^2} - \frac{1}{a^2 + z_0^2 z_1^2} \right) \\ & + 7 \log \frac{(a^2 + z_0^2 z_1^2) (b^2 + z_0^2 z_2^2)}{(a^2 + z_0^2 z_2^2) (b^2 + z_0^2 z_1^2)} + \left(16 z_0^2 (z_1 - z_2) (z_1 + z_2 + 2) \right) \left(\frac{1}{b^2} - \frac{1}{a^2} \right) \\ & + 16 z_0 \left\{ (z_2 + 2) \left(\frac{\sqrt{b^2 + z_0^2 z_2^2}}{b^2} - \frac{\sqrt{a^2 + z_0^2 z_2^2}}{a^2} \right) + (z_1 + 2) \left(\frac{\sqrt{a^2 + z_0^2 z_2^2}}{a^2} - \frac{\sqrt{b^2 + z_0^2 z_1^2}}{b^2} \right) \right\} \\ & \left. + \frac{15 z_0}{b} \left\{ \tan^{-1} \left(\frac{z_0 z_2}{b} \right) - \tan^{-1} \left(\frac{z_0 z_1}{b} \right) \right\} + \frac{15 z_0}{a} \left\{ \tan^{-1} \left(\frac{z_0 z_1}{a} \right) - \tan^{-1} \left(\frac{z_0 z_2}{a} \right) \right\} \right], \end{aligned} \quad (5.39)$$

where $z_{1,2} = -1 + e^{\kappa t_{1,2}}$. If one takes the future slice at $t_2 \rightarrow \infty$ and then takes $b \rightarrow \infty$ limit, then the integral diverges, which means that if one wants to write down a physical process first law for an asymptotic slice besides integrating over the complete slices, then it fails. This was pointed out in (Jacobson and Parentani 2003). There is, of course, a way to avoid this problem. It is possible to get a finite result (ΔS) with an asymptotic slice if one restricts the change of area to some open region of the horizon slice. We will demonstrate this and explain the consequences. If one takes $t_2 \rightarrow \infty$ and subsequently does the ρ integration for some finite a, b , then the above expression (Eq.

(5.39)) becomes,

$$\begin{aligned}
& \frac{\pi \kappa m^2}{4} \left[-\frac{2z_0^2 z_1 (z_1 + 1)(a - b)(a + b)}{(a^2 + z_0^2 z_1^2)(b^2 + z_0^2 z_1^2)} + 15\pi z_0 \left(\frac{1}{b} - \frac{1}{a} \right) + 14 \log \frac{(a^2 + z_0^2 z_1^2)}{(b^2 + z_0^2 z_1^2)} \right. \\
& \quad \left. + 32z_0(z_1 + 2) \left(\frac{(z_0 z_1 - \sqrt{b^2 + z_0^2 z_1^2})}{b^2} - \frac{(z_0 z_1 - \sqrt{a^2 + z_0^2 z_1^2})}{a^2} \right) \right. \\
& \quad \left. + 32 \log \frac{(\sqrt{b^2 + z_0^2 z_1^2} + z_0 z_1)}{(\sqrt{a^2 + z_0^2 z_1^2} + z_0 z_1)} + 30z_0 \left\{ \frac{\tan^{-1}(\frac{z_0 z_1}{a})}{a} - \frac{\tan^{-1}(\frac{z_0 z_1}{b})}{b} \right\} \right]. \quad (5.40)
\end{aligned}$$

One can see that this quantity is finite for some finite value of b , but has a logarithmic term which diverges as $b \rightarrow \infty$. One would think that this can be avoided by putting an upper bound on the size of the particle. This, however, remains to be seen and will be addressed in some future work. Another way to obtain a finite value for ΔS is the following. If one keeps the final slice to be at some finite Killing time but integrates over the entire horizon cross-section ($b \rightarrow \infty$), the corresponding expression (Eq. (5.39)) is again finite.

$$\begin{aligned}
& -\frac{\pi \kappa m^2}{2} \left[\frac{16z_0^2}{a^2} \left(z_1(z_1 + 2) - z_2(z_2 + 2) \right) - \frac{16z_0(z_1 + 2)\sqrt{a^2 + z_0^2 z_1^2}}{a^2} \right. \\
& \quad \left. + 7 \log \frac{(a^2 + z_0^2 z_2^2)}{(a^2 + z_0^2 z_1^2)} + 16 \log \frac{(\sqrt{a^2 + z_0^2 z_1^2} + z_0 z_1)}{(\sqrt{a^2 + z_0^2 z_2^2} + z_0 z_2)} - \frac{z_0^2 z_1 (z_1 + 1)}{a^2 + z_0^2 z_1^2} + \frac{z_0^2 z_2 (z_2 + 1)}{a^2 + z_0^2 z_2^2} \right. \\
& \quad \left. + \frac{16z_0(z_2 + 2)\sqrt{a^2 + z_0^2 z_2^2}}{a^2} + \frac{15z_0}{a} \left(\tan^{-1} \left(\frac{z_0 z_2}{a} \right) - \tan^{-1} \left(\frac{z_0 z_1}{a} \right) \right) \right]. \quad (5.41)
\end{aligned}$$

We will use this feature to write a modified PPFL. Note that this problem arises only for the case of a Rindler horizon. In the case of a black hole horizon, there is a natural cut-off set by the curvature scale of the background black hole geometry, beyond which the Rindler approximation breaks down. In one of the following sections, we will show that this divergent feature does not arise in higher dimensions, even for Rindler horizons. That explains the necessity to write the first law between arbitrary slices at least in 4 spacetime dimensions. The other motivation for writing such a modified

PPFL is, of course, evading the lower bound on the radius of the object. We, therefore, conclude this section with an expression for ΔS between arbitrary slices but with ρ integration in the range $[a, \infty)$.

$$\begin{aligned} \Delta S = \frac{\pi m^2}{8a^2} & \left[7a^2 \log \frac{(a^2 + z_0^2 z_1^2)}{(a^2 + z_0^2 z_2^2)} - 16a^2 \log \frac{(\sqrt{a^2 + z_0^2 z_1^2} + z_0 z_1)}{(\sqrt{a^2 + z_0^2 z_2^2} + z_0 z_2)} \right. \\ & - 16z_0 z_1 \sqrt{a^2 + z_0^2 z_1^2} + 16z_0 z_2 \sqrt{a^2 + z_0^2 z_2^2} + 16z_0^2 (z_1 - z_2)(z_1 + z_2) \\ & \left. + 15a z_0 \left(2z_2 \tan^{-1} \left(\frac{z_0 z_2}{a} \right) - 2z_1 \tan^{-1} \left(\frac{z_0 z_1}{a} \right) + \pi(z_1 - z_2) \right) \right]. \end{aligned} \quad (5.42)$$

This expression, however, does not take into account the matter stress-energy tensor of the body itself. This contribution can only be calculated if one considers a realistic body for which the metric and the matter content of the interior is known. Note that if the size of the particle satisfies the bound found in section (5.3.1)³, then the initial slice (t_1) can be taken to be at the bifurcation surface, else, t_1 must satisfy $t_1 > \tau$, where τ is given in Eq. (5.33). The upper limit t_2 cannot, however, be taken to ∞ , if the integration over the cross-sections is taken up to $\rho \rightarrow \infty$, for Rindler horizons in four spacetime dimension. This expression, therefore, incorporates relaxation of both the assumptions discussed in section (5.4).

5.4.2 Dimensions greater than four

One can define the first law for the horizon cross-sections in higher dimensions, if one considers the evolution satisfying the assumptions detailed in section (5.4). But, as explained before, while calculating the change in entropy using Eq. (5.32), one should ensure that the integration does not diverge. Interestingly, in dimensions greater than four, the change in entropy is finite even if one considers the evolution of the generators up to infinite Killing time and over the entire horizon cross-sections (excluding $\rho = 0$). To see this, we analyze the expression for the change in entropy for arbitrary slices in higher dimensions. Similar to the case of 4 dimensions, the first term in the expression of entropy change (Eq. (5.32)) is finite even for large values of both ρ and t . But, one

³However, note that there is, of course, another bound that the radius must satisfy. The radius cannot be less than the Schwarzschild radius of the perturbing body.

should check the second term carefully to look for any divergences. We will explicitly calculate this particular term and show that unlike the case of four dimensions, the change in entropy is finite for dimensions higher than 4. First, we consider the evolution of the Rindler horizon in 5 dimensions. The radial component of the electric part of the Weyl tensor which generates shear is given by,

$$\varepsilon_{\rho\rho} = -\frac{32 m\rho^2 \kappa^2 z_0^2 e^{2\kappa t}}{3\pi \left(\rho^2 + z_0^2 (e^{\kappa t} - 1)^2\right)^3}. \quad (5.43)$$

The expression for the horizon shear is obtained as,

$$\sigma_{\rho\rho}(t) = \frac{4\kappa m z_0 e^{\kappa t}}{3\pi\rho^3} \left[\frac{\rho z_0 (e^{\kappa t} - 1) \left(5\rho^2 + 3z_0^2 (e^{\kappa t} - 1)^2\right)}{\left(\rho^2 + z_0^2 (e^{\kappa t} - 1)^2\right)^2} + 3 \tan^{-1} \left(\frac{z_0 (e^{\kappa t} - 1)}{\rho} \right) \right] - \frac{2\kappa z_0 m e^{\kappa t}}{\rho^3}. \quad (5.44)$$

Now, one can calculate the expansion of geodesics using Eq. (5.13).

$$\begin{aligned} \theta(t) = & \frac{2\kappa m^2 z_0 e^{\kappa t}}{9\pi^2 \rho^6} \left[-\frac{6\rho^2 (12\pi\rho + z_0 (e^{\kappa t} - 1))}{\rho^2 + z_0^2 (e^{\kappa t} - 1)^2} + \frac{16\rho^6 z_0 (e^{\kappa t} - 1)}{\left(\rho^2 + z_0^2 (e^{\kappa t} - 1)^2\right)^3} - 54\pi^2 z_0 e^{\kappa t} \right. \\ & + 6 \left\{ -37\rho + \frac{24\rho^3}{\rho^2 + z_0^2 (e^{\kappa t} - 1)^2} + 36\pi z_0 (e^{\kappa t} - 1) \right\} \tan^{-1} \left(\frac{z_0 (e^{\kappa t} - 1)}{\rho} \right) \\ & \left. - 216z_0 (e^{\kappa t} - 1) \tan^{-1} \left(\frac{z_0 (e^{\kappa t} - 1)}{\rho} \right)^2 + \frac{68\rho^4 z_0 (e^{\kappa t} - 1)}{\left(\rho^2 + z_0^2 (e^{\kappa t} - 1)^2\right)^2} + \pi(37\rho + 18\pi z_0) \right]. \end{aligned} \quad (5.45)$$

Note that the shear and the expansion are zero when evaluated at $t = \infty$, similar to the case of four dimensions. Also, the contribution to the entropy change from the first term of Eq. (5.32) is finite. Therefore, as in the case of four dimensions, we are worried about the second term in Eq. (5.32). We explicitly perform the integration to obtain the entropy change. The full expression for $\int (\Sigma(t_2) - \Sigma(t_1)) \rho^2 d\rho d\Omega_2$ integrated over $t \in [t_1, t_2]$ and $\rho \in [a, b]$ can also be found. One would then be able to see that the

$t_2 \rightarrow \infty$ and the subsequent $b \rightarrow \infty$ gives a finite result,

$$\begin{aligned}
& \frac{4}{9} \pi \kappa m^2 \left(-\frac{18z_0^2 z_1^2}{a^3} + \frac{36z_0 z_1 (2a - \pi z_0)}{\pi a^3} + \frac{18(\pi^2 - 4)a + 39\pi z_0}{\pi^2 a^2} - \frac{8(a^3 - az_0^2 z_1)}{\pi^2 (a^2 + z_0^2 z_1^2)^2} \right. \\
& \quad + \frac{72z_0^2 z_1 - 60a^2}{\pi^2 (a^3 + az_0^2 z_1^2)} - \frac{6(2z_1 + 1) \cot^{-1} \left(\frac{z_0 z_1}{a} \right)}{\pi^2 z_0 z_1^2} - \frac{6}{\pi^2 a z_1} + \frac{6z_1 + 3}{\pi z_0 z_1^2} \\
& \quad - \left(12(z_0^2 z_1 (z_1 + 2) - a^2) \tan^{-1} \left(\frac{z_0 z_1}{a} \right) + az_0 (24z_1 + 13) + 12\pi (a^2 - z_0^2 z_1 (z_1 + 2)) \right) \\
& \quad \left. \times \left(\frac{z_0 z_1}{a} \right) \frac{6}{\pi^2 a^3} \tan^{-1} \right). \tag{5.46}
\end{aligned}$$

Therefore, in the case of Rindler horizons in five spacetime dimension, the first assumption made in section (5.4) continues to hold. Hence there is no necessity to take the future slice to be at a finite Killing time. However, in principle, one can write an expression for entropy when the future slice is taken at some finite Killing time. The relaxation of the second condition can still be done (section (5.4)). The corresponding expression for entropy change is found to be,

$$\begin{aligned}
\Delta S = & \frac{m^2}{9\pi a^3 z_0 z_1 (a^2 + z_0^2 z_1^2)} \left[z_0 z_1 \left(2(9\pi^2 - 67)a^4 + 33\pi a^3 z_0 z_1 \right. \tag{5.47} \\
& + 6(6\pi^2 - 23)a^2 z_0^2 z_1^2 + 33\pi a z_0^3 z_1^3 + 18\pi^2 z_0^4 z_1^4 \right) + 6(a^2 + z_0^2 z_1^2) \tan^{-1} \left(\frac{z_0 z_1}{a} \right) \\
& \left. \times \left(a^3 + 12z_0 z_1 (a^2 + z_0^2 z_1^2) \tan^{-1} \left(\frac{z_0 z_1}{a} \right) - 12\pi a^2 z_0 z_1 - 11a z_0^2 z_1^2 - 12\pi z_0^3 z_1^3 \right) \right].
\end{aligned}$$

This expression again does not take into account the matter stress-energy tensor of the body itself. The future slice has been taken at the asymptotic Killing time. If a does not satisfy the bound given by Eq. (5.26), on the radius then t_1 must satisfy the bound $t_1 > \tau$, where τ is given by Eq. (5.33). If a satisfies the bound then t_1 can be taken at $-\infty$. For completeness, we will briefly outline the results obtained for six-dimensional Rindler space-time. In 6 dimensions, we have the following expressions for the electric

part of Weyl tensor.

$$\varepsilon_{\rho\rho} = -\frac{45 m\rho^2 \kappa^2 z_0^2 e^{2\kappa t}}{4\pi \left(\rho^2 + z_0^2 (e^{\kappa t} - 1)^2\right)^{\frac{7}{2}}}. \quad (5.48)$$

The expression for shear is given by,

$$\sigma_{\rho\rho}(t) = \frac{3\kappa m z_0^2 e^{\kappa t} (e^{\kappa t} - 1) \left(15\rho^4 + 8z_0^4 (e^{\kappa t} - 1)^4 + 20\rho^2 z_0^2 (e^{\kappa t} - 1)^2\right)}{4\pi\rho^4 \left(\rho^2 + z_0^2 (e^{\kappa t} - 1)^2\right)^{5/2}} - \frac{6\kappa m z_0 e^{\kappa t}}{\pi\rho^4}. \quad (5.49)$$

This expression is zero at $t = \infty$. One proceeds to calculate the expansion and is found to be zero at $t = \infty$, which ensures the future equilibrium configuration of the horizon. The contribution to the entropy change from the first term of Eq. (5.32) is finite. Therefore, we calculate the term $\int (\Sigma(t_2) - \Sigma(t_1)) \rho^3 d\rho d\Omega_3$ integrated over $t \in [t_1, t_2]$ and $\rho \in [a, b]$. The $t_2 \rightarrow \infty$ and the subsequent $b \rightarrow \infty$ again gives a finite result. The corresponding expression for change in entropy of Rindler horizon in 6 dimensions is calculated to be,

$$\Delta S = \frac{9m^2}{2048} \left[\frac{1890z_0z_1}{a^3} \cot^{-1} \left(\frac{z_0z_1}{a} \right) + \frac{2(73a^2 + 67z_0^2z_1^2)}{(a^2 + z_0^2z_1^2)^2} + \frac{158}{a^2} + \frac{4096z_0z_1 \left(z_0z_1 - \sqrt{a^2 + z_0^2z_1^2} \right)}{a^4} \right]. \quad (5.50)$$

We have analyzed the behavior of the entropy change for a Rindler horizon in different dimensions. An interesting observation thus made is, in 4 dimensions the expression for entropy change is infinite if one considers the evolution of all the geodesics for $\rho \in (0, \infty]$, and $t \rightarrow \infty$ limit. But such divergences do not arise for dimensions five and six. Therefore, by looking at the behavior of the expression for the entropy change, we conjecture that the change in horizon entropy is finite even the horizon evolution is taken up to $t \rightarrow \infty$ for dimensions greater than 4. We will analyze the same problem for space-times with non-zero cosmological constant below.

5.5 Horizon perturbation in arbitrary dimensional de-Sitter spacetime

As the final step of our analysis on the validity of PPFL, we consider the perturbation of a black hole horizon in $(n + 2)$ dimensional spacetime with a non-zero cosmological constant (Λ). Such space-times demand similar studies in their own rights owing to their importance in cosmology and holography. The interesting question now is how the introduction of a cosmological constant changes our previous results. We will be dealing with de-Sitter space-time only since the examination with the anti-de-Sitter is quite similar. In a small enough region, the event horizon of a Schwarzschild-de Sitter black hole can be approximated by a horizon, as perceived by an accelerating observer in Minkowski spacetime (Appendix B). We shall exploit this advantage to simplify our calculations. We will be considering only the perturbation of the black hole horizon (r_h) throughout this work since the cosmological horizon is of less importance for the study we are having. Basically, the calculations deal with the perturbation of the Rindler horizon in flat-space-time and the effect of Λ comes from the horizon perturbing matter. At the end of the calculations, we will revert the results back to the case of Schwarzschild-de Sitter black hole, as explained in Appendix B. We follow the same procedure as before to find the expansion of the horizon due to an infalling spherically symmetric object. We assume the mass m of the perturbing object is small so that one can treat the problem perturbatively. This allows us to consider the perturbing metric as a solution of linearized Einstein's equations in the presence of a positive cosmological constant. In isotropic coordinate system $(T, Z, \rho, \Omega_{n-1})$, the metric for the perturbing object is given by (Astefanesei et al. 2004),

$$ds^2 = - \left(1 - \frac{Cme^{-(n-1)H_0T}}{\left(\sqrt{\rho^2 + (Z - z_0)^2}\right)^{(n-1)}} \right) dT^2 \quad (5.51)$$

$$+ e^{2H_0T} \left(1 + \frac{Cme^{-(n-1)H_0T}}{(n-1)\left(\sqrt{\rho^2 + (Z - z_0)^2}\right)^{(n-1)}} \right) (dZ^2 + d\rho^2 + \rho^2 d\Omega_{n-1}^2),$$

where $\rho^2 = \sum_{i=1}^n x_i^2$ and $H_0^2 = 2\Lambda/(n(n+1))$. The constant $C = \frac{16\pi}{n\Omega_n}$, with Ω_n being the volume of S^n . The non-zero components of the electric part of the Weyl tensor are

calculated along the horizon ($Z - T = 0$).

$$\begin{aligned} \varepsilon_{\rho\rho} &= -\frac{(n-1)}{g_{\theta_i\theta_i}} \varepsilon_{\theta_i\theta_i} \\ &= -\frac{(n-1)Cm\kappa^2 Z^2 e^{-(n-1)H_0 Z}}{2\left(\sqrt{\rho^2 + (Z-z_0)^2}\right)^{(n+3)}} \left(\rho^2 (n + e^{2H_0 Z}) + (Z-z_0)^2 (e^{2H_0 Z} - 1) \right). \end{aligned} \quad (5.52)$$

Proceeding with the same analysis as before, we approximate the electric part of the Weyl tensor with a delta function centered at $\bar{t} = 0$, where \bar{t} is the shifted Killing time.

$$\varepsilon_{\rho\rho}(\bar{t}) = -\frac{(n-1)}{g_{\theta_i\theta_i}} \varepsilon_{\theta_i\theta_i} = -\frac{(n-1)}{n\Omega_{n-1}} \frac{8\pi m\kappa z_0}{\rho^n} e^{-(n-1)H_0 z_0} (n-1 + e^{2H_0 z_0}) \delta(\bar{t}). \quad (5.53)$$

This expression reduces to the one obtained in [Amsel et al. \(2008\)](#) for $H_0 = 0$. We calculate the shear of the horizon using Eq. [\(5.12\)](#) and the expansion using Eq. [\(5.13\)](#).

$$\begin{aligned} \theta(\bar{t}) &= \frac{n}{(n-1)\kappa} \left(\frac{(n-1)}{n\Omega_{n-1}} \frac{8\pi m\kappa z_0}{\rho^n} e^{-(n-1)H_0 z_0} (n-1 + e^{2H_0 z_0}) \right)^2 \\ &\quad \times e^{\kappa\bar{t}} (1 - e^{\kappa\bar{t}}) \Theta(-\bar{t}). \end{aligned} \quad (5.54)$$

The condition on θ such that a caustic forms, now reads,

$$\left(\frac{\theta}{n\kappa} \right)_{max} \geq 1. \quad (5.55)$$

This gives a limit on the size of the perturbing object to keep the horizon evolution quasi-stationary. Therefore, caustic formation along the horizon is avoided if,

$$r > \left(\frac{4\pi\sqrt{n-1}mz_0}{n\Omega_{n-1}} e^{-(n-1)H_0 z_0} (n-1 + e^{2H_0 z_0}) \right)^{\frac{1}{n}}, \quad (5.56)$$

where we have approximated the radial coordinate ρ with the radius of the object. One can check that for $\Lambda = 0$; this condition reduces the expression obtained in Eq. [\(5.26\)](#). For the case of black holes, the condition on the radius of perturbing matter to avoid caustic formation can be obtained as described in Appendix [\(B\)](#). One can see from the above expression that the allowed (no caustic) values for the radius of the perturbing

object get larger as the dimensionality increases.

Our analysis on the validity of PPFL for various perturbation set-ups completes here. We have investigated different cases of horizon perturbations and obtained conditions on the size of the object so that caustic will not form along the horizon, hence ensuring the validity of the first law. In the next section, we consider the case of modified PPFL relation discussed in (Mishra et al. 2018), where authors have obtained a first law relation for arbitrary horizon cross-sections. In the next section, we analyze the characteristics of the entropy change for a space-time with non-zero cosmological constant.

5.5.1 PPFL for arbitrary horizon cross sections in de-Sitter space-time

In this section, we look for a duration of horizon evolution in de-Sitter space-time, where one can establish the first law even if caustics form. As discussed before, caustic may develop along the horizon if the radius of the perturbing object doesn't obey Eq. (5.56). In the case of the horizon perturbation in Schwarzschild space-time, we have already explained the appropriate way to develop the notion of the first law in section (5.4). Now, we develop the same in the case of black hole perturbation in de-Sitter space-time, exploiting the results obtained above.

Before proceeding, let us recap the motive behind considering the horizon evolution between arbitrary slices. We have explained in section (5.2) that if the expansion of the black hole horizon becomes comparable to 2κ , where κ is the surface gravity of the black hole before perturbation, due to the infall of some matter at time $t = 0$, caustic will inevitably form along the horizon at some finite earlier time ($t < 0$). Evidently, the quasi-stationary approximation of the horizon evolution breaks down hence invalidating the first law. Interestingly, it has been shown in (Mishra et al. 2018), that one can still study the horizon evolution by excluding the non-quasi-stationary part of the evolution. This is achieved by slightly modifying the form of the first law as in section (5.4). Also, we have explained how this works in the case of the horizon perturbation of the Schwarzschild black hole. Here we give yet another simple calculation to exemplify the modified version of PPFL.

Consider the perturbation of a $(n + 2)$ dimensional Rindler horizon in de-Sitter spacetime by a spherically symmetric object. Suppose the radius of the object violates the condition to avoid caustic formation ($\theta < n\kappa$), at some point of horizon evolution ($t = \tau$). This spoils the quasi-stationarity nature of the process for $t < \tau$. But, one can still study the first law for $\tau < t < \infty$. The value of τ , for this case, can be calculated as,

$$\tau = \frac{1}{\kappa} \ln \left[\frac{1}{2} \left(1 - \sqrt{1 - N^{-1}} \right) \right], \quad (5.57)$$

where,

$$N = \frac{8(n-1)}{n} \left(\frac{\pi m z_0}{\Omega_{n-1} \rho^n} e^{-\frac{(n-1)H_0}{\kappa}} \left(n - 1 + e^{\frac{2H_0}{\kappa}} \right) \right)^2. \quad (5.58)$$

One can safely use Eq. (5.32) to obtain the change in entropy within the range $\tau < t < \infty$. Also, it will be interesting to check whether the change in entropy is finite. Since the calculation of area change for arbitrary dimensional de Sitter space-time is quite laborious, we consider four (4D) as well as six-dimensional (6D) cases only. The expansion and shear calculated for 4D and 6D are well behaved except when ρ becomes zero, just like the case of Rindler horizon in flat space-time. This divergence is, however, not our concern since we are looking for the evolution of those geodesics which do not intersect the perturbing object. Further, the first term in the expression of entropy change Eq. (5.32) is finite for both 4D and 6D cases even if one considers the $\rho \rightarrow \infty$ limit. Hence, just like the case of flat space-time, divergences come from the second term of Eq. (5.32). In 4D, we denote this term as $\int (\Sigma(t_2) - \Sigma(t_1)) \rho d\rho d\theta$, where $\Sigma(t)$ is the time integral of σ^2 . This quantity is finite if either one of the variables (ρ or t_2) varies till infinity, but other is held finite. But diverges if both tend to infinity. This can be seen by the following argument. If one evaluates the above integration over the cross-section area, where ρ varies between $[a, b]$, then an asymptotic expansion around $t_2 = \infty$ gives

the following expression:

$$\begin{aligned} & \frac{\pi \kappa m^2 e^{-2H_0 z_0}}{4a^2 b^2} \left[z_0(a-b) \left\{ a \left(\pi b (8e^{2H_0 z_0} + 8e^{4H_0 z_0} - 1) - 8z_0 (e^{2H_0 z_0} + 1)^2 \right) \right\} \right. \\ & - 32a^2 b^2 e^{2H_0 z_0} \log\left(\frac{a}{b}\right) \cosh(H_0 z_0) \left\{ \cosh(H_0 z_0) + 2 \left(\log(2z_0) - 1 \right) \sinh(H_0 z_0) \right\} \\ & \left. - 8bz_0^2(a-b) (e^{2H_0 z_0} + 1)^2 \right], \end{aligned}$$

as the leading order term. However, this expression contains $\log b$ term and therefore diverges when the $b \rightarrow \infty$ limit is taken. But if we consider higher-dimensional de-Sitter spacetimes ($D \geq 5$), this divergence goes away, giving finite results for entropy change, similar to the case of Rindler horizon in flat space-time. The expression calculated for the change in entropy of Rindler horizon in six dimensions, obtained by taking both $t \rightarrow \infty$ and $\rho \rightarrow \infty$ limits is given,

$$\begin{aligned} \Delta S = & \frac{9m^2 e^{-4H_0 z_0}}{2048} \left[\frac{5z_0 z_1 (16e^{2H_0 z_0} (e^{2H_0 z_0} + 5) + 93) (\pi - 2 \tan^{-1}(\frac{z_0 z_1}{a}))}{a^3} \right. \\ & + \frac{1}{z_0^2 z_1^2} \left\{ \frac{2z_0 z_1}{a^4 (a^2 + z_0^2 z_1^2)^{5/2}} \left(128z_0^7 z_1^7 (e^{2H_0 z_0} + 3)^2 \left(\sqrt{a^2 + z_0^2 z_1^2} - z_0 z_1 \right) \right. \right. \\ & - 64a^8 (2e^{2H_0 z_0} + e^{4H_0 z_0} - 3) + a^2 z_0^5 z_1^5 \left((1648e^{2H_0 z_0} + 304e^{4H_0 z_0} + 2223) \sqrt{a^2 + z_0^2 z_1^2} \right. \\ & - 64z_0 z_1 (e^{2H_0 z_0} + 3) (7e^{2H_0 z_0} + 17) \left. \right) + a^4 z_0^3 z_1^3 \left(-192z_0 z_1 (e^{2H_0 z_0} + 3) (3e^{2H_0 z_0} + 5) \right. \\ & + (112e^{2H_0 z_0} (2e^{2H_0 z_0} + 9) + 1041) \sqrt{a^2 + z_0^2 z_1^2} - 8a^6 z_0 z_1 (8z_0 z_1 (e^{2H_0 z_0} + 3) \\ & \left. \left. \times (5e^{2H_0 z_0} + 3) + (-16e^{2H_0 z_0} - 6e^{4H_0 z_0} + 3) \sqrt{a^2 + z_0^2 z_1^2} \right) \right) \left. \right\} \\ & - 64 (2e^{2H_0 z_0} + e^{4H_0 z_0} - 3) \left(\log(a^2 + z_0^2 z_1^2) - 2 \log \left(\sqrt{a^2 + z_0^2 z_1^2} + z_0 z_1 \right) \right) \left. \right]. \end{aligned} \tag{5.59}$$

One can see that the above expression is finite. Therefore, for a Rindler horizon in a space-time with non-zero cosmological constant, the change in horizon entropy, when considered between asymptotic cross-sections, is finite for dimensions greater than four.

This result is the same as of a Rindler horizon in flat space-time.

Finally, we would like to emphasize the usefulness of the recipe for obtaining a period of horizon evolution in which the process is quasi-stationary. As presented in (Mishra et al. 2018), one doesn't always have to worry about the bifurcation surface to establish the first law for the black hole horizon. Instead, it can be achieved by considering any arbitrary horizon slices, provided the quasi-stationarity approximation is valid in between such cross-sections, and the first law looks like Eq. (5.32). We have explicitly calculated the value of the time slice in terms of the parameters of the perturbing object.

5.6 Discussions

The first law of black hole mechanics has molded much of our views about black holes. However, checking the limits of application of the first law of black hole mechanics is an important aspect that can be explored. As emphasized before, the questions posed in this paper are analogous to the question of which processes are quasi-static in usual thermodynamics. However, there is an important difference. In usual thermodynamics, if one starts with an initial equilibrium state, then a non-quasi-static process will evolve the state through non-equilibrium states. Due to the teleological nature of the event horizon, one has to ask the opposite question in the case of black hole thermodynamics. That is if one assumes that the final state is a stationary black hole, what are the processes that ensure that the initial state was stationary? The breakdown of the assumptions in PPFL and the onset of caustics to the past, of the event of an object crossing the horizon, precisely means that the initial state was non-stationary and that the initial bifurcation surface never existed.

While this has been pointed out several times in the literature, it has also been argued that Rindler horizons present itself in a unique way, due to non-compact cross-sections. In (Jacobson and Parentani 2003), it has been pointed out that though the shear remains small throughout the process, the total shear obtained by integrating over the cross-sections contributes infinitely to the change in entropy. In this article, the main focus is to demonstrate this precisely. In four dimensions, we show, that this indeed is true. However, in higher dimensions, this is not so, at least for the case when the perturbation

is due to a spherical body. We attribute this behavior to the fall-off condition of the Weyl tensor in asymptotically flat space times in four dimensions. It is possibly similar in spirit to the logarithmic behavior of the electric potential in two dimensions. Assuming that the occurrence of such pathologies is generic; we provide a recipe to obtain finite results by restricting ourselves to finding changes only within a finite interval of horizon evolution (modified PPFL).

A similar study has been done in the case where the background is de-sitter. The results obtained have been compared with the case of zero cosmological constant. In effect, we observe that the set of allowed values for the size of the perturbing object, so that the PPFL remains valid, gets reduced due to the presence of the cosmological constant. Also, our results show that this effect of the cosmological constant is the same in all dimensions. The motivation for the analysis in arbitrary dimensions is mainly due to the growing interest in “the large dimension” limits of Einstein’s equation and its solutions. The results obtained show that the allowed range of values of the radius of the object monotonically increases as the dimensions increase.

Another important aspect is the following. Even if caustics form to the future of the bifurcation surface, it is plausible that the PPFL still holds for an interval of time after caustics set in. However, in this case, the limits of integration are different from those assumed in the original derivation of PPFL. The effect of such a choice of integration limits is a modified version of PPFL suggested in (Mishra et al. 2018). This motivates one to find a horizon time beyond which this modified PPFL continues to hold. This is precisely what we have calculated in sections 5.4 and 5.5.1. This lends support and provides an example for the suggestions put forward in (Mishra et al. 2018).

Chapter 6

Summary and future work

The general theory of relativity (GR) is, beyond any doubt, an elegant description of classical gravity. However, our nature works according to the principles of quantum mechanics. Naturally, one expects a quantum mechanical explanation of gravity. It is a puzzle to the community that the quantization procedures fail when it comes to the case of GR since it is perturbatively non-renormalizable. There are many approaches active toward a unified theory of both quantum mechanics and gravity such as string theory and loop quantum gravity, but a “quantum gravity” theory remains elusive to this date. There is yet another way to the problem at hand, i.e., exploration of black holes. To be more precise, the thermodynamic and statistical understanding of black holes may lead us to some positive results in the pursuit. In this prospect, we have investigated a few aspects of black hole thermodynamics through this thesis.

In the extended phase space, asymptotically AdS black holes undergo a vdW-like first-order phase transition between small black hole (SBH) and large black hole phase (LBH). The realization that black holes behave like the van der Waal system has opened up an intriguing way to explore black hole micro-structure. The first part of this thesis deals with the microstructure of the dRGT massive black hole in an anti-de Sitter background by exploiting the Ruppeiner (Ruppeiner 1995a) geometry. The construction was carried out by defining a normalized curvature scalar R_N in the parameter space of pressure P and the volume V , which are the fluctuation coordinates, via the adiabatic compressibility κ . Our results show that the microstructure details of the dRGT massive black holes

are similar to the charged AdS black holes. The small black hole phase has microstructures analogous to anyon gas with attractive and repulsive interactions. On the other hand, the LBH exhibits only attractive interactions all over the parameter space, which is similar to a boson gas. Further, we observe that the repulsive interaction is suppressed by the graviton mass. The effect of the topology on the repulsive interaction was also investigated, which shows a trend of stronger to weaker in the order $k = -1, 0, 1$. In both the small and large black hole phases, the attractive interactions of the black hole microstructure have the same dependence on the space-time parameters m and k . The effect of charge on the microstructure was also explored, which we find negligible. We would like to extend these calculations to various modified theories of gravity.

Another critical aspect of thermodynamic studies is the dynamics of phase transitions. We have studied various aspects of the phase transition of the dRGT massive black hole in an anti-de Sitter background using the underlying free energy landscape. A detailed investigation of the dynamics and kinetics of phase transitions using the stochastic Fokker-Planck equation was presented, and the results are qualitatively similar to the case of black holes in AdS space-time. The dynamics of switching between the small and large black hole phases due to the thermal fluctuation is probed by calculating the first passage time. Further, we have analyzed the effect of topology and the mass parameter on the evolution of black hole phases. We believe that the variation of switching time from small black holes to large black hole states with respect to the mass as well as the topology is connected to the stability of black holes and will be addressed in future works. Also, we would like to revisit the properties of black hole phase transitions by incorporating Hawking radiation.

Finally, we have investigated one of the versions of the first law of black hole thermodynamics, i.e., the physical process first law (PPFL). The physical process version of the first law can be obtained for horizons with certain assumptions. However, one has to restrict to situations where the horizon evolution is quasi-stationary. We have revisited the analysis of this assumption considering the horizon perturbations of a Rindler horizon with a spherically symmetric object. Our results show that even if the quasi-stationary assumption holds, the change in entropy, in four space-time dimen-

sions, diverges when considered between asymptotic cross-sections. However, these divergences do not appear in higher dimensions. We have also analyzed these features in the presence of a positive cosmological constant and obtained similar results. Further, we have provided a method to set up the physical process first law even if the caustic forms in the past.

Recently, there are many advancements that explore the relationship between black hole thermodynamics, holography, and conformal symmetry. These studies reveal intriguing phase behavior and critical phenomena within the context of black hole thermodynamics in extended phase space. (Ahmed et al. 2023, Frassino et al. 2023, Cong et al. 2022). We would like to extend our research works incorporating these aspects as well.

Appendices

Appendix A

Komar integrals in AdS space

The metric for the AdS_4 spacetime is given by,

$$ds^2 = -\frac{r^2}{l^2}dt^2 + \frac{l^2}{r^2}dr^2 + r^2d\Omega_2^2. \quad (\text{A.1})$$

where $\Lambda = 3/l^2$, l is the AdS radius. By calculating the Komar integral for this AdS spacetime,

$$Q_\xi = \frac{1}{4\pi G} \int_{\partial\Sigma} dS_{\mu\nu} \nabla^\nu \xi^\mu = \frac{1}{4\pi G} \int_{\partial\Sigma} n_\mu \sigma_\nu \nabla^\mu \xi^\nu \quad (\text{A.2})$$

$$= \frac{1}{4\pi G} \int_{\partial\Sigma} d\theta d\phi r^2 \sin\theta n_t \sigma_r \nabla^t \xi^r = \frac{1}{4\pi G} \int_{\partial\Sigma} d\theta d\phi r^2 \sin\theta \frac{r}{l^2}. \quad (\text{A.3})$$

This integral is diverging at $r \rightarrow \infty$. So this relation is need to modify for arriving Smarr relation. There are various ways to resolve these divergences. Method of Brown-York quasi-local stress-energy tensor, by adding a counter term to cancel divergence, Hamiltonian formalism of Hawking and Horowitz. We using definition of a Komar potential $\omega^{\mu\nu}$ to resolve this issue (Kastor et al. 2009a). From the Killing equation, we write,

$$\nabla_\mu \xi^\mu = 0. \quad (\text{A.4})$$

This enable us to define an antisymmetric potential $\omega^{\mu\nu}$, such that derivative of potential is same as the Killing vector ξ^ν ,

$$\xi^\nu = \nabla_\mu \omega^{\mu\nu}. \quad (\text{A.5})$$

The new potential $\omega^{\mu\nu} = \omega^{\mu\nu} + \lambda^{\mu\nu}$ still satisfies the Killing equation since killing potential is not unique one. We can also add an exact term $\lambda^{\mu\nu} = \nabla_\alpha \eta^{\alpha\mu\nu}$, where $\eta^{\alpha\mu\nu}$ is antisymmetric tensor. That will not change the value of the final Komar integral. With the potential term as a counter term, it prevents the divergence issue. The Komar integral reads as,

$$Q_\xi = \frac{1}{4\pi G} \int_{\partial\Sigma} dS_{\mu\nu} (\nabla^\nu \xi^\mu + \Lambda \omega^{\mu\nu}). \quad (\text{A.6})$$

Consider the case of Schwarzschild-AdS spacetime with metric given by,

$$ds^2 = -f(r)dt^2 + \frac{dr^2}{f(r)} + r^2 d\Omega_2^2, \quad f(r) = 1 - \frac{m}{r} - \frac{\Lambda}{3}r^2, \quad (\text{A.7})$$

where m is the mass parameter, which is related to total mass of black hole M through the Komar integral.

$$M = \frac{(d-2)}{16\pi} \omega_{d-2} m, \quad \omega_{d-2} = \frac{2\pi^{(d-1)/2}}{\Gamma(d-1)/2}, \quad (\text{A.8})$$

where $\omega_{(d-2)}$ is the volume of unit $S^{(d-2)}$ sphere. As the only Killing vector associated is $\xi^\mu = \left(\frac{\partial}{\partial t}\right)^\mu = (1, 0, 0, 0)$, we have to determine only rt component of Killing potential $\omega^{\mu\nu}$. Using the definition of Killing potential (eqn. [A.5](#))

$$\frac{1}{r^2} \partial_r (r^2 \omega^{rt}) = 1 \quad (\text{A.9})$$

Integrating the above equation, we get

$$\omega^{rt} = \frac{r}{3} + \frac{C}{r^2}. \quad (\text{A.10})$$

$C = 0$ corresponds to AdS spacetime. For Schwarzschild-AdS metric this can be written

as,

$$\nabla_r \xi_t = \frac{1}{2} \nabla_r (g_{tt} \xi^t) = -\frac{1}{2} \partial_r (f(r)). \quad (\text{A.11})$$

Evaluating Komar integral for pure AdS spacetime, we have

$$Q_\xi = \frac{1}{4\pi G} \int_{\partial\Sigma} dS_{rt} (\nabla^r \xi^t + \Lambda \omega^{rt}) \quad (\text{A.12})$$

$$= \frac{1}{4\pi G} \int_{\partial\Sigma} dS_{rt} \left(\frac{r}{l^2} - \frac{r}{l^2} \right) = 0. \quad (\text{A.13})$$

The same procedure can be applied to derive Smarr relation for Schwarzschild-AdS case. As Komar charge $Q = 0$, we can write the enhanced Komar integral in the D -dimensional spacetime as,

$$\frac{D-2}{8\pi G} \int_{\Sigma} \left(\nabla^\mu \xi^\nu + \frac{2\Lambda}{D-2} \omega^{\mu\nu} \right) = 0. \quad (\text{A.14})$$

Where the $(D-1)$ hypersurface Σ connects the horizon and infinity, infact Σ is bounded by two surfaces, \mathcal{H} on the event horizon and S_∞ at the spatial infinity. Evaluating above integral at the two surfaces, we get

$$0 = \frac{D-2}{8\pi G} \left(\int_{S_\infty} dS_{\mu\nu} \left(\nabla^\mu \xi^\nu + \frac{2\Lambda}{D-2} \omega^{\mu\nu} \right) - \int_{\mathcal{H}} dS_{\mu\nu} \left(\nabla^\mu \xi^\nu + \frac{2\Lambda}{D-2} \omega^{\mu\nu} \right) \right) \quad (\text{A.15})$$

Schwarzschild-AdS spacetime integral will give a finite value, nevertheless it can be removed by infinite background subtraction as prescribed in (?). Adding and subtracting $\omega_{AdS}^{\mu\nu}$ potential will do the trick,

$$0 = \frac{D-2}{8\pi G} \int_{S_\infty} dS_{\mu\nu} \left(\left\{ \nabla^\mu \xi^\nu + \frac{2\Lambda}{D-2} \omega_{AdS}^{\mu\nu} \right\} + \frac{2\Lambda}{D-2} \omega^{\mu\nu} - \frac{2\Lambda}{D-2} \omega_{AdS}^{\mu\nu} \right) \quad (\text{A.16})$$

$$- \frac{D-2}{8\pi G} \int_{\mathcal{H}} dS_{\mu\nu} \left(\nabla^\mu \xi^\nu + \frac{2\Lambda}{D-2} \omega^{\mu\nu} \right). \quad (\text{A.17})$$

Rearranging the terms, we get

$$\frac{D-2}{8\pi G} \int_{S_\infty} dS_{\mu\nu} \left(\nabla^\mu \xi^\nu + \frac{2\Lambda}{D-2} \omega_{AdS}^{\mu\nu} \right) = \frac{D-2}{8\pi G} \int_{\mathcal{H}} dS_{\mu\nu} \nabla^\mu \xi^\nu \quad (\text{A.18})$$

$$+ \frac{D-2}{8\pi G} \frac{2\Lambda}{D-2} \left(\int_{\mathcal{H}} dS_{\mu\nu} \omega^{\mu\nu} - \int_{S_\infty} dS_{\mu\nu} (\omega^{\mu\nu} - \omega_{AdS}^{\mu\nu}) \right). \quad (\text{A.19})$$

We have already evaluated various terms in the above expression, where l.h.s is the definition of Komar mass M ,

$$\frac{D-2}{8\pi G} \int_{S_\infty} dS_{\mu\nu} \left(\nabla^\mu \xi^\nu + \frac{2\Lambda}{D-2} \omega_{AdS}^{\mu\nu} \right) = (D-3)M. \quad (\text{A.20})$$

The integral of first term in the r.h.s is the product of surface gravity κ and area of event horizon,

$$\frac{D-2}{8\pi G} \int_{\mathcal{H}} dS_{\mu\nu} \nabla^\mu \xi^\nu = (D-2) \frac{\kappa A}{8\pi}. \quad (\text{A.21})$$

The remaining terms left in eqn. [A.19](#) are denoted by Θ , which can be seen later as the conjugate volume,

$$\Theta = \int_{\mathcal{H}} dS_{\mu\nu} \omega^{\mu\nu} - \int_{S_\infty} dS_{\mu\nu} (\omega^{\mu\nu} - \omega_{AdS}^{\mu\nu}). \quad (\text{A.22})$$

Combining terms together, we get the Smarr formula

$$(D-3)M = (D-2) \frac{\kappa A}{8\pi G} - 2 \frac{\Theta}{8\pi G} \Lambda. \quad (\text{A.23})$$

Appendix B

Rindler approximations of black hole space-times

We outline the idea of the Rindler approximation of black hole horizon, which shows that the near horizon geometry of a stationary non extremal black hole is that a Rindler spacetime. Though we have considered Schwarzschild and Schwarzschild-de Sitter space-times for our case studies, this idea is applicable to more general cases. We consider a general spherically symmetric metric of the form,

$$ds^2 = -f(r)dt^2 + \frac{dr^2}{f(r)} + r^2 d\Omega^2. \quad (\text{B.1})$$

We expand the function $f(r)$ around the black hole horizon as,

$$f(r) = f(r_+) + f'(r_+)(r - r_+) + O((r - r_+)^2), \quad (\text{B.2})$$

where r_+ represents the position of black hole horizon. If we restrict the region of interest sufficiently close to the horizon, one can approximate the above relation as,

$$f(r) \approx 2\kappa(r - r_+), \quad (\text{B.3})$$

where $\kappa = \frac{1}{2}f'(r_+)$ is the surface gravity of the corresponding horizon. Introducing a new radial coordinate (α) which vanishes at the horizon and increases outwards as,

$$\alpha = \sqrt{2\kappa(r-r_+)} + O\left((r-r_+)^{\frac{3}{2}}\right). \quad (\text{B.4})$$

The line element becomes,

$$ds^2 = -\alpha^2 dt^2 + \frac{d\alpha^2}{\kappa^2} + r_+^2 d\Omega^2. \quad (\text{B.5})$$

Now one can express the above metric in cartesian coordinates in a small region of space-time sufficiently close to the horizon ($\alpha \ll 1$) around a specific direction $\theta = \theta_0$ as follows

$$x = r_+ \sin(\theta_0) \phi, \quad (\text{B.6})$$

$$y = r_+ (\theta - \theta_0),$$

$$z = \frac{\alpha}{\kappa}.$$

The metric in this coordinates will look like,

$$ds^2 = -\kappa^2 z^2 dt^2 + dx^2 + dy^2 + dz^2. \quad (\text{B.7})$$

This is the Rindler spacetime and it will be obvious if we do another coordinate transformation as,

$$T = z \sinh(\kappa t) \text{ and } Z = z \cosh(\kappa t). \quad (\text{B.8})$$

And the metric becomes,

$$ds^2 = -dT^2 + dx^2 + dy^2 + dZ^2. \quad (\text{B.9})$$

The Rindler approximation of the black hole horizon was justified by the following assumptions. The region under consideration is within $\alpha \ll 1$, which means on the trajectory, $z_0 \ll \frac{1}{\kappa}$ and is within a patch of horizon cross-section which is small compared to the total area of the horizon cross-sections. To recover the results for black

holes, we relax these approximations so that $\kappa z_0 = \alpha_0 \approx 1$. Where α_0 is the initial radial distance of the perturbing object from the horizon (Suen et al. 1988).

Bibliography

- Ahmed, M. B., Cong, W., Kubizňák, D., Mann, R. B., and Visser, M. R. (2023). Holographic Dual of Extended Black Hole Thermodynamics. *Phys. Rev. Lett.*, 130(18):181401.
- Amsel, A. J., Marolf, D., and Virmani, A. (2008). The Physical Process First Law for Bifurcate Killing Horizons. *Phys. Rev. D*, 77:024011.
- Astefanesei, D., Mann, R. B., and Radu, E. (2004). Reissner-Nordstrom-de Sitter black hole, planar coordinates and dS / CFT. *JHEP*, 01:029.
- Bardeen, J. M., Carter, B., and Hawking, S. W. (1973a). “The four laws of black hole mechanics”. *Communications in mathematical physics*, 31(2):161–170.
- Bardeen, J. M., Carter, B., and Hawking, S. W. (1973b). The Four laws of black hole mechanics. *Commun. Math. Phys.*, 31:161–170.
- Bekenstein, J. D. (1972). Black holes and the second law. *Lett. Nuovo Cim.*, 4:737–740.
- Bekenstein, J. D. (1973). Black holes and entropy. *Phys. Rev.*, D7:2333–2346.
- Bhattacharjee, S. and Sarkar, S. (2015). Physical process first law and caustic avoidance for rindler horizons. *Phys. Rev. D*, 91:024024.
- Boulware, D. G. and Deser, S. (1972). Can gravitation have a finite range? *Phys. Rev. D*, 6:3368–3382.
- Cai, R.-G., Cao, L.-M., Li, L., and Yang, R.-Q. (2013). P-V criticality in the extended phase space of Gauss-Bonnet black holes in AdS space. *JHEP*, 09:005.

- Cai, R.-G., Hu, Y.-P., Pan, Q.-Y., and Zhang, Y.-L. (2015). Thermodynamics of Black Holes in Massive Gravity. *Phys. Rev. D*, 91(2):024032.
- Capozziello, S. and Laurentis, M. D. (2011). Extended theories of gravity. *Physics Reports*, 509(4-5):167–321.
- Carter, B. (1979). The general theory of the mechanical, electromagnetic and thermodynamic properties of black holes. In Hawking, S. W. and Israel, W., editors, *General Relativity: An Einstein centenary survey*, pages 294–369.
- Chabab, M., El Moumni, H., Iraoui, S., and Masmar, K. (2019). Phase transitions and geothermodynamics of black holes in dRGT massive gravity. *Eur. Phys. J. C*, 79(4):342.
- Clifton, T., Ferreira, P. G., Padilla, A., and Skordis, C. (2012). Modified gravity and cosmology. *Physics Reports*, 513(1-3):1–189.
- Cong, W., Kubiznak, D., Mann, R. B., and Visser, M. R. (2022). Holographic CFT phase transitions and criticality for charged AdS black holes. *JHEP*, 08:174.
- Dayyani, Z., Sheykhi, A., Dehghani, M. H., and Hajkhalili, S. (2018). Critical behavior and phase transition of dilaton black holes with nonlinear electrodynamics. *Eur. Phys. J. C*, 78(2):152.
- de Rham, C., Gabadadze, G., and Tolley, A. J. (2011). Resummation of massive gravity. *Phys. Rev. Lett.*, 106:231101.
- Dehyadegari, A., Sheykhi, A., and Wei, S.-W. (2020). Microstructure of charged AdS black hole via $P - V$ criticality. *Phys. Rev. D*, 102(10):104013.
- Dolan, B. P. (2011a). Pressure and volume in the first law of black hole thermodynamics. *Class. Quant. Grav.*, 28:235017.
- Dolan, B. P. (2011b). The cosmological constant and the black hole equation of state. *Class. Quant. Grav.*, 28:125020.

- Fernando, S. (2016). Phase transitions of black holes in massive gravity. *Mod. Phys. Lett. A*, 31(16):1650096.
- Fierz, M. and Pauli, W. (1939). On relativistic wave equations for particles of arbitrary spin in an electromagnetic field. *Proc. Roy. Soc. Lond. A*, 173:211–232.
- Frassino, A. M., Pedraza, J. F., Svesko, A., and Visser, M. R. (2023). Higher-Dimensional Origin of Extended Black Hole Thermodynamics. *Phys. Rev. Lett.*, 130(16):161501.
- Ghosh, A. and Bhamidipati, C. (2020a). Thermodynamic geometry and interacting microstructures of BTZ black holes. *Phys. Rev. D*, 101(10):106007.
- Ghosh, A. and Bhamidipati, C. (2020b). Thermodynamic geometry for charged Gauss-Bonnet black holes in AdS spacetimes. *Phys. Rev.*, D101(4):046005.
- Hawking, S. W. (1972). Black holes in general relativity. *Commun. Math. Phys.*, 25:152–166.
- Hawking, S. W. (1975). Particle Creation by Black Holes. *Commun. Math. Phys.*, 43:199–220. [,167(1975)].
- Hawking, S. W. (1975). Particle creation by black holes. *Communications in Mathematical Physics*, 43(3):199–220.
- Hawking, S. W. and Hartle, J. B. (1972). Energy and angular momentum flow into a black hole. *Commun. Math. Phys.*, 27:283–290.
- Hawking, S. W. and Page, D. N. (1983a). Thermodynamics of Black Holes in anti-De Sitter Space. *Commun. Math. Phys.*, 87:577.
- Hawking, S. W. and Page, D. N. (1983b). Thermodynamics of Black Holes in anti-De Sitter Space. *Commun. Math. Phys.*, 87:577.
- Hendi, S. H., Eslam Panah, B., and Panahiyan, S. (2016). Thermodynamical Structure of AdS Black Holes in Massive Gravity with Stringy Gauge-Gravity Corrections. *Class. Quant. Grav.*, 33(23):235007.

- Hendi, S. H., Eslam Panah, B., Panahiyan, S., Liu, H., and Meng, X. H. (2018). Black holes in massive gravity as heat engines. *Phys. Lett. B*, 781:40–47.
- Hendi, S. H., Mann, R. B., Panahiyan, S., and Eslam Panah, B. (2017a). Van der Waals like behavior of topological AdS black holes in massive gravity. *Phys. Rev. D*, 95(2):021501.
- Hendi, S. H., Mann, R. B., Panahiyan, S., and Eslam Panah, B. (2017b). Van der waals like behavior of topological ads black holes in massive gravity. *Phys. Rev. D*, 95:021501.
- Jacobson, T. and Parentani, R. (2003). Horizon entropy. *Foundations of Physics*, 33:323–348.
- Janyszek, H. and Mrugaa, R. (1990). Riemannian geometry and stability of ideal quantum gases. *Journal of Physics A: Mathematical and General*, 23(4):467–476.
- Johnson, C. V. (2014). Holographic Heat Engines. *Class. Quant. Grav.*, 31:205002.
- Kastor, D. (2008). “Komar integrals in higher (and lower) derivative gravity”. *Classical and Quantum Gravity*, 25(17):175007.
- Kastor, D., Ray, S., and Traschen, J. (2009a). Enthalpy and the Mechanics of AdS Black Holes. *Class. Quant. Grav.*, 26:195011.
- Kastor, D., Ray, S., and Traschen, J. (2009b). “Enthalpy and the mechanics of AdS black holes”. *Classical and Quantum Gravity*, 26(19):195011.
- Kubiznak, D. and Mann, R. B. (2012). P-V criticality of charged AdS black holes. *JHEP*, 07:033.
- Kubizňák, D. and Mann, R. B. (2012). “P- V criticality of charged AdS black holes ”. *Journal of High Energy Physics*, 2012(7):33.
- Lan, S.-Q. (2019). Joule-Thomson expansion of neutral AdS black holes in massive gravity. *Nucl. Phys. B*, 948:114787.

- Li, R. and Wang, J. (2020). Thermodynamics and kinetics of hawking-page phase transition. *Phys. Rev. D*, 102:024085.
- Li, R., Zhang, K., and Wang, J. (2020). Thermal dynamic phase transition of Reissner-Nordström Anti-de Sitter black holes on free energy landscape. *JHEP*, 10:090.
- Liu, B., Yang, Z.-Y., and Yue, R.-H. (2020). Tricritical point and solid/liquid/gas phase transition of higher dimensional AdS black hole in massive gravity. *Annals Phys.*, 412:168023.
- May, H.-O., Mausbach, P., and Ruppeiner, G. (2013). Thermodynamic curvature for attractive and repulsive intermolecular forces. *Phys. Rev. E*, 88:032123.
- Miao, Y.-G. and Xu, Z.-M. (2018). Parametric phase transition for a Gauss-Bonnet AdS black hole. *Phys. Rev. D*, 98(8):084051.
- Mirza, B. and Mohammadzadeh, H. (2008). Ruppeiner geometry of anyon gas. *Phys. Rev. E*, 78:021127.
- Mirza, B. and Sherkatghanad, Z. (2014). Phase transitions of hairy black holes in massive gravity and thermodynamic behavior of charged AdS black holes in an extended phase space. *Phys. Rev. D*, 90(8):084006.
- Mishra, A., Chakraborty, S., Ghosh, A., and Sarkar, S. (2018). On the physical process first law for dynamical black holes. *JHEP*, 09:034.
- Mo, J.-X. and Liu, W.-B. (2014). $P - V$ criticality of topological black holes in Lovelock-Born-Infeld gravity. *Eur. Phys. J. C*, 74(4):2836.
- Naveena Kumara, A., Rizwan, C. L. A., Hegde, K., Ali, M. S., and M, A. K. (2020). Microstructure of five-dimensional neutral Gauss-Bonnet black hole in anti-de Sitter spacetime via $P - V$ criticality.
- Ning, S.-L. and Liu, W.-B. (2016). Black Hole Phase Transition in Massive Gravity. *Int. J. Theor. Phys.*, 55(7):3251–3259.

- Ökcü, O. and Aydiner, E. (2017). Joule–Thomson expansion of the charged AdS black holes. *Eur. Phys. J. C*, 77(1):24.
- Oshima, H., Obata, T., and Hara, H. (1999). Riemann scalar curvature of ideal quantum gases obeying gentile’s statistics. *Journal of Physics A: Mathematical and General*, 32(36):6373–6383.
- Rajagopal, A., Kubizňák, D., and Mann, R. B. (2014). Van der Waals black hole. *Phys. Lett. B*, 737:277–279.
- Ruppeiner, G. (1995a). Riemannian geometry in thermodynamic fluctuation theory. *Rev. Mod. Phys.*, 67:605–659. [Erratum: *Rev. Mod. Phys.* 68, 313–313 (1996)].
- Ruppeiner, G. (1995b). Riemannian geometry in thermodynamic fluctuation theory. *Rev. Mod. Phys.*, 67:605–659. [Erratum: *Rev. Mod. Phys.* 68, 313 (1996)].
- Ruppeiner, G. (2008a). Thermodynamic curvature and phase transitions in Kerr–Newman black holes. *Phys. Rev. D*, 78:024016.
- Ruppeiner, G. (2008b). Thermodynamic curvature and phase transitions in Kerr–Newman black holes. *Phys. Rev.*, D78:024016.
- Safir, T. K., Rizwan, C. L. A., and Vaid, D. (2022). Ruppeiner geometry, $P - V$ criticality and interacting microstructures of black holes in dRGT massive gravity. *Int. J. Mod. Phys. A*, 37(25):2250158.
- Suen, W. M., Price, R. H., and Redmount, I. H. (1988). Membrane Viewpoint on Black Holes: Gravitational Perturbations of the Horizon. *Phys. Rev. D*, 37:2761–2789.
- Teitelboim, C. (1985). “The cosmological constant as a thermodynamic black hole parameter”. *Physics Letters B*, 158(4):293–297.
- Thorne, K. S., Price, R. H., and Macdonald, D. A., editors (1986). *BLACK HOLES: THE MEMBRANE PARADIGM*.
- Vegh, D. (2013). Holography without translational symmetry.

- Wald, R. M. (1995a). Quantum field theory in curved space-time. In *14TH INTERNATIONAL CONFERENCE ON GENERAL RELATIVITY AND GRAVITATION (GR14)*, pages 401–415.
- Wald, R. M. (1995b). *Quantum Field Theory in Curved Space-Time and Black Hole Thermodynamics*. Chicago Lectures in Physics. University of Chicago Press, Chicago, IL.
- Wei, S.-W. and Liu, Y.-X. (2013). Critical phenomena and thermodynamic geometry of charged gauss-bonnet ads black holes. *Phys. Rev. D*, 87:044014.
- Wei, S.-W. and Liu, Y.-X. (2015a). Insight into the Microscopic Structure of an AdS Black Hole from a Thermodynamical Phase Transition. *Phys. Rev. Lett.*, 115(11):111302. [Erratum: *Phys.Rev.Lett.* 116, 169903 (2016)].
- Wei, S.-W. and Liu, Y.-X. (2015b). Insight into the Microscopic Structure of an AdS Black Hole from a Thermodynamical Phase Transition. *Phys. Rev. Lett.*, 115(11):111302. [Erratum: *Phys. Rev. Lett.* 116,no.16,169903(2016)].
- Wei, S.-W., Liu, Y.-X., and Mann, R. B. (2019a). Repulsive Interactions and Universal Properties of Charged Anti-de Sitter Black Hole Microstructures. *Phys. Rev. Lett.*, 123(7):071103.
- Wei, S.-W., Liu, Y.-X., and Mann, R. B. (2019b). Ruppeiner Geometry, Phase Transitions, and the Microstructure of Charged AdS Black Holes. *Phys. Rev.*, D100(12):124033.
- Weinhold, F. (1975). Metric geometry of equilibrium thermodynamics ii. *The Journal of Chemical Physics*, 63:2479–2483.
- Wu, B., Wang, C., Xu, Z.-M., and Yang, W.-L. (2021). Ruppeiner geometry and thermodynamic phase transition of the black hole in massive gravity. *Eur. Phys. J. C*, 81(7):626.
- Xu, J., Cao, L.-M., and Hu, Y.-P. (2015). P-V criticality in the extended phase space of black holes in massive gravity. *Phys. Rev. D*, 91(12):124033.

- Xu, Z.-M. (2020). The correspondence between thermodynamic curvature and isoperimetric theorem from ultraspinning black hole. *Phys. Lett. B*, 807:135529.
- Xu, Z.-M., Wu, B., and Yang, W.-L. (2020a). Diagnosis inspired by the thermodynamic geometry for different thermodynamic schemes of the charged BTZ black hole.
- Xu, Z.-M., Wu, B., and Yang, W.-L. (2020b). Ruppeiner thermodynamic geometry for the Schwarzschild-AdS black hole. *Phys. Rev. D*, 101(2):024018.
- Yazdikarimi, H., Sheykhi, A., and Dayyani, Z. (2019). Critical behavior of gauss-bonnet black holes via an alternative phase space. *Phys. Rev. D*, 99:124017.
- Yerra, P. K. and Bhamidipati, C. (2020a). Critical heat engines in massive gravity. *Class. Quant. Grav.*, 37(20):205020.
- Yerra, P. K. and Bhamidipati, C. (2020b). Ruppeiner Geometry, Phase Transitions and Microstructures of Black Holes in Massive Gravity. *Int. J. Mod. Phys. A*, 35(22):2050120.
- Zou, D.-C., Yue, R., and Zhang, M. (2017). Reentrant phase transitions of higher-dimensional AdS black holes in dRGT massive gravity. *Eur. Phys. J. C*, 77(4):256.
- Zou, D.-C., Zhang, S.-J., and Wang, B. (2014). Critical behavior of born-infeld ads black holes in the extended phase space thermodynamics. *Phys. Rev. D*, 89:044002.

CURRICULUM VITAE



SAFIR T. K.

Permanent Address :

Kalikulangara House, Cheruvayoor,
Vazhakkad, Malappuram Dist,
Kerala, India - 673645

Mobile:(+91)-9946635799

E-mail: stkphy@gmail.com,

Academic Qualifications :

Master of Science Score : 72%

M.G University,
Kottayam, Kerala, India

Bachelor of Education Score : 76%

Kerala University,
Trivandrum, kerala India

Bachelor of Science Score : 70%

Calicut University,
Calicut, kerala India

Research Publications :

Articles in International Journals : 2

Workshops and Schools attended : 25+